



Separator

1287-1

1. Report No. FHWA/TX-94/1287-1	2. Government Accession No.	3. Recipient's Catalog No.	
4. Title and Subtitle RECOMMENDATIONS FOR ASSESSING STRUCTURAL CONTRIBUTION OF STABILIZED BASES AND SUBBASES:		5. Report Date November 1994	
		6. Performing Organization Code	
7. Author(s) Dallas N. Little, and Jasim Bhuiyan		8. Performing Organization Report No. Research Report 1287-1	
9. Performing Organization Name and Address Texas Transportation Institute The Texas A&M University System College Station, Texas 77843-3135		10. Work Unit No. (TRIS)	
		11. Contract or Grant No. Study No. 0-1287	
12. Sponsoring Agency Name and Address Texas Department of Transportation Research and Technology Transfer Office P. O. Box 5080 Austin, Texas 78763-5080		13. Type of Report and Period Covered Interim: September 1991-June 1993	
		14. Sponsoring Agency Code	
15. Supplementary Notes Research performed in cooperation with the Texas Department of Transportation and the U.S. Department of Transportation, Federal Highway Administration. Research Study Title: Recommendations for Assessing Structural Contribution of Stabilized Bases and Subbases			
16. Abstract The Texas Department of Transportation uses stabilized bases and subgrades extensively in flexible pavements. A method of integrating the structural benefits derived from these bases into current TxDOT flexible pavement design and analysis procedures for considering stabilized layers as candidate layers in flexible pavements is needed. This report describes approaches documented in the literature for evaluating the structural contribution of stabilized bases and subbases.			
17. Key Words Stabilization, Bases, Subgrade Stabilization, Structural Benefits, Flexible Pavements		18. Distribution Statement No restrictions. This document is available to the public through NTIS: National Technical Information Service 5285 Port Royal Road Springfield, Virginia 22161	
19. Security Classif.(of this report) Unclassified	20. Security Classif.(of this page) Unclassified	21. No. of Pages 148	22. Price

RECOMMENDATIONS FOR ASSESSING STRUCTURAL CONTRIBUTION OF STABILIZED BASES AND SUBBASES

by

Dallas N. Little
Research Engineer
Texas Transportation Institute

and

Jasim Bhuiyan
Graduate Research Assistant
Texas Transportation Institute

Research Report 1287-1
Research Study Number 0-1287
Research Study Title: Recommendations for Assessing Structural
Contribution of Stabilized Bases and Subbases

Sponsored by the
Texas Department of Transportation
In Cooperation with
U.S. Department of Transportation
Federal Highway Administration

November 1994

TEXAS TRANSPORTATION INSTITUTE
The Texas A&M University System
College Station, Texas 77843-3135

IMPLEMENTATION STATEMENT

This report is a summary of pertinent literature regarding the structural characterization of stabilized bases and subbases. The approaches to structural characterization discussed in this report provide the basis for the development of the mixture design and assignment of structural properties to stabilized layers presented in report 1287-2F.

This is a literature review and evaluation of the applicability of the literature to research project 1287.

DISCLAIMER

The contents of this report reflect the views of the authors who are responsible for the facts and the accuracy of the data presented herein. The contents do not necessarily reflect the official view or policies of the Texas Department of Transportation (TxDOT), or the Federal Highway Administration (FHWA). This report does not constitute a standard, specification, or regulation nor is it intended for construction, bidding, or permit purposes. The engineer in charge of the project is Dallas N. Little, P.E. #40392.

TABLE OF CONTENTS

	Page
LIST OF FIGURES	xi
LIST OF TABLES	xii
SUMMARY	xiv
CHAPTER 1 - OBJECTIVES AND PURPOSE OF THE INTERIM REPORT	1
INTRODUCTION	1
OBJECTIVES OF THE INTERIM REPORT	1
CHAPTER 2 - FINDINGS OF THE CHARACTERIZATION AND DESIGN OF STABILIZED LAYERS TO ACCOMMODATE THE EVALUATION OF THEIR ROLE AND CONTRIBUTION IN PAVEMENT PERFORMANCE	3
CHARACTERIZATION AND PERFORMANCE EVALUATION OF LIME STABILIZED BASES	3
CHARACTERIZATION AND PERFORMANCE EVALUATION OF PORTLAND CEMENT STABILIZED SUBGRADES	19
CHARACTERIZATION AND PERFORMANCE EVALUATION OF LIME-FLY ASH AND CEMENT-FLY ASH STABILIZED BASES	23
CONCLUSIONS	29
CHAPTER 3 - WORK NECESSARY TO VERIFY, UPGRADE AND/OR REPLACE CURRENT PERFORMANCE ALGORITHMS	33
LIME STABILIZED SUBGRADES	33
LIME STABILIZED BASES	35
PORTLAND CEMENT STABILIZED BASES AND SUBGRADES	35
FLY ASH STABILIZED BASES AND SUBGRADES	36
SUMMARY OF DELIVERABLES	36

TABLE OF CONTENTS

	Page
REFERENCES	37
APPENDIX SURVEY OF PERTINENT LITERATURE	A-1
LIME STABILIZATION	A-1
CEMENT STABILIZATION	A-43
LIME-FLY ASH-STABILIZED BASES AND SUBBASES	A-83

LIST OF FIGURES

Figure	Page
1 The quantity of lime required to produce pozzolanic reaction is influenced by the mineralogy of the soil being stabilized (Eades and Grim, 1960)	8
2 The resilient modulus of the tama B soil are significantly influenced by lime stabilization even after 10 freeze-thaw cycles (Thompson, 1985)	12
3 Comparison of strength after 7 days at 43°C (110°F) with strength increases at 22°C (72°F) (Alexander, 1978)	17
4 Structural layer coefficient, a_2 , as determined by Thompson, as a function of compressive strength for lime stabilized layers. (Thompson, 1970)	18
5 Variation in cement-treated bases with base strength parameter (AASHTO, 1986)	22
6 Typical relationship of stress ratio to traffic conditions (ESALs - 18 kip equivalent single axle loads) (Flexible Pavement Manual, 1991)	28
7 Typical PSM thickness design chart	30

LIST OF TABLES

Table	Page
1 Unconfined compressive strengths of selected soils	7
2 Resilient moduli of lime stabilized subgrade (LSS's) backcalculated from falling weight deflectometer (FWD) data	10
3 Average values of bulk stress, Θ , within the flexible base (aggregate base) layer as a function of hot mix asphalt concrete thickness and subgrade support (AASHTO Guide, 1986)	14
4 Typical variation in the resilient modulus of flexible base (aggregate base) as a function of moisture condition and stress states (AASHTO Guide, 1986)	14
5 Summary of octahedral stress ratios developed within hot mix asphalt concrete surfaces as a function of the supporting modulus of the flexible base course layers	15
6 Recommended physical and chemical requirements * for fly ash for use in pozzolanic stabilized mixtures (PSMs) (Flexible Pavement Manual, 1991)	24
7 Suggested AASHTO structural layer coefficient (a_2) for PSM base layers (Flexible Pavement Manual, 1990)	31

SUMMARY

Stabilized subgrades, subbases and bases are an important component of many of the roadways of Texas. Unfortunately, stabilized subgrades are frequently not accounted for in the pavement design process largely because of concerns regarding the permanency of stabilization. Furthermore, the existing Flexible Pavement System (FPS) does not adequately address stabilized base design.

The importance of ascertaining the structural characteristics of stabilized layers in Texas pavements has been widely accepted by Texas Department of Transportation (TxDOT) district personnel. Districts have provided great cooperation and invaluable assistance in establishing and conducting laboratory and in situ field testing on lime stabilized subgrades, lime stabilized bases, portland cement stabilized bases and subgrade and fly ash stabilized bases and subgrades.

Because of the interest level demonstrated by district personnel in establishing pertinent engineering properties of stabilized layers, it was decided to concentrate more in project 1287 on establishing in situ characteristics of stabilized layers and on appropriate structural performance models or algorithms for these layers.

CHAPTER 1

OBJECTIVES AND PURPOSE OF THE INTERIM REPORT

INTRODUCTION

Stabilized subgrades, subbases and bases are an important component of many of the roadways of Texas. Unfortunately, stabilized subgrades are frequently not accounted for in the pavement design process largely because of concerns regarding the permanency of stabilization. Furthermore, the existing Flexible Pavement System (FPS) does not adequately address stabilized base design.

The importance of ascertaining the structural characteristics of stabilized layers in Texas pavements has been widely accepted by Texas Department of Transportation (TxDOT) district personnel. Districts have provided great cooperation and invaluable assistance in establishing and conducting laboratory and in situ field testing on lime stabilized subgrades, lime stabilized bases, portland cement stabilized bases and subgrade and fly ash stabilized bases and subgrades.

Because of the interest level demonstrated by district personnel in establishing pertinent engineering properties of stabilized layers, it was decided to concentrate more in project 1287 on establishing in situ characteristics of stabilized layers and on appropriate structural performance models or algorithms for these layers.

OBJECTIVES OF THE INTERIM REPORT

The objectives of this interim report are

1. Identify the structural performance algorithms that can most effectively be used to evaluate the structural contribution of stabilized layers to the pavement system.
2. Identify what additional work is necessary in order to upgrade existing structural performance algorithms or to develop alternative structural algorithms to satisfactorily evaluate the role of the stabilized layer in the pavement system.

CHAPTER 2

FINDINGS OF THE CHARACTERIZATION AND DESIGN OF STABILIZED LAYERS TO ACCOMMODATE THE EVALUATION OF THEIR ROLE AND CONTRIBUTION IN PAVEMENT PERFORMANCE

CHARACTERIZATION AND PERFORMANCE EVALUATION OF LIME STABILIZED BASES

Mechanisms of Stabilization

The basic mechanisms of stabilization in lime stabilized clay soils are (1) cation exchange, (2) flocculation and agglomeration, (3) pozzolanic reaction and (4) carbonation. These reactions are explained in detail by Little et al., (1987) and Little (1992). This report will not attempt to review the mechanisms of lime stabilization in detail. However, it is pertinent to review the basic physical property changes that occur upon the addition of lime to soil.

Soil Modification

Upon the addition of lime with soils containing a significant clay fraction, at least approximately 10 percent, the rapidly occurring reactions of cation exchange, flocculation and agglomeration and some rapidly occurring pozzolanic reactions lead to a significant reduction in plasticity and swell potential. These reactions have been shown to occur with virtually all fine-grained soils and can occur at relatively low lime contents.

As a result of the textural and plasticity changes that occur in the lime treated soils, shear strength increases and a significant increase in stiffness or resilient modulus has also been documented. However, the effects of modification of the soil with lime need to be differentiated from the effects of stabilization of the soil with lime. Therefore, modification should be defined as the reduction of plasticity and/or swell potential to an acceptable level to meet design requirements. This modification usually also carries with it strength and stiffness improvements and a significant improvement in workability, constructability and textural changes.

Soil Stabilization

Soil stabilization is a permanent change in the properties of the lime treated soils. This stabilization reaction requires a significant level of pozzolanic reactivity. The pozzolanic reaction is discussed in detail by Little et al., (1987) and Little (1992). Succinctly stated, this reaction entails the development of a high pH environment in the soil-lime-water system through the addition of the appropriate level of lime to trigger the high pH environment. The result of this high pH system is that the clay minerals (comprised of alternating layers of silicates and

aluminates) are partially dissolved, since the solubility of both silica and alumina is very high in high pH systems. When the optimum amount of lime is added to a soil-water system, the pH exceeds 12.4 at 25°C (77°F). This pH is well above the level required to dissolve clay silica and clay alumina.

The reaction among clay silica and clay alumina and calcium hydroxide (lime) and water results in products referred to as calcium-aluminate-hydrates and calcium-silicate-hydrates. The reaction is referred to as pozzolanic because it relies on pozzolans provided by the clay. These pozzolans are clay silica and clay alumina.

The pozzolanic products which form have been shown to be permanent reaction products by Little et al (1982), Kennedy and Tahmoressi (1987), and Eades and Grim (1960). The products formed at the surface of the clay mineral represent a change in mineralogy and result in a significant increase in stiffness (resilient modulus). The pozzolanic reaction continues with time and proper conditions for the reaction, i.e., temperature above 4°C, time and the presence of the reactants (calcium and pozzolans). The only way to insure the continuation of the reaction is to provide the appropriate level of lime to continue to keep the pH high and the supply of calcium adequate until an appreciable level of the pozzolanic product has been developed.

The pozzolanic product represents a permanent change in the clay mineral. The permanency and durability of this product has been documented by many researchers and durability studies, i.e., McCallister and Petry (1990), Eades and Grim (1960), Kelley (1972), Little (1994), Gutschick (1985). The key to permanency is that appropriate steps have been taken in the mixture design process to insure that an adequate lime content has been added to promote the pozzolanic reaction. If too little lime is added, it is possible to promote cation exchange without the development pozzolanic products. The result can be improved workability and reduced plasticity and reduced swell. However, since these physical changes can be predominately the result of cation exchange, leaching action can possibly reverse this process. However, the reversal of the pozzolanic reaction is very unlikely as demonstrated by McCallister and Petry (1990).

Therefore, lime stabilization as the result of pozzolanic reaction results in a pavement layer of substantial strength, stiffness and durability. This is required if the lime is to be used to produce a structural layer. Since the pozzolanic reaction is evidenced by the development of shear strength, shear strength tests have been used to measure pozzolanic reactivity.

Lime Stabilization in Base Courses

Lime stabilization of base course materials has received increased attention during the last several years. Essentially the same mechanisms of stabilization are involved as with lime stabilization of subgrade materials. In most cases where lime is used to stabilize base courses, the base material to be stabilized is comprised by a substantial amount of clay binder. The binder fraction of the base course is usually defined as the percentage of the gradation passing the number 40 sieve. When the plasticity index of this fraction exceeds 10 percent and the fines (fraction passing the number 200 sieve) is greater than about 25 percent, lime is a possible

stabilizer (Little et al., 1987).

Lime has been successfully used to stabilize aggregate base courses with plastic binder (minus 40 sieve fraction) by using low percentages of lime. For example Little (1990) documents the success encountered when an Arizona granite aggregate base course with plastic fines (PI ranging from 12 to 17) was stabilized with 1 percent lime by weight of the aggregate base course. This level of stabilizer, of course, is in the order of 5 or 6 percent by weight of the fines and is, therefore, typical of the amount generally required for the development of pozzolanic reactivity.

Little (1990) documented that engineering properties of the lime stabilized (1 percent by weight of the aggregate) were substantially and statistically superior to the unstabilized control sections. The engineering properties measured were the unconfined compressive strength and the in situ resilient modulus, determined from Falling Weight Deflectometer (FWD) deflection basins. The average resilient modulus of the control (unstabilized) aggregate base layers was approximately 140 MPa (20,000 psi) while the average resilient modulus of the stabilized layers was approximately 1,575 MPa (225,000 psi).

The level of resilient modulus achieved in the granite aggregate base course is in a good range for performance of a base course. The stiffness is high enough to provide good protection of underlying layers and good support of the hot mix asphalt concrete surface. Yet, the stiffness is not so high as to develop a brittle, rigid slab effect as is often the case when the layer is stabilized with higher percentages of stabilizers. The level of resilient modulus achieved in this case may be said to be highly compatible with the moduli of the other layers within the system. In this case compatibility is defined as the ratio of layer stiffnesses.

The unconfined compressive strengths of the lime stabilized aggregate base course were sufficiently high to produce durable material. The unconfined compressive strengths were in the range of 2,800 KPa (400 psi).

Lime stabilization has been successfully used in Texas to alter the properties of bank run river gravel aggregate. Little (1994) documents the stabilization of a high fines content, high plasticity (PI of approximately 30) bank run Colorado River gravel with the use of from 3 to 5 percent lime. The need for the high percentage of lime is due to the high binder content and the high plasticity of the fines. The addition of the lime increased the California Bearing Ratio (CBR) of the aggregate from approximately 40 to approximately 100 and increased the unconfined compressive strength from approximately 350 KPa (50 psi) to approximately 840 KPa (120 psi).

One of the most interesting uses of lime has been to enhance the properties of carbonate aggregate bases. The Corpus Christi, Yoakum and Bryan Districts, among others, have successfully used lime to enhance the properties of limestone bases with lime. In some cases these limestones have had enough plastic fines to react with the lime pozzolanically. However, in many cases the limestone base has been devoid of plastic, clay fines. Yet, the lime has still reacted with the carbonate base to produce substantially improved compressive strengths and substantially improved resilient modulus responses.

The explanation of the reaction of the lime with the carbonate aggregate was provided by Graves et al. (1992) who documented this reaction with limestone aggregates in Florida. Graves explained that the reaction is due to substantial development of calcium carbonate. It is well known that calcium carbonate develops when calcium hydroxide reacts with carbon dioxide from the atmosphere. This forms a cement. However, the reaction has traditionally been labeled as somewhat unreliable as it uses lime which could have reacted pozzolanically with clay. However, in the case of carbonate material without clay, the development of a carbonate cementitious matrix represents a substantial improvement in mixture properties. It has also been established that carbonate aggregates without lime tend to "set up" through carbonation. Graves et al. (1992) explains that the addition of low percentages of lime "catalyzes" and enhances this reaction.

An additional interesting finding of the study by Graves et al. (1992) is that the interfacial bonding of lime treated aggregates was a key to strength development. Graves reported that strength development of all aggregates was a function of calcite to quartz ratios. Higher ratios result in greater strength due to the more complete development of carbonate bonding.

Graves et al. (1992) also reported that granite aggregates stabilized with portland cement produce high strengths but that the weak link in their strength is the interfacial bond. Microfractures in this bond, developed during cyclic wetting and drying or freezing and thawing, may result in reduced strength. However, when the granite aggregate was pretreated with Ca(OH)_2 the residual strength was significantly higher. Scanning electron microscopic (SEM) analysis showed that the lime treated aggregate developed a better interfacial bond between the cement paste and the aggregate than was developed without the lime pretreatment. Furthermore, SEM analysis documented the nature of the carbonate cement matrix in calcareous aggregates. The addition of relatively low levels of CaCO_3 was shown to develop a much denser CaCO_3 cement matrix that developed in the aggregate without lime.

Material Characteristics Due to Stabilization

When adequate lime is added to optimize the pozzolanic reaction with soils substantial improvement in shear strength and resilient moduli can be realized. Table 1 illustrates typical improvement levels in strength and stability for various classifications of soils.

Table 1 demonstrates the strength levels achieved when testing five lime stabilized Texas soils with very different mineralogies. It is well known that the mineralogy and conditions of weathering substantially influence the reactivity of lime with soils (Thompson, 1985).

The soils in Table 1 are all reactive with lime. However, the Beaumont clay is the least reactive. This clay possesses what is referred to by soil scientists as non-specific acidity. This acidity refers to the presence of poorly structured aluminate layers interdispersed within the clay structure. As a result of the influence of the aluminate layers, the Beaumont clay requires more lime than most soils for stabilization and a longer curing time. The variation among different soils in terms of lime reactivity is further illustrated by Figure 1. In this figure, it is apparent that some soils begin developing pozzolanic reaction with low levels of lime, i.e., the kalonite clays.

Table 1. Unconfined compressive strengths of selected soils.

Soil	Percent Lime	Accelerated Strength*, KPa (psi)	28-Day Strength**, KPa (psi)
Arlington Clay	4	1,225 (175)	
	6	2,170 (310)	
	8	2,450 (350)	4,830 (690)
Beaumont Clay	4	490 (70)	
	6	490 (70)	
	8	700 (100)	1,540 (220)
Burleson Clay	4	630 (90)	
	6	1,400 (200)	
	8	1,750 (250)	2,310 (330)
Denver, Co. Sandy Clay	4	2,100 (300)	
	6	2,030 (290)	2,870 (410)
	8	1,750 (250)	
Victoria Clay	4	700 (100)	
	6	8,050 (1,150)	
	8	1,470 (210)	1,425 (275)

* 2 day at 35°C

** 28-days at 22°C

1 psi = 6,894 Pa

However, the montmorillonite soils require a substantial amount of lime prior to the development of strength. This indicates that a substantial amount of lime is necessary to satisfy cation exchange effects and cation or $\text{Ca}(\text{OH})_2$ molecule crowding effects prior to the development of pozzolanic reactivity. This would seem logical for the high surface area and highly negatively charged montmorillonite minerals.

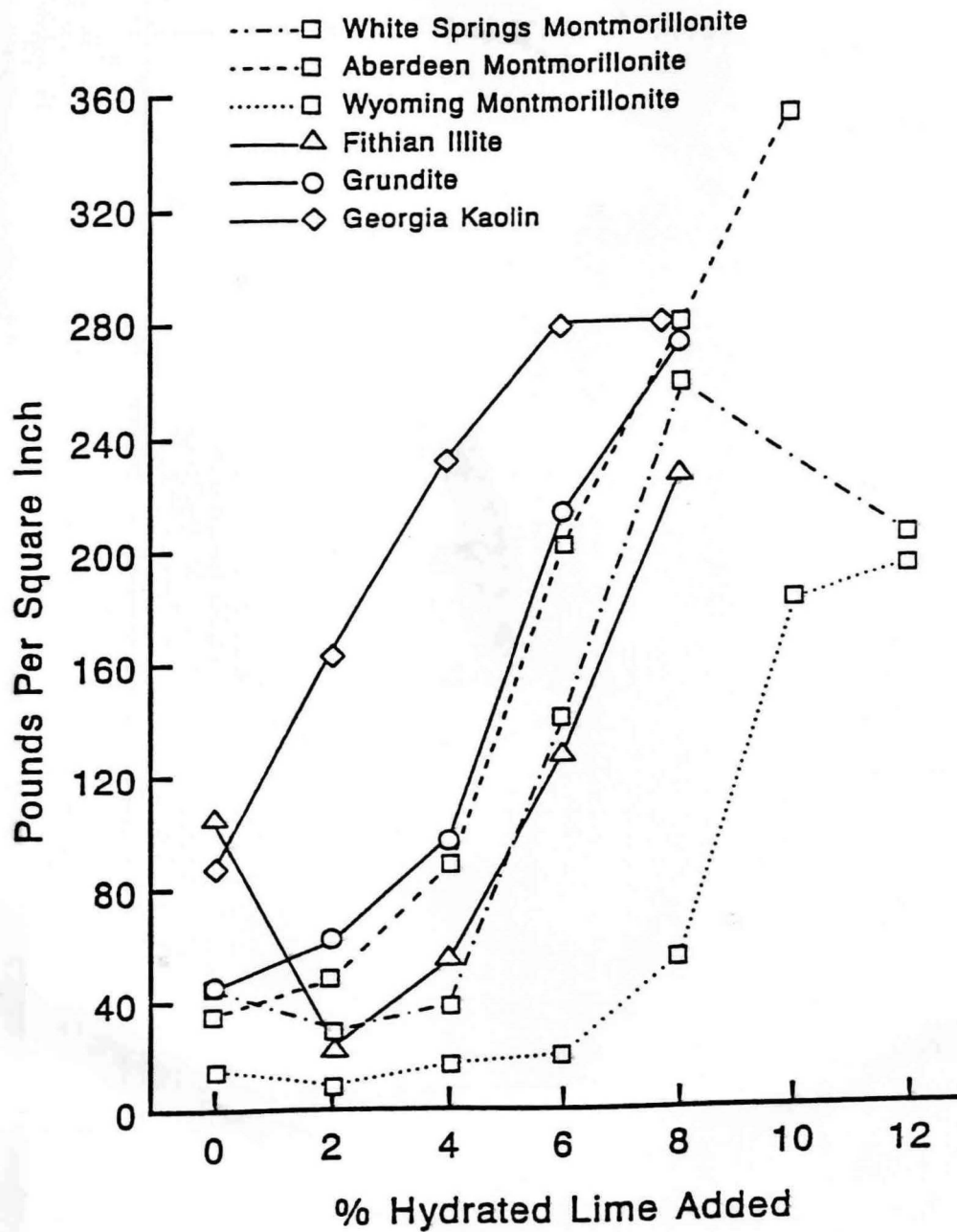


Figure 1. The quantity of lime required to produce pozzolanic reaction is influenced by the mineralogy of the soil being stabilized (Eades and Grim, 1960).
(1 psi = 6, 894 Pa)

Typical values of resilient moduli measured in situ for various Texas soils are summarized in Table 2. From this table the following conclusions may be drawn:

1. The range of resilient moduli values determined through in situ measurements is quite large from about 175 MPa (25,000 psi) to about 6,511 MPa (930,000 psi). However, in every case the resilient modulus determined represents a significant and substantial improvement over the native, unstabilized subgrade.
2. The average value of the in situ moduli are from four to twenty times the in situ moduli of the natural, unstabilized soil.
3. Lime stabilized subgrades produce moduli which are high enough to add structurally to the flexible pavement system, and this structural benefit should be considered in pavement design and pavement systems considerations.
4. Most of the LSS layers evaluated had been in-place for over 10 years which is indicative of the durability of the layers and the permanence of the reaction. The TTI research annex LSS layers were tested after 2-years of very wet (much higher than average rainfall) conditions without cover.

Influence of Material Improvements on Pavement Performance

The improved shear strength and improved resilient modulus of lime stabilized subgrades can influence the structural performance of the flexible pavement system in the following ways:

1. The increased shear strength achieved through pozzolanic reaction reduces the potential of the stabilized layer to deform excessively through being overstressed under heavy wheel loads. This is particularly important in clay soils under wet conditions or in clayey soils which have been subjected to cyclic moisture effects such as freeze-thaw and/or wet-dry cycling. Figure 2 illustrates this situation for a Tama B soil from Illinois.
2. The increased stiffness or resilient modulus produced in a lime stabilized subgrade layer produces two additional effects on the pavement system:
 - a. Protection of the natural subgrade under the lime stabilized layer from being overstressed which could lead to pavement roughness and/or deep layer rutting.
 - b. Better support of the overlying layers including the flexible base layer and the hot mix asphalt concrete layer.

Table 2. Resilient moduli of lime stabilized subgrade (LSS's) backcalculated from falling weight deflectometer (FWD) data.

Highway	Pavement Section	In Place Resilient Modulus, MPa (psi)	
		Natural Subgrade	Lime Treated Subgrade
IH40	254-mm (10-in) HMA 381-mm (15-in) ABC 368-mm (14.5-in) LSS Clay Sand	91 (13,000)	644 (92,000)
SH105	51-mm (2-in) HMA 244-mm (9.6-in) ABC 165-mm (6.5-in) LSS Clay Sand	133 (19,000)	820 (260,000)
US77	190-mm (7.5-in) HMA 305-mm (12-in) ABC 152-mm (6-in) LSS Silt	84 (12,000)	3,010 (430,000)
SH19	279-mm (11-in) HMA 152-mm (6-in) ABC 203-mm (8-in) LSS Sandy Clay	105 (15,000)	1,120 (160,000)
SH23	76-mm (3-in) HMA 279-mm (18-in) ABC 203-mm (8-in) LSS Clay Sand	126 (18,000)	770 (110,000)
SH21	216-mm (8.5-in) HMA 279-mm (11-in) ABC 114-mm (4.5-in) LSS Clay Sand	126 (18,000)	5,600 (800,000)
IH37	178-mm (7-in) HMA 254-mm (10-in) ABC 152-mm (6-in) LSS Sandy Clay	175 (25,000)	6,510 (930,000)

Highway	Pavement Section	In Place Resilient Modulus, MPa (psi)	
		Natural Subgrade	Lime Treated Subgrade
SH19	51-mm (2-in) HMAC 279-mm (11-in) ABC 229-mm (9-in) LSS Sandy Clay	175 (25,000)	2,100 (300,000)
US83	254-mm (10-in) HMAC 265-mm (10.5-in) Soil- Aggregate 140-mm (5.5-in) LSS Clay	97 (13,000)	1,995 (285,000)
US77	51-mm (2-in) HMAC 279-mm (11-in) ABC 178-mm (7-in) LT-Sand Sand	105 (15,000)	98 (14,000)
US59	51-mm (2-in) HMAC 203-mm (8-in) ABC 229-mm (9-in) LS Clay Sand	70 (10,000)	245 (35,000)
IH37	254-mm (10-in) HMAC 432-mm (17-in) Soil- Aggregate 152-mm (6-in) LSS Sandy Clay	182 (26,000)	931 (133,000)
TTI Research Annex	152-mm (6-in) LSS (before traffic) 304-mm (12-in) LSS (before traffic) 304-mm (12-in) LSS (after traffic)	7-28 (1,000-4,000) 7-28 (1,000-4,000) 7-28 (1,000-4,000)	237-546 (34,000-78,000) 175-490 (25,000-70,000) 238-280 (34,000-40,000)
Houston, Texas City Streets	152-mm (6-in) (approx. 6 locations)	21 - 52.5 (3,000-7,5000)	140-490 (20,000-70,000)

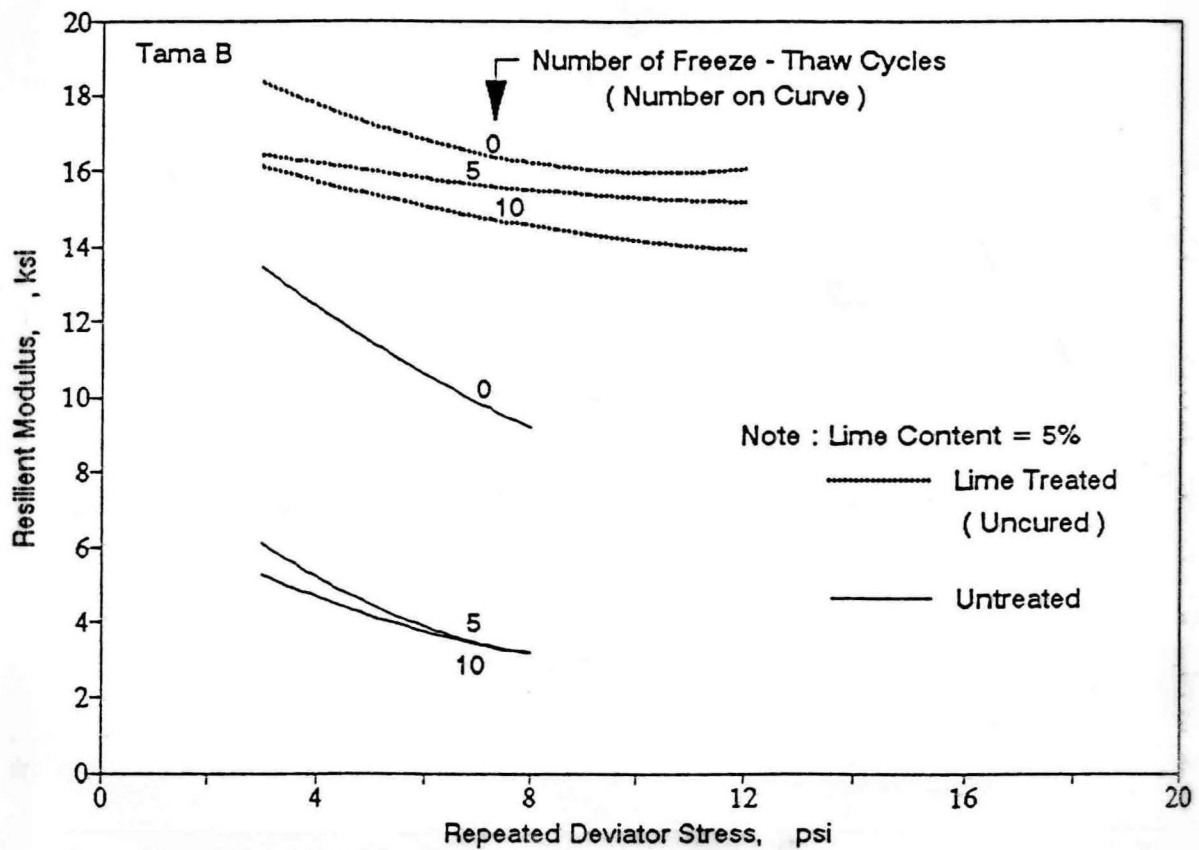


Figure 2. The resilient modulus of the tama B soil are significantly influenced by lime stabilization even after 10 freeze-thaw cycles (Thompson, 1985). (1 psi = 6,894 Pa)

Superior support of the granular, flexible base course layers results in improved performance of these layers. It has long been accepted that the resilient modulus response of aggregate base courses is stress and moisture dependent. This stress dependency of resilient modulus, M_R , is defined by the general law:

$$M_R = K\Theta^n$$

where K and n are regression constants and Θ is the bulk stress invariant, defined as the sum of the principal stresses.

The 1986 AASHTO pavement design guide (AASHTO, 1986) illustrates that the supporting power of the subgrade substantially affects the average value of Θ within the flexible base, and hence, substantially influences the value of the resilient modulus of the flexible base. Tables 3 and 4, taken directly from the 1986 design guide, illustrate this effect. Little (1994) used finite element elastic analysis to evaluate the effects of lime stabilization in enhancing the resilient modulus of the flexible base. Little's study demonstrated the effect of lime stabilization on resilient modulus on the Tama B soil, shown in Figure 2 after 10 freeze-thaw cycles. The pavement section considered consisted of 89-mm (3.5-in) of hot mix asphalt concrete, 305-mm (12-in) of flexible base and Tama B subgrade subjected to 10 freeze/thaw cycles. Verification of the effect of the support of lime stabilized soft clay subgrade of flexible base moduli and performance is an important part of this study. Two cases were evaluated. In Case A, the unstabilized Tama B subgrade was evaluated. In Case B, the identical pavement structure was evaluated except that the top 203-mm (8-inches) of the Tama B subgrade was stabilized with lime. Under a 80-KN (18-kip) single axle load, the resilient modulus of the flexible base increased from 140 MPa to 196 MPa (20,000 psi to 28,000 psi) due to the superior support of the lime stabilized layer.

Since, according to the 1986 AASHTO design guide the structural layer coefficient, a_2 , is a function of the resilient modulus as:

$$a_2 = 0.249 \log M_R - 0.977$$

the increase in M_R of the flexible base in this example results in an increase in a_2 from 0.09 to 0.14 for the flexible base layer. This increase in the structural layer coefficient results in approximately a 100 percent increase in performance life, according to the 1986 AASHTO design equation.

Little (1990) demonstrated that the level of shear stresses induced in hot mix asphalt concrete surfaces is substantially reduced when the modulus ratio between the hot mix surface and the flexible base is reduced. Little (1990) used the octahedral shear stress ratio as the factor associated with rutting or distortion potential in the hot mix surface. This ratio of induced shear stress within the surface layer and shear strength of the surface hot mix layer is indeed an indicator of distortion or rutting potential within the layer. Little (1986) demonstrated that as this ratio approaches 0.70, rutting potential becomes high.

Table 3. Average values of bulk stress, Θ , within the flexible base (aggregate base) layer as a function of hot mix asphalt concrete thickness and subgrade support (AASHTO Guide, 1986).

Asphalt Concrete Thickness, mm (inches)	Roadbed Soil Resilient Modulus, KPa (psi)		
	21,000 (3,000)	52,500 (7,500)	105,000 (15,000)
Less than 5 (2)	140 (20)	175 (25)	210 (30)
51-102 (2-4)	70 (10)	105 (15)	140 (20)
102-152 (4-6)	35 (5)	70 (10)	105 (15)
Greater than 152 (6)	35 (5)	35 (5)	35 (5)

Table 4. Typical variation in the resilient modulus in MPa (psi) of flexible base (aggregate base) as a function of moisture condition and stress states (AASHTO Guide, 1986).

Moisture State	Equation	Stress State MPa (psi)			
		$\Theta=35(7)$	$\Theta=70 (7)$	$\Theta=140 (20)$	$\Theta=210 (30)$
Dry	$8000\Theta^{0.6}$	147 (21,012)	223 (31,848)	338 (48,273)	431 (61,569)
Damp	$4000\Theta^{0.6}$	74 (10,506)	111 (15,924)	169 (24,136)	215 (30,784)
Wet	$3200\Theta^{0.6}$	59 (8,404)	89 (12,739)	135 (19,309)	172 (24,627)

Table 5 summarizes moduli of the flexible base layers and the octahedral shear stress ratios developed within the Arizona pavements discussed earlier. Note that the ratio is above the 0.70 value for all of the unstabilized layers (low moduli of the flexible base or high surface to base modulus ratio). On the other hand, the stress ratio for the pavements with lime stabilized bases is much lower, below the 0.70 value in each case, as a result of the lower surface to base modulus ratios due to stabilization of the flexible base with lime. The same effect results when the response modulus of the flexible base is increased through the superior support offered by the stabilized subgrade layer. Verification of the influence of shear stress ratios on hot mix asphalt concrete surface layer performance is another important part of this study.

Table 5. Summary of octahedral stress ratios developed within hot mix asphalt concrete surfaces as a function of the supporting modulus of the flexible base course layers.

Pavement Section Identification	Resilient Modulus of Flexible Base, MPa (psi)	Stress Ratio, OSSR
Section 7 89-mm (3.5-in) HMAC 254-mm (10-in) flex. base	245 (35,000)	0.70
Section 8 (Same as section 7)	97 (13,000)	0.78
Section 9 (Same as section 7)	140 (20,000)	0.75
Section 1 89-mm (3.5-in) HMAC 254-mm (10-in) flex. base (1% lime stabilization)	378 (54,000)	0.65
Section 3 (Same as section 1)	1,568 (224,000)	0.50
Section 6 (Same as section 1)	2,849 (407,000)	0.45

Recommended Structural Performance Algorithms

The primary function of the lime stabilized subgrade or lime stabilized base course layer in a flexible pavement system is to improve the shear strength of the stabilized layer, protect the underlying layers and native subgrade from being overstressed, enhance the response modulus generated by the flexible base layer due to the improved support of the lime stabilized subgrade, and reduce in shear stresses within the hot mix asphalt concrete surface as a result of the better support offered by the lime stabilized subgrade layer and the improved response modulus of the flexible base layer.

The interim recommendations for accounting for the structural effect of the lime stabilized subgrade are as follows:

1. Assign a structural layer coefficient, which can be used in accordance with the AASHTO performance equation to determine pavement serviceability, based on the unconfined compressive strength of the lime stabilized subgrade layer.

Presently, test method TEX-121-E requires that the unconfined compressive strength of lime stabilized material be determined using 152-mm (6-inch) diameter by 203-mm (8-inch) high samples using the Texas Triaxial testing method. The curing method in this test requires 7-days of moist curing followed by 6-hours of drying at 60°C (140°F). This relatively short term curing may not be a satisfactory indication of the strength likely to develop in many lime-soil mixtures as the pozzolanic development in many of these mixtures is considerably slower than in Portland cement stabilized or lime and fly ash stabilized materials. This is illustrated by Alexander (1978) in Figure 3. The long term curing effects required for the Beaumont clay, discussed earlier is a good example of the requirement for long term evaluation of strength gain in some lime-soil mixtures. Further research is required in this area as discussed in Chapter 4.

At this time it seems prudent to assign a structural layer coefficient of 0.09 to 0.11 to lime stabilized layers (according to Figure 4 Thompson 1975) if the unconfined compressive strength of the mixture exceeds 100 psi when tested in accordance with TEX 121-E.

2. Assign a structural layer coefficient to the flexible base layer as a function of its resilient modulus as defined by the 1986 AASHTO pavement design guide. This approach requires additional study and verification.
3. Develop an algorithm which utilizes shear stresses induced in the hot mix surface layer or a shear stress ratio concept to predict rutting potential within the surface layer.
4. In special case pavements where the lime stabilized layer comprises the major structural layer, use the above approach in addition to the Thompson approach (1985), (discussed on pages A-67 through A-81 of the literature review section of this report), to insure that flexural, load-induced fatigue is not a problem.

In this special case the lime stabilized layer must be stabilized and not modified. The pavement section is essentially a two layered system with the two layers consisting of a native subgrade and a composite structural layer of lime stabilized subgrade and a thin asphaltic surface treatment the composite layer function, with a "slab-effect." The basic steps in this approach are to determine the compressive strength of the lime stabilized layer, determine or approximate the resilient modulus of the native soil, approximate the maximum induced flexural tensile stress within the lime stabilized layer by means of the regression equation discussed in Appendix A and evaluate the fatigue damage potential within the stabilized layer according to the stress ratio concept outlined in pages A-58 through A-67.

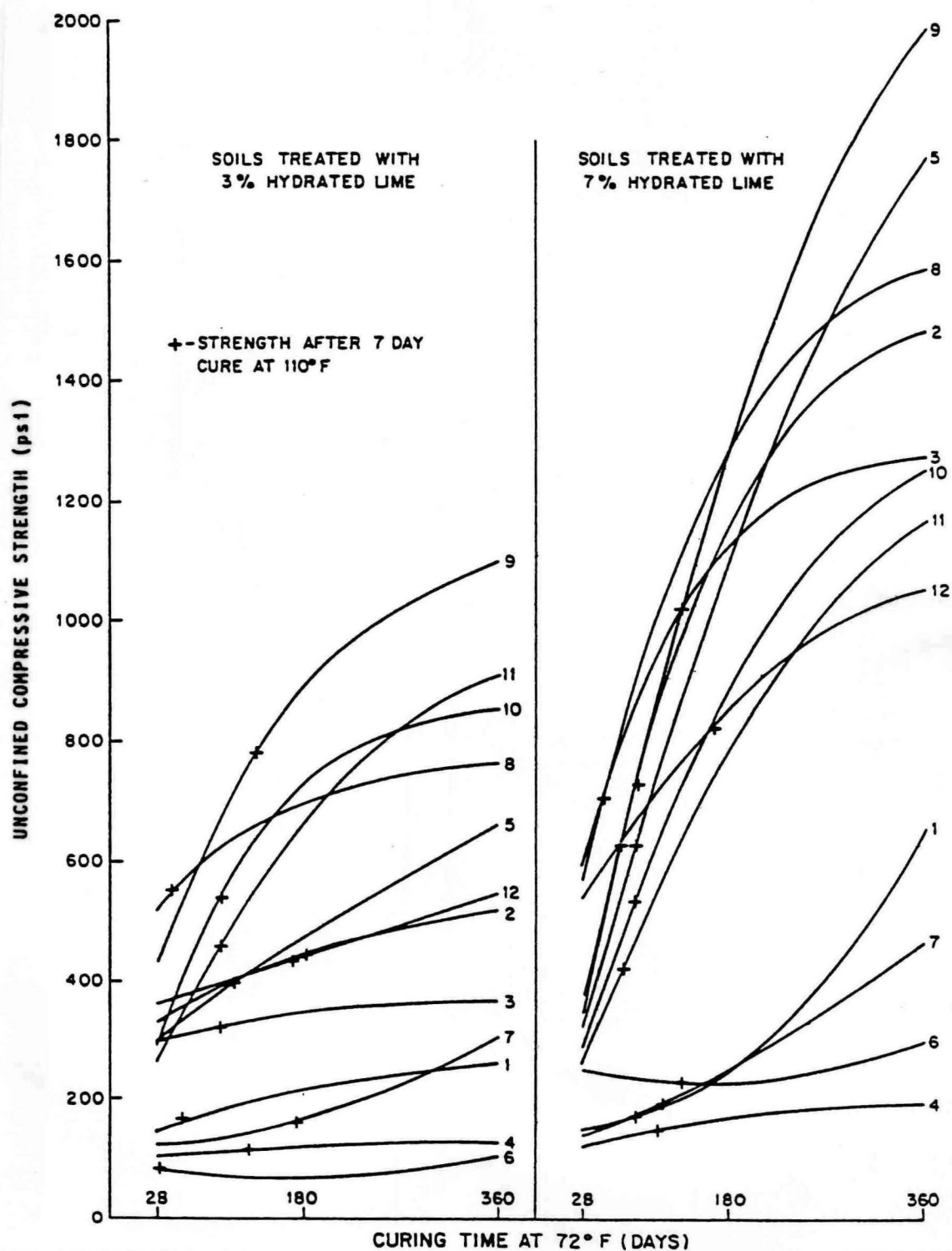


Figure 3. Comparison of strength after 7 days at 43°C (110°F) with strength increases at 22°C (72°F) (Alexander, 1978). (1 psi = 6,894 Pa)

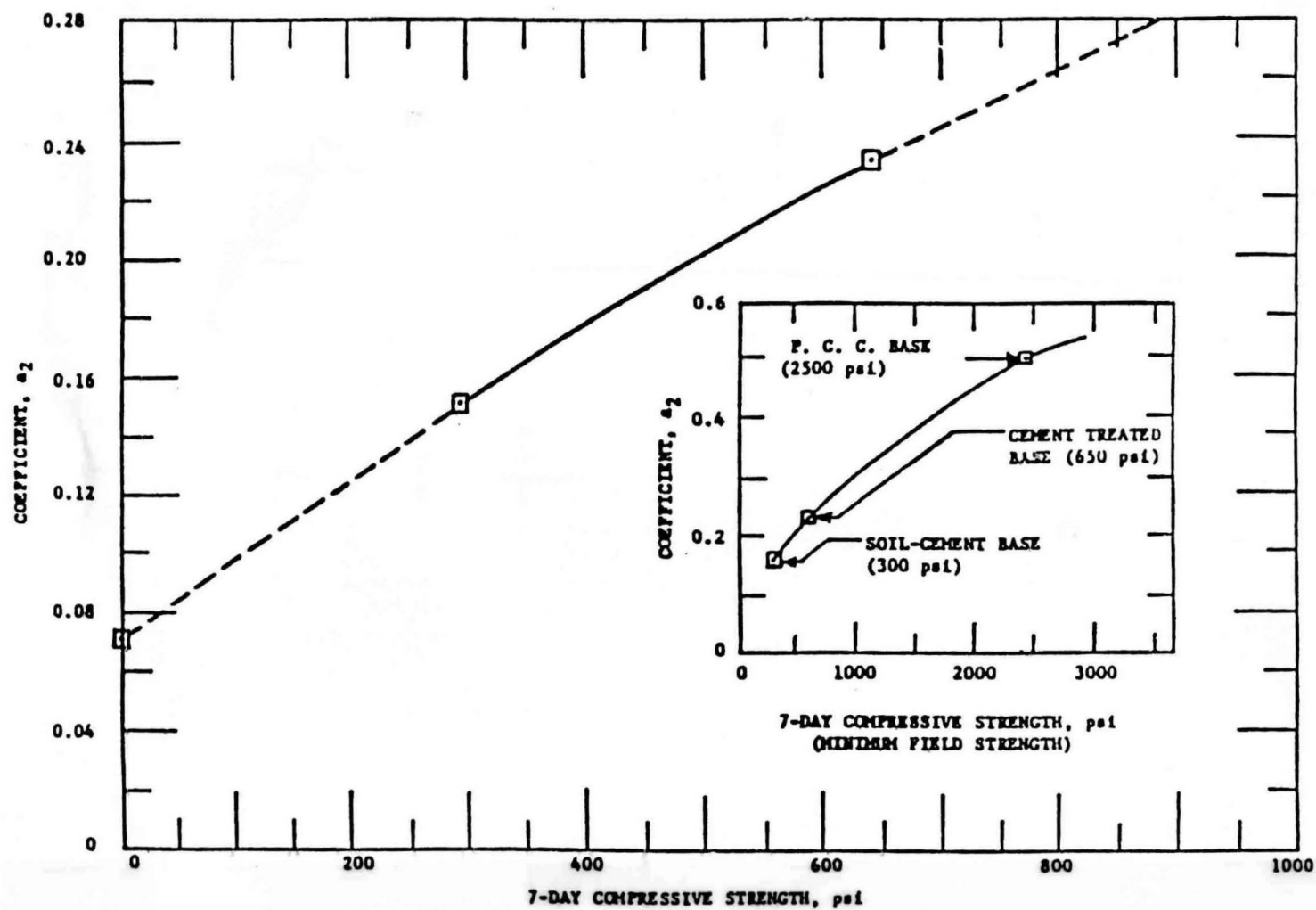


Figure 4. Structural layer coefficient, a_2 , as determined by Thompson, as a function of compressive strength for lime stabilized layers. (Thompson, 1970). (1 psi = 6,894 Pa)

CHARACTERIZATION AND PERFORMANCE EVALUATION OF PORTLAND CEMENT STABILIZED SUBGRADES

Basic Reactions and Mechanisms of Stabilization

The basic reactions between portland cement and soil are the following: (1) cation exchange, (2) flocculation and agglomeration, (3) pozzolanic reaction between the available calcium in the Portland cement and the soil, (4) cementitious reaction and (5) carbonation.

The reactions of cation exchange, flocculation and agglomeration, pozzolanic reaction and carbonation are the same reactions that occur during lime stabilization. These reactions are initiated and driven by the presence of available lime and available calcium. Although a chemical oxide analysis will indicate that Portland cement is predominately calcium oxide (about 63 percent by weight), the great majority of the CaO is combined with aluminates and silicates and is not available for reaction with the soil. In the hydration process, the availability of the CaO increases markedly, but the practical aspects of a short mixing time may limit to some extent the potential for cation exchange, flocculation and agglomeration and pozzolanic reaction in highly plastic soils.

Lime is generally used with more plastic soils because of the availability of large amounts of free calcium to trigger cation exchange and flocculation and agglomeration. These reactions result in plasticity reduction and a reduction in swell potential. The key to the success of lime in ameliorating the physical properties of plastic soils is not only the large quantities of available calcium but also the slow pozzolanic reaction time between lime and soil. This slow "strength-developing" reaction allows a long period of mixing during which the plastic soil can be broken down and mixed intimately with the lime. This mixing period can extend up to several days, including several mixing periods and intermediate mellowing periods, without detrimental effects on the final product.

Mixing with Portland cement and compaction must occur within several hours, 4 to 8. Otherwise, the hydration of the cementitious product within the Portland cement will result in a rapid strength gain which will prevent necessary compaction. If this compaction is achieved it will occur at the expense of irreversibly destroying the cementitious product. Therefore, although Portland cement can be used to stabilize plastic soils, it must be mixed intimately over a very short time frame, less than 4 to 8 hours.

The main component of Portland cement stabilized soils is the cementitious reaction which can develop considerable compressive strengths within the stabilized soil. This cementitious reaction is due to the hydration of calcium silicate and calcium aluminate to form calcium silicate hydrates and calcium aluminate hydrates.

Material Characteristics Due to Stabilization

It is well known that cement stabilization can be used effectively over a wide range of soil types and classifications. Granular soils at optimum cement contents typically have 7-day unconfined compression strengths of 2.1-4.2 MPa (300-600 psi) and 28-day unconfined compression strengths of 2.8-7 MPa (400-1,000 psi). Highly plastic, fine-grained soils may have 7-day strengths of 100-400 psi and 28-day strengths of from 1.75-4.2 MPa (250-600 psi) (Bulletin 292, Highway Research Board, 1961) if they can be intimately mixed with the stabilizer during the 4 to 8 hour period before compaction is necessary.

Unlike lime stabilized soils, the strength gain in Portland cement stabilized soils is rather rapid with as much as 50 percent of the 28-day compressive strength occurring within the first 7-days. Although strength gain can continue for very long periods of time the great majority of strength gain usually occurs in the first 28-days or so of curing.

The high compressive strengths developed in Portland cement stabilized soils lead to high stiffnesses or resilient moduli of the resulting pavement layers. In many cases the strengths are so high and the stiffnesses so great that the cement stabilized layer must be treated as a structural slab.

Influence of Material Improvements on Pavement Performance

The 1972 AASHTO interim pavement design guide demonstrates the substantial level of structural improvement that a Portland cement stabilized layer can add to the pavement system. Structural layer coefficients for cement treated bases can be considerably higher than the structural layer coefficients for unbound aggregate base courses. However, in order to achieve this considerable level of structural contribution, the 1972 and 1986 AASHTO design guides require that a high 7-day unconfined compressive strength be achieved in order to assure durability.

Recent work by South African and Australian researchers, discussed in Appendix A, provides considerable insight into the mechanism of failure of cement stabilized bases and provides pertinent input to the level of strength required to achieve a certain level of structural contribution. The South African study (Jordaan, 1992) indicates that in situ moduli are considerably less than previously reported and vary considerably with depth. It is imperative that the failure mechanism postulated by the South Africans and the stiffness gradient within the stabilized layer identified by the South Africans be verified in this study. This is discussed in Appendix A.

Although the studies referenced above may cause some reassessment of the design approaches of cement treated bases and subbases, the considerable strength increases achieved in cement stabilized layers and the considerable stiffnesses, often in the range of 7,000 to 14,000 MPa (1,000,000 to 2,000,000 psi), usually requires the designer to treat the layer as rigid slab. This is because the modulus ratio between the stabilized layer and the underlying native subgrade is often very high. This high modulus ratio results in high tensile flexural stresses being induced

in the slab which can result in flexural fatigue cracking and the ultimate deterioration of the structural slab. Several design approaches based on the concept of preventing excessive flexural fatigue cracking within the Portland cement stabilized layer are presented in Chapter 3.

Recommended Structural Performance Algorithms

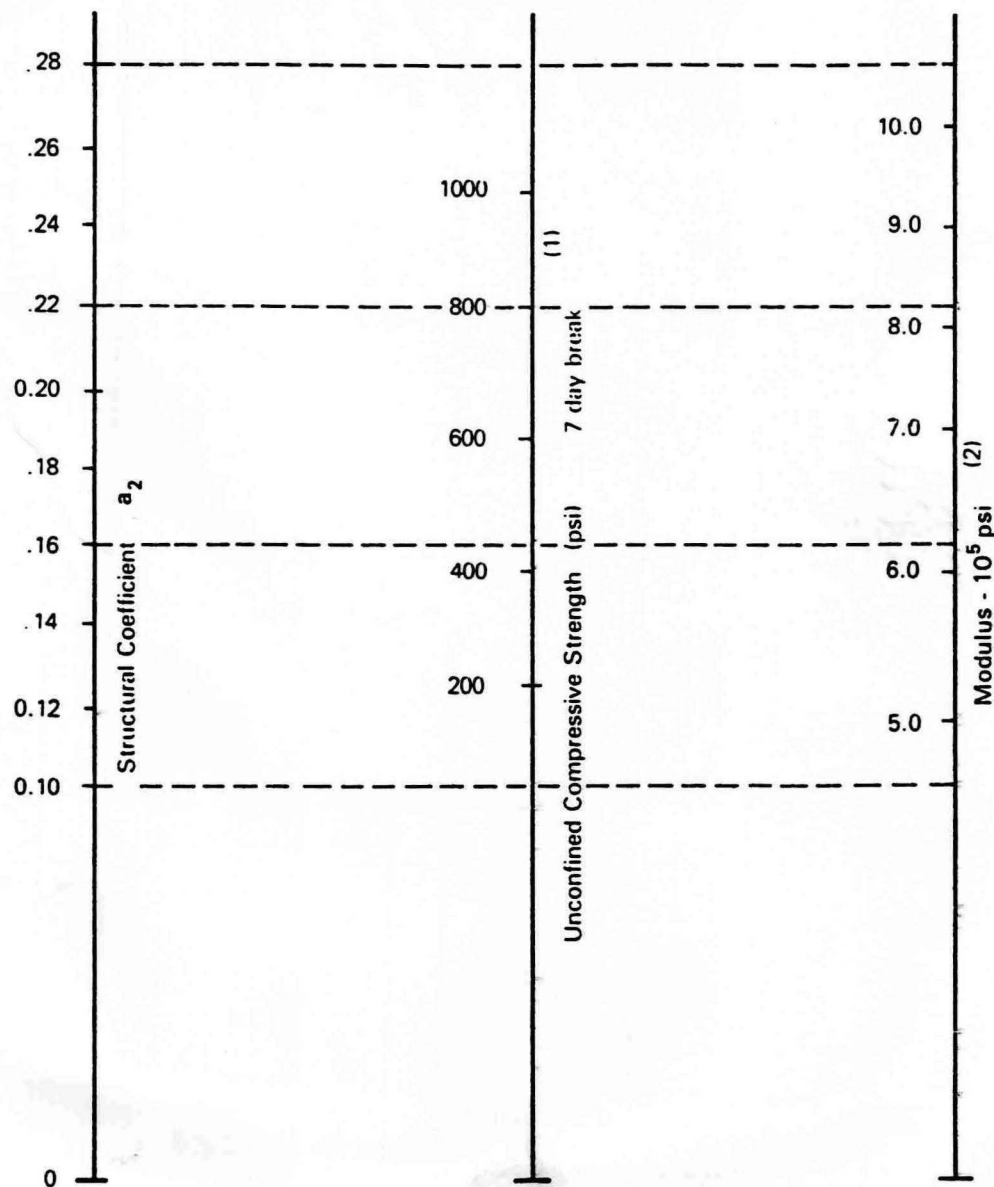
The Griffith model as modified by Raad (1977) offers a rather simple and realistic approach by which to evaluate the response of a Portland cement stabilized layer under loading. The approach evaluates the susceptibility of the stabilized, slab-like layer to develop flexural fatigue based on the principles of crack propagation and fracture mechanics.

The Griffith approach as modified by Raad is attractive in that the only structural property required of the cement treated layer is the unconfined compressive strength. The major and minor principle stresses, σ_1 and σ_3 , respectively, are then determined to identify the stress state and the stress intensity field. Based on the material property of unconfined compressive strength and the stress conditions of major and minor principle stresses, the fatigue life of the Portland cement stabilized layer is determined as discussed in Appendix A, pages A-101 through A-106.

Once the structural integrity of the slab is insured in terms of adequate resistance to flexural fatigue cracking according to the modified (by Raad) Griffith approach, the serviceability of the pavement section can be predicted using the 1986 AASHTO performance design guide by assigning the appropriate structural layer coefficient to the Portland cement stabilized base in accordance with Figure 5.

Raad (1980) demonstrates that Portland cement stabilized layers are bi-modular. This means that the tensile modulus is not equal to the compressive modulus. His research offers a relationship by which to characterize one from the other. It is imperative that when performing the structural analysis for fatigue potential, the appropriate flexural tensile modulus be used. It is important, therefore, in this study to define the relationship between the appropriate modulus to be used in design (based on an approach such as Raad's) and the in situ determined modulus.

It is imperative that research continue in the area of investigation of the mode of failure of Portland cement stabilized bases in both flexible and rigid pavement systems. This vital and continuing research will determine whether the fatigue approach is sufficient or whether it is necessary to investigate different approaches of the evaluation of the structural performance of cement stabilized bases. This critical research is discussed in Chapter 3.



- (1) Scale derived by averaging correlations from Illinois, Louisiana and Texas.
 (2) Scale derived on NCHRP project (3).

Figure 5. Variation in cement-treated bases with base strength parameter (AASHTO, 1986).

CHARACTERIZATION AND PERFORMANCE EVALUATION OF LIME-FLY ASH AND CEMENT-FLY ASH STABILIZED BASES

Basic Reactions and Mechanisms of Stabilization

The basic reactions between fly ash and soil are very similar to those that occur between Portland cement and soil. These reactions include (1) cation exchange, (2) flocculation and agglomeration, (3) pozzolanic reaction, (4) cementitious reaction and (5) carbonation.

As with lime and Portland cement the immediate reactions that influence plasticity reduction and reduction in swell potential, i.e., cation exchange and flocculation and agglomeration, occur due to available lime. Available lime is defined as CaO that is not combined with other compounds and is available or "free" to react with the soil. Of course some fly ashes have little or no CaO (type F) while others (type C ashes), contain an appreciable level of CaO, from 10 to 30 percent by weight. However, the vast majority of this CaO is combined with silicates and aluminates as in the case of Portland cement. The CaO is not available as it is in lime.

Type C fly ashes can be very reactive when moisture is added and a vigorous cementitious reaction can result. However, most ashes require the addition of an activator such as lime or Portland cement to trigger the reaction of the fly ash. These activators react pozzolanically with the silicates and aluminates in the fly ash.

In order to successfully function as a pozzolan, fly ash should meet certain physical and chemical requirements summarized in Table 6.

The chemical requirements of a minimum of 70 percent $\text{SiO}_2 + \text{Al}_2\text{O}_3 + \text{Fe}_2\text{O}_3$ for type F ash and a minimum of 50 percent for type C ash are based on the need for a plentiful supply of silicates and aluminates to develop a significant pozzolanic reaction with the activator.

Material Characteristics Due to Stabilization

Fly ash and lime fly ash stabilized soils develop the same type of improvement as discussed under lime and Portland cement stabilization. These improvements include physical property changes of the soil such as reduction in plasticity and reduction in swell potential. However, the main purpose of fly ash stabilization is to improve the shear strength and the resilient modulus or stiffness of the stabilized soil layer.

Soils suitable for fly ash stabilization include coarse-grained soils and fine-grained soils. However, when plastic clays are encountered, it is often necessary to add additional lime to reduce plasticity prior to fly ash mixing. The ability of the fly ash alone to react with the soil to reduce plasticity is dependent on the amount and reactivity of the CaO contained in the fly ash. Type F fly ashes without CaO could not be considered alone as a stabilizer of plastic or clayey soils.

Table 6. Recommended physical and chemical requirements* for fly ash for use in pozzolanic stabilized mixtures (PSMs) (Flexible Pavement Manual, 1990).

A. Physical Requirements		
	Class of Fly Ash	
	F	C
Fineness - (amount retained on No. 325 sieve prior to dampening)	34% max	34% max
Strength index with Portland cement - (percent of control at 28 days)	75% min	75% min
Strength index with lime - (compressive strength at 7 days)	5.6 MPa 800 psi	--
B. Chemical Requirements		
	Class of Fly Ash	
	F	C
$\text{SiO}_2 + \text{Al}_2\text{O}_3 + \text{Fe}_2\text{O}_3$	70% min	50% min
SO_3	5% max	5% max
Loss on Ignition (LOI)	10% max	6% max

- * The requirements of industry specifications, ASTM C593 ⁽²⁾ and ASTM C 618 ⁽³⁾, have been applied in Table 6 to coal fly ash for PSM base layers for flexible pavement systems; however, sources of fly ash meeting various local standards for physical and chemical characteristics and related uniformity requirements, have been used with highly satisfactory results. The physical and chemical characteristics shown in Table 6 can be determined for a given source of fly ash using standardized test methods which are found in ASTM C 311 ⁽⁸⁾. Fly ash not conforming to the requirements of Table 6 may be proposed for use in a PSM, and such proposals should be supported by laboratory trials and/or field performance data demonstrating the suitability of PSMs containing the non-conforming fly ash.

For a more complete discussion on suitable soils for stabilization with fly ash the reader should consult the "Flexible Pavement Manual," published by the American Coal Ash Association (1991) and Little et al. (1987).

The levels of shear strength and stiffness achieved by fly ash stabilization or stabilization with fly ash plus an activator can be quite considerable and can approach or equal those obtained due to stabilization with Portland cement. Little and Alam (1984) used deflection data to evaluate in situ stiffnesses of fly ash and lime and fly ash stabilized pavement layers in 10 test sites throughout the State of Texas. As expected, the study demonstrated that a wide range of stiffnesses can be encountered depending on the soil being stabilized and the percentages and combinations of each additive used. The study also demonstrated the stiffnesses can be considerably high - well over 7,000 MPa (1,000,000 psi). Little and Alam (1984) determined that in 8 of the 10 sites evaluated, that the use of lime as an activator considerably improved the reactivity of the fly ash as reflected by a higher back-calculated resilient modulus.

Influence of Material Improvements on Pavement Performance

As previously discussed under the sections dealing with lime and Portland cement stabilization, the shear strength enhancing and stiffening effect added to the pavement layer by means of fly ash or fly ash plus activator stabilization can be considerable. In summary, the stabilization of a pavement layer with fly ash or with fly ash plus an activator may influence pavement performance in the following ways:

1. Reduce the potential of the stabilized layer to deform under heavy loads (high shear stresses) by considerably increasing the shear strength of the stabilized layer. This, of course, requires that proper mixture design be used to optimize the shear strength achieved for the soil and fly ash mixture.
2. Protect the layers underlying the fly ash stabilized layer from being overstressed by increasing the stiffness of the layer stabilized with fly ash or with fly ash and activator. The increased stiffness or increased resilient modulus allows the stabilized layer to more efficiently spread the wheel induced loads and, hence, more effectively protect the underlying layers.
3. Provide better support of the surface hot mix asphalt concrete layer and, hence, reduce flexural stresses and shearing stresses within that layer. The net result of this effect is to reduce the potential for rutting, shoving or other forms of surface deformation.

Recommended Structural Performance Algorithms

Pozzolanically stabilized materials (PSM's) are expected to achieve very high stiffnesses with full curing. The American Coal Ash Association (1991) refers to the development of elastic moduli of in excess of 14,000 MPa (2,000,000 psi) with full curing.

With elastic moduli of this level the PSM base behaves as a slab. The American Coal Ash Association (1990) states that plate-load tests have clearly shown that a fully-cured PSM base layer behaves as a slab and that its ultimate load-carrying capacity under a single static load is greater by a significant amount than that predicted by elastic slab theory.

PSM layers have also been shown to exhibit autogenous healing (Little et al., 1987) because of the effect of long-term pozzolanic reactions which may continue for several years if the temperature remains above 4°C (40°F).

Because of the high stiffnesses achieved by PSM layers, it is necessary to consider the slab effect of these layers in pavement design and pavement performance prediction. Also because of the stiffness of the PSM layer and the slab effect, faulting of transverse pavement cracks may occur under extremely heavy traffic volumes. Sawed and sealed joints tend to moderate the faulting phenomenon (American Coal Ash Association, 1991).

The American Coal Ash Association (1990) recommends that the thickness of a PSM base layer for a flexible pavement system can be determined by one of three methods:

1. Method A - AASHTO flexible pavement design procedures, using structural layer coefficients,
2. Method B - Mechanistic pavement design procedures, using resilient modulus values for the pavement layers, and
3. Method C - A combination of Method A and Method B, using mechanistic design concepts for determining pavement layer coefficients.

The basic philosophy of these three design approaches are discussed in the following paragraphs. The detailed design approaches can be found on pages 23 through 41 of the American Coal Ash Association's Flexible Pavement Manual (1991).

In Method A, the AASHTO performance equation is used to predict pavement serviceability. The widely used and well established AASHTO performance equation as set forth in the 1986 design guide uses the structural number to account for the structural contribution of the pavement layers. The structural number is defined as:

$$SN = a_1 D_1 + a_2 D_2 m_2 + a_3 D_3 m_3$$

where D represents the layer thicknesses, a_i represents the structural layer coefficients of the various layers and m_i represents the drainage coefficients for the base and subbase layers. For a PSM base the drainage coefficient is 1.0.

According to the Flexible Pavement Manual (1991), the main factors influencing the variation in the structural layer coefficient are the unconfined compressive strength and the elastic modulus of the layer. The field design strength, determined after 56 days of moist curing at 22°C (73°F) (or other curing conditions required by individual agencies), is the compressive strength value used to determine the structural layer coefficient for PMS's.

According to the AASHTO design guide, a relationship exists between the modulus of elasticity (E_{psm}), the field design compressive strength (CS) and the structural layer coefficient. The relationship between E_{psm} and CS can be defined as:

$$E_{psm} = 500 + CS$$

where E_{psm} is in ksi and CS is in psi. The normal range of a_2 in the AASHTO design guide for PSM layers is from 0.20 to 0.28 with the 0.20 value being assigned to mixtures with a minimum compressive strength of 2.8 MPa (400 psi).

In the mechanistic design approach (Method B) the required thickness of the PSM is based on the potential of the mixture to fatigue or fatigue consumption. Fatigue consumption is related to the number of load applications and the stress ratio, SR, which is calculated for the PSM layer as:

$$SR = (\text{PSM Design Flexural Stress})/(\text{PSM Flexural Strength}).$$

Figure 6 shows permissible SR values for various design reliabilities and traffic conditions (in terms of equivalent 80 KN (18,000 pound) axle loads, ESAL's).

For a given wheel load, PSM strength and pavement thickness are the primary factors that control the PSM design flexural stress. The pavement thickness factor is quantified by the equivalent thickness, T_{EQ} , which is defined as:

$$T_{EQ} = 0.5 T_{AC} + T_{PSM}$$

where T_{EQ} is the asphalt wearing course thickness in inches and T_{PSM} is the thickness of the PSM base layer in inches.

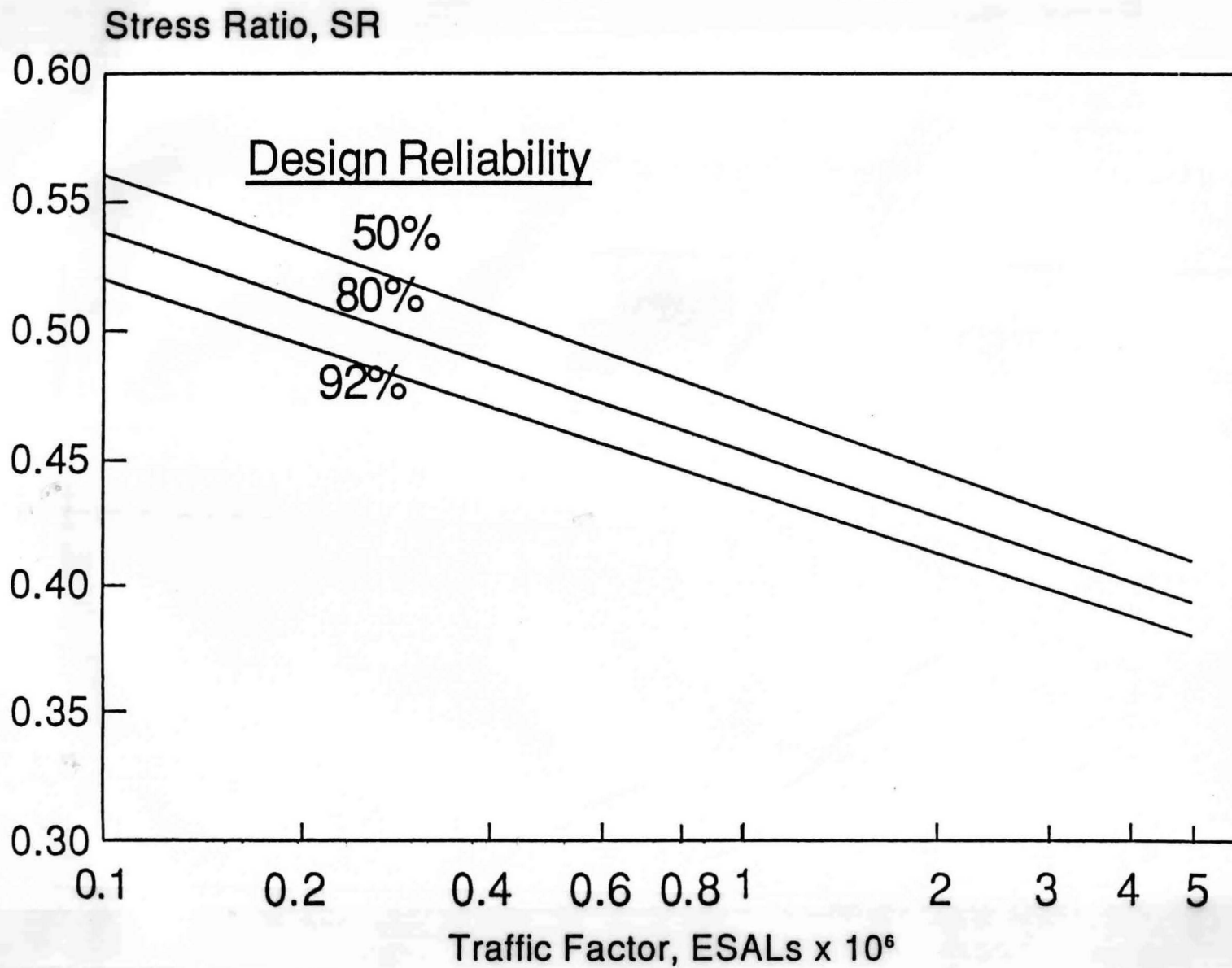


Figure 6. Typical relationship of stress ratio to traffic conditions (ESALs - 80 KN (18 kip) equivalent single axle loads) (Flexible Pavement Manual, 1991).

The Flexible Pavement Manual (1991) uses the relationship graphically presented in Figure 7 to determine the required T_{EQ} for routine pavement design. The use of this Figure 7 requires values for the design SR and the "field design compressive strength" (CS). The maximum design SR that should be used is 0.65. The compressive strength which should be used is the compressive strength (CS) for curing conditions of 56 days at 23°C (73°F) and 100 percent relative humidity.

Recommended minimum asphalt concrete surface layer thicknesses are presented in Table 5 of the Flexible Pavement Manual, and the minimum PSM layer thickness is recommended to be 6-inches.

The AASHTO thickness design of flexible pavements using mechanistic concepts is the third method (Method C) presented in the Flexible Pavement Manual (1991).

In this method the required structural number (SN) is determined as in the normal AASHTO method. However, in this procedure the structural layer coefficient of the PSM base layer relates not only to the unconfined compressive strength of the layer but also to the base-layer thickness as illustrated in Table 7.

For more details on Methods A, B or C, the Flexible Pavement Manual (1991) should be consulted.

CONCLUSIONS

The literature provides the type of information necessary to formulate a design strategy for pavements including stabilized layers. Two basic approaches are available for design and selection of appropriate pavement sections incorporating stabilized layers: (1) thickness design based on minimum strength or engineering properties of the various layers or based on a mechanistic analysis of the pavement system under realistic conditions of climate and traffic and with realistic engineering properties of the various layers and (2) selection of the appropriate engineering properties that a stabilized layer; must possess in order to function successfully in a specific environment (specific climate, traffic condition and structural cross section).

Although both of the approaches listed above are addressed in this study, the latter will be the focus of this effort. This study will identify the engineering properties of stabilized pavement layers that are necessary for the pavement to function properly. The approach will be to identify the traffic, native subgrade, climatic and pavement structural cross-section to be employed and to then recommend the appropriate engineering properties of the stabilized layers necessary for the stabilized layer to function within the specific pavement system identified.

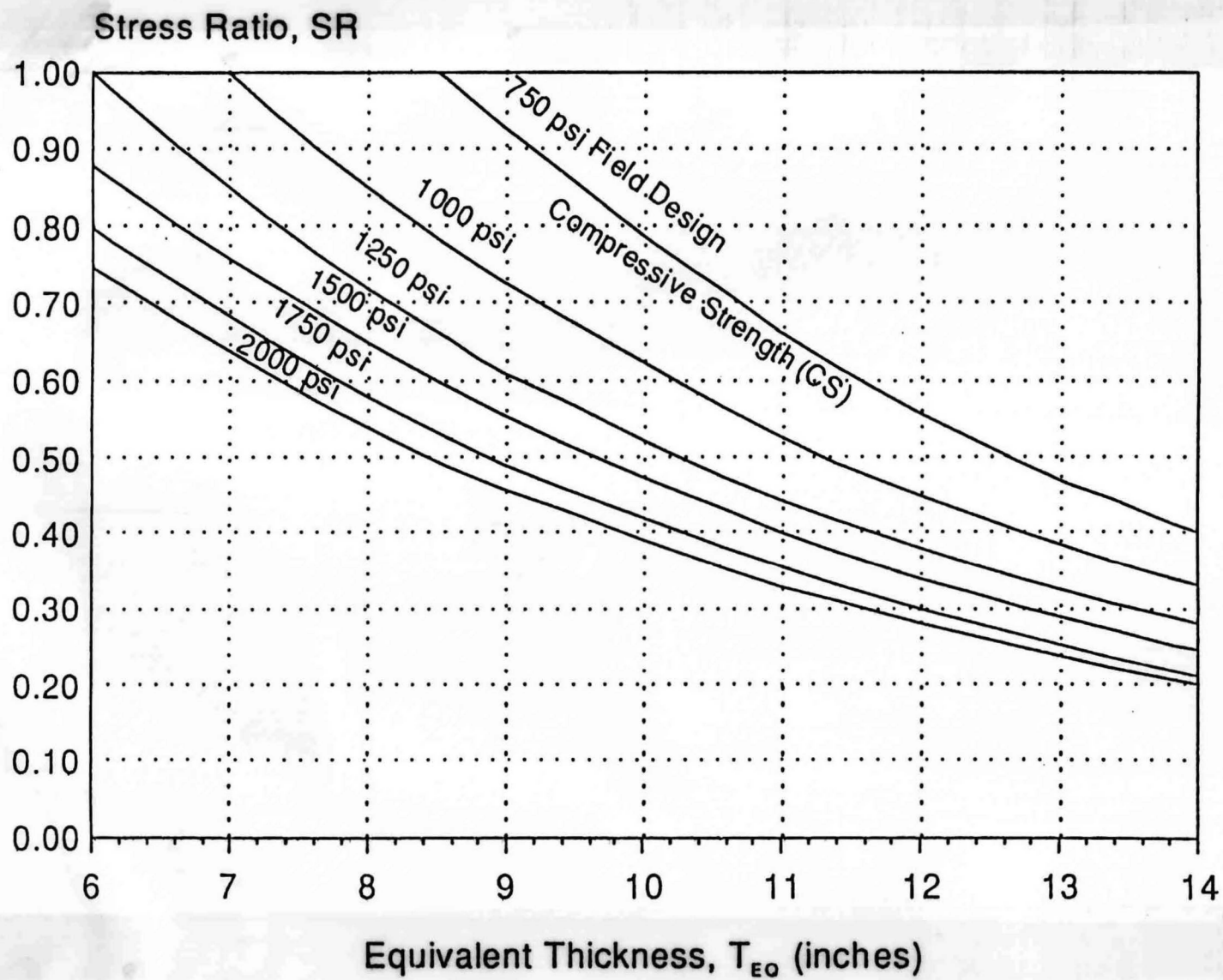


Figure 7. Typical PSM thickness design chart. (1 in = 25.4 mm, 1 psi = 6,894 Pa)

Table 7. Suggested AASHTO structural layer coefficient (a_2) for PSM base layers (After Flexible Pavement Manual, 1991).

Field Design Compressive Strength (CS), MPa (psi)	Coefficient (a_2 for PSM Base Layers)				
	PSM Base Layer Thickness, mm (inches)				
	152 (6)	203 (8)	254 (10)	305 (12)	356 (14)
5.25 (750)	0.20	0.20	0.20	0.30	0.40
7 (1000)	0.20	0.20	0.30	0.40	0.40
8.75 (1250)	0.20	0.26	0.38	0.40	0.40
10.5(1500)	0.20	0.37	0.40	0.40	0.40
14 (2000)	.30	.40	0.40	0.40	0.40

All pertinent modes of distress will be considered: deep layer and surface deformation, fatigue cracking, thermal cracking and reflection cracking. Based on the consideration of these distress conditions the requirements will be developed for the following:

1. Minimum resilient modulus and/or acceptable range of resilient moduli of the stabilized layer.
2. Minimum compressive strength and/or acceptable range of compressive strength of the stabilized layer.
3. Minimum compressive strength of the stabilized layer to provide acceptable durability or resistance to moisture-induced damage.

It may also be appropriate to measure and specify tensile and compressive strength requirements.

CHAPTER 3

WORK NECESSARY TO VERIFY, UPGRADE AND/OR REPLACE CURRENT PERFORMANCE ALGORITHMS

LIME STABILIZED SUBGRADES

Structural Role of Lime Stabilized Subgrades

As discussed in Chapter 2, the contribution of lime stabilization of the subgrade to the performance of the flexible pavement system is comprised of 3 components:

1. Reduction of the swell potential of the stabilized layer and concomitant improvement in textural and physical properties of this layer which affect constructability,
2. A significant shear strength increase within the stabilized layer resulting in resistance of the layer to being overstressed, and
3. A significant stiffening of the stabilized layer resulting in
 - a. Protection of the underlying sublayers from being overstressed,
 - b. Better support of the flexible base course which may exist on top of the lime stabilized subgrade, resulting in an improved resilient modulus response of the flexible base due to a more favorable stress condition within the flexible base, and
 - c. Better support of the hot mix asphalt concrete surface resulting in the reduction of flexural tensile stresses, which may lead to fatigue cracking, and shear stresses, which may lead to surface distortion, within the hot mix asphalt concrete surface layer.

Evaluation of the Structural Role of the Lime Stabilized Subgrade

The pavement performance algorithms suggested to model the lime stabilized layers address the roles discussed in the preceding section. Probably the best way to insure that the stresses induced within the lime stabilized subgrade do not result in distortion of the layer is to insure that the compressive diviatoric stress induced within the lime stabilized layer is less than one-half of the unconfined compressive strength of the mixture, or that the compressive strain induced within the lime stabilized layer is less than one-half of the strain at failure in the unconfined compressive strength test (which is normally about 1 percent strain).

Induced strains within the lime stabilized layer kept at below one-half of the failure strain and induced deviatoric stresses which are kept below one-half of the unconfined compressive strength of the mixture remain, essentially, in the elastic region and do not result in permanent deformation. At values above these levels, strain softening of the mixture or pavement layer begins to occur. Thus a simple algorithm and either a layered elastic or finite element structural model could easily evaluate the potential of shear deformation based on this concept. This check should be made within the lime stabilized layer to evaluate distortion potential and within the underlying natural subgrade where a compressive strength and/or strain at failure could be assigned to the natural subgrade layer depending on soil classification.

In order to evaluate the applicability of this concept, we plan to extract cores from lime stabilized layers where possible and to fabricate lime stabilized samples from the natural soil at several test sights. These samples will be tested for unconfined compressive strength according to method TEX 121-E. This testing will be performed at established locations in Districts 2, 11, 14, 17 and 19.

The level of the modulus of the lime stabilized layer is perhaps the most important component of the stabilized layer to the pavement system. The level of modulus developed in lime stabilized soils typically represents five to twenty-fold increase over the modulus of the native soil. In some cases it is lower, and in some cases it is substantially higher. Nevertheless, the modulus developed in the lime stabilized layer is generally substantially less than that produced in Portland cement stabilized sands. In most cases the lime stabilized subgrade is probably not stiff enough to be concerned about designing for the "slab effect."

Since the ability of the lime stabilized layer to protect underlying layers and to support overlying layers is so heavily tied to the in situ modulus of the layer, it is imperative that field studies identify the in situ moduli of these layers. In this investigation the effects of seasonal variation, soil type and mineralogy and pavement structure must also be considered. These studies will be performed in Districts 2, 11, 14, 17 and 19.

One of the most important studies in 1287 will be in situ verification that higher stiffness subgrades provide a superior resilient modulus response for flexible bases. In order to study this question, pavement sections have been and are being identified in which aggregate bases or flexible bases exist over both stabilized and unstabilized, or control, subgrades. The primary focus of this research will be in pavement test sites identified in Districts 14 and 17. In addition, existing pavement test sections at the TTI Research Annex will be used to evaluate this question. These test sections include pavements with limestone bases over native subgrade and over lime stabilized subgrades. These test sections also contain stabilized flexible bases layers (with both Portland cement and lime).

LIME STABILIZED BASES

Lime stabilized bases consist of base courses which use lime to upgrade properties of the base through pozzolanic reaction between the lime and the clay soil fraction or due to the development of and enhancement of carbonation as in limestone bases stabilized with low percentages of lime. Addition of the stabilizer has two important effects: improvement of the shear strength of the base layer and stiffening of the base or enhancement of the resilient modulus.

The measure of the performance of lime stabilized bases in a pavement system is most closely tied to the resilient modulus of the base layer. Since the structural layer coefficient of a flexible base is tied directly to the resilient modulus of the flexible base, it is logical that the structural coefficient of a lime stabilized base would be also. This is especially true since lime treatment of most bases does not stiffen the base to the point in which the layer acts as a rigid slab.

The resilient modulus of the stabilized base is the key to performance prediction. Therefore, the value of in situ stiffness of these layers must be determined with proper consideration given to the following variables: seasonal effects, layer thickness effects, base type and mineralogy and age of the base layer and traffic effects on the base layer.

Particular attention will be placed on studies of limestone bases stabilized with low percentages of lime in Districts 13, 16 and 17. This study will evaluate the mechanism of stabilization and the level of stiffness and compressive strength that can be achieved in these layers through carbonation and pozzolanic reactions.

PORTLAND CEMENT STABILIZED BASES AND SUBGRADES

Since Portland cement stabilized bases and subgrades often develop very high resilient moduli, the slab effect of these layers must be evaluated. Consequently, most design and analysis philosophies call for a flexural fatigue analysis of the stabilized layer. This is discussed in some detail in Chapter 2 and Appendix A.

Recent studies by the South Africans and Australians (Jordaan (1992) and Caltabiano and Rawlings (1992)) indicate that cement stabilized bases may fail in a different mode than flexural fatigue, and that the modulus of the stabilized layers varies considerably with depth and is not nearly as high as generally considered in pavement design approaches.

Work in this study, especially in District 12, will concentrate heavily on defining the mode of failure of stabilized subgrades and stabilized bases and in the determination of the composite moduli of the pavement layer and as a function of depth. The evaluation of the change in moduli with depth will be determined using multi-depth deflectometers.

FLY ASH STABILIZED BASES AND SUBGRADES

The same general approach will be taken to evaluate the performance of in situ fly ash stabilized bases as for Portland cement stabilized bases. It is logical that the failure mechanism of fly ash stabilized bases and subgrades should be similar to Portland cement stabilized bases. This is because the fly ash stabilized bases and subgrades tend to develop high strengths and slab action in a similar manner to the Portland cement stabilized bases.

Field evaluations of the mode of failure and of in situ values of lime and fly ash stabilized subgrades and bases have been planned in District 11 and District 4.

SUMMARY OF DELIVERABLES

This study will provide the following deliverables:

Lime-Stabilized Subgrades

1. Appropriate range of resilient moduli and/or confined compressive strengths for acceptable performance in specific pavement sections (i.e., specific structural cross sections, design traffic levels, climatic regions and native subgrade characteristics).
2. Risk assessment based on deviations from the recommended ranges and/or minimums of resilient modulus or compressive strength.
3. Recommended mixture design approach to help insure durability and permanency of reaction.

Lime-Stabilized Marginal Aggregates and Flexible Bases

The same items as provided for lime-stabilized subgrades (1 through 3) will be provided for lime stabilized bases and marginal aggregates. Typical improvements in lime stabilized flexible bases and non-stabilized flexible bases will be discussed based on the improvement in resilient modulus.

Portland Cement and Fly Ash Stabilized Bases

The same items as provided for the lime-stabilized layers will be provided for Portland cement and fly ash stabilized layers. However, in addition to recommendations for appropriate ranges in engineering properties, i.e., compressive strength and resilient modulus, the structural slab action of the stabilized layers will be evaluated for susceptibility to deterioration based on flexural fatigue and to deterioration through other mechanisms.

REFERENCES

Ahlberg, H. L., and McVinnie, William W., "Fatigue Behavior of Lime-Fly Ash-Aggregate Mixtures," Highway Research Bulletin 335, 1962, pp 1-10.

Alexander, M. L., and Doty, R. N., "Determination of Strength **Equivalency** Factors for the Design of Lime-Stabilized Roadways", Final Report, Office of Transportation Laboratory, California Department of Transportation, 1978.

Alexander, M. L., "Determination of Strength Equivalency Factors for Design of Lime-Stabilized Roadways," Report No. FHWA-CA-TL-78-37, December, 1978.

Amerigaznon, M. and Little, D. N., "Permanent Deformation Potential in Asphalt Concrete Overlays Over PCC Pavements," Research Report No. 452-3F, Texas Transportation Institute, 1988.

Barenberg, E. J. and Thompson, M. R., " Design, Construction, and Performance of Lime, Fly Ash, and Slag Pavement," Transportation Research Record 839, 1982.

Bendana, J., "Equivalent Wheel Load Factors for Airfield Pavement on Stabilized Base," Ph.D. Dissertation, Texas A&M University, 1988.

Caltabiano, M. A., Rawlings, R. E., "Treatment of Reflection Cracks in Queensland," Proceedings of 7th International Conference on Asphalt Pavements, 1992.

Crockford, W. W. and Little, D. N., "Tensile Fracture and Fatigue of Cement Stabilized Soil," Journal of Geotechnical Engineering, American Society of Civil Engineers, ASCE, Vol 113 No.5: 1987 pp 502-519.

Design Coefficients for Lime-Soil Mixtures, Research Project IHR-28 Report, Illinois Division of Highway, Bureau of Research and Development and U.S. Department of Transportation, Federal Highway Administration, Bureau of Public Roads, 1970, pp 1-20, (NTIS) PB189-910.

Eades, J. L. and Grim, R. E., "A Quick Test to Determine Lime Requirements for Lime Stabilization," Highway Research Record 139, HRB, National Research Council Washington, D.C., 1966, pp 61-72.

Eades, J. L. and Grim, R. E., "Reaction of Hydrated Lime with Pure Clay Minerals in Soil Stabilization," Highway Research Bulletin No. 262, Washington, D.C., 1960, pp 51-63.

Fernando, E. G., and Lytton, R. L., "Demonstration of the Potential Benefits of Performance - Oriented Specifications," Transportation Research Record 1353, Transportation Research Board, Washington, D.C., 1992, pp. 73-81.

Flexible Pavement Manual, American Coal Ash Association, 1991, pp 21-42.

Graves, R. E., Eades, J. L., and Smith, L. L., "Calcium Hydroxide Treatment of Construction Aggregates for Improved Cementation Properties," STP 1135, ASTM, 1992, pp 65-78.

Griffith, A. A., "Theory of Rupture," Proceedings, 1st International Congress for Applied Mechanics, Delft, Netherlands, 1924.

Guide for the Design of Pavement Structures, AASHTO, 1986.

Gutschick, K. S., "Canal Lining Stabilization Proves Successful," Pitt and Quarry, May, 1985.

Jayawickrama and Lytton, "Methodology for Predicting Asphalt Concrete Overlay Life Against Reflection Cracking," Proceedings of 6th International Conference on Structural Design of Asphalt Pavements, Vol 1 The University of Michigan, 1987, pp 912-924.

Jordaan, G. J. "Towards Improved Procedures for the Mechanistic Analysis of Cement Treated Layers in Pavements," Proceedings of 7th International Conference on Asphalt Pavement, 1992, pp 209-223.

Jordaan, G. J., "Towards Improved Procedures for the Mechanistic Analysis of Cement Treated Layers in Pavements," Proceedings of 7th International Conference on Asphalt Pavement, 1992, pp 209-223.

Kelley, C. M., "A Long-Range Durability Study of Lime Stabilized Bases at Military Posts in the Southwest," Bulletin No. 320, National Lime Association, Washington, D. C., 1977.

Kennedy, T. W. and Tahmoressi, M., "Lime and Cement Stabilization," Updates on Lime Applications in Construction, National Lime Association, Issue No. 2, Waco, Texas, 1987.

Kim, Y. S. and Little, D. N., " Prediction of Fracture Fatigue Parameters from Creep Testing of Soils-Cement," Journal of Geotechnical Engineering, ASTM, Vol 10 No.3: 1987, pp 97-104.

Larsen, T. J. and Nussbaum, P. J., "Fatigue of Soil-Cement," Portland Cement Association Research and Development Laboratories, Vol. 9 No. 2, 37-59 May 1967, pp 47.

Larsen, T. J. and Nussbaum, P. J., " Research on Thickness Design for Soil-Cement Pavements," Portland Cement Association, Bulletin D142, 1969, pp 14.

"Lime-Fly Ash-Stabilized Bases And Subbases," NCHRP Synthesis of Highway Practice 37, Transportation Research Board, 1976, pp 10-13

Little, D. N., et al., " Soil Stabilization for Roadways and Airfields" Final Report, Dallas N. Little & Associates, Airforce Engineering and Services Center, 1982, pp 21-72 108-120.

Little, D. N., "Lime Stabilization Handbook," National Lime Association, Kendall-Hunt Publishers, 1994.

Little, D. N., "Comparison of In-Situ Resilient Moduli of Aggregate Base Courses with and without Low Percentages of Lime Stabilization," STP 1135, ASTM, 1992, pp 8-22.

Little, D. N., Terrel, R., Epps, J. A., Thompson, M. R. and Barenberg, E., "Stabilization of Roadways and Airfields," Technical Report ESL-TR-86-19, Air Force Engineering and Services Center, Tyndall AFB, Panama City, Florida, 1987.

Little, D. N., "Basic Reactions of Soil-Lime Mixtures," Bulletin 331, National Lime Association, 1986.

Little, D. N. and Alam, S., "Evaluation of Fly Ash Test Sites Using a Simplified Elastic Theory Model and Field Measurements," Research Report 240-2F, Texas Transportation Institute, March, 1984.

Little, D. N., et al., Soil Stabilization for Roadways and Airfields, Final Report, Dallas N. Little & Associates, Air Force Engineering and Services Center, 1982, pp 21-72, 108-120.

McCallister, L. D., and Petry, T. M., "Property Changes in Lime Treated Expansive Clays Under Continuous Leaching," Technical Report GL-90-17, September, 1990.

McDowell, C., "Flexible Pavement Design Guide," Bulletin 327, National Lime Association, Arlington, Virginia, 1972.

Moore, R. K. , Kennedy, T. W., and Kozuh, J. A., "Tensile Properties for Design of Lime-Treated Materials," Center for Highway Research, University of Texas at Austin. Highway Research Record 351, 1971, pp 78-86.

Nguyen-van-Hue, " The Effect of Repeated Loading on the Strength and Deformation of TaYlor Marl Clay Stabilized with Lime, Thesis, Master of Science in Engineering, The University of Texas at Austin, January 1966.

Nussbaum, P. J. and Larsen, T. J., " Load-Deflection Characteristics of Soil-Cement Pavements," Portland Cement Association, Bulletin D96, 1965, pp 11-12.

Paris, P., and Erdogan, F., "A Critical Analysis of Crack Propagation Laws," Transactions of the ASME, Journal of Basic Engineering, Series D, 85, No. 3, 1963.

Raad, et al., "Fatigue Behavior of Cement-Treatment Materials," Transportation Research Record N641, pp 7-11, 1977.

Raad, L., Figueroa, J. L., "Load Response of Transportation Support Systems," Transportation Engineering Journal, 1980, pp 111-128.

Raad, L., "Behavior of Stabilized Layers Under Repeated Loads," Transportation Research Record 1022, 1985, pp 72-79.

Robnett, Q. L. and Thompson, M. R., "Effect of Lime Treated on the Resilient Behavior of Fine-Grained Soils," Transportation Research Record 560, 1976, pp 11-20.

Schapery, R. A., "Non-Linear Fracture Analysis of Viscoelastic Composite Materials Based on a Generalized J Integral Theory," Proceedings, Japan-USA Conference on Composite Materials, Tokyo, 1981.

Schapery, R. A., "Continuum Aspects of Crack Growth in Time Dependent Materials", Report MM4665-83-2, Mechanics and Materials Center, Texas A&M University, February 1983.

Swanson, T. E. and Thompson, M. R., "Flexural Fatigue Strength of Lime-soil Mixtures," Highway Research Record 198, 1967.

Thompson, M. R. , Figueroa, J. L. , "Mechanistic Thickness Design Procedure for Soil-Lime Layers," Transportation Research Record 754, 1980.

Thompson, M. R., "Soil-Lime Mixtures for Construction of Low Volume Roads," Special Report 160, Transportation Research Board 1975.

Thompson, M. R. , and Robnett, Q. L. , " Resilient Properties of Subgrade Soils", Transportation Engineering Journal 1979, pp 71-89.

Thompson, M. R., "Final Report - Subgrade Stability," Report No. FHWA-IL-UI-169, 1985.

APPENDIX

SURVEY OF PERTINENT LITERATURE

Significant studies have been done on fatigue behavior and reflection cracking of stabilized bases. A brief summary of the literature review is given below:

LIME STABILIZATION

Improvements of Engineering Properties of Stabilized Soils and Aggregates

Unconfined Compression

Unconfined compression strength increases of greater than 700 KPa (100 psi) are achieved with many soils, and some soil-lime mixtures strength continues to increase with time up to 10 years with extended curing. Substantial strength increases indicate that the soil is reactive with lime and can probably be stabilized to produce a structural layer quality material (Little, et al., 1982).

Shear Strength

The major effect of lime on the shear strength of a reactive fine-grained soil is to produce a substantial increase in cohesion. The cohesion of the mixtures is increased compared to natural soils. Cohesion increases with increased mixture compressive strength and is approximately 30 percent of the unconfined compression strength (Little et al., 1982).

California Bearing Ratio (CBR)

Large CBR values of many cured soil-lime mixtures indicate the extensive development of pozzolanic cementing agents. For CBR values greater than 100 the results have little significance. CBR may serve as a general strength indicator if extensive pozzolanic cementing action has not developed due to a lack of curing time or non-reactivity of the treated soil (Little et al., 1982).

Tensile Strength

Split-tensile test strengths show large variations depending on the soil-lime mixture and curing conditions. The ratio of split-tensile strength to unconfined compressive strength of the mixtures is approximately 0.13. The Flexural test strength (modulus of rupture) is approximately 25 percent of the unconfined compressive strength of the cured soil-lime mixture (Little et al. 1982).

Fatigue Strength

Flexural fatigue is an important consideration since for pavement loading conditions, flexural strength of reactive soil-lime mixtures will probably be the limiting factor in applications as subbase and base course structural layers. The fatigue strengths of soil-lime mixtures vary for different mixtures but are approximately 50 - 55 percent of the ultimate mixture flexural strength. The ultimate strength of the soil-lime mixtures is a function of curing period and temperature. Since the magnitude of the flexural stress repetitions applied to the mixture are relatively constant, the ultimate strength of the material increases due to curing, the stress level (as a percent of ultimate flexural strength) will decrease and the fatigue life of the mixture will increase (Little et al. 1982).

Shrinkage

Lime treatment decreases shrinkage potential associated with the loss of moisture from the stabilized soil relative to the problem of shrinkage cracking of the materials and reflective cracking through overlying paving layers. Calculations based on laboratory and field data indicate that for typical field service conditions shrinkage of cured soil-lime mixtures will not be extensive. Hence, reflective cracking through the surface course will not occur frequently (Little et al., 1982).

Design Considerations for Lime Stabilized Bases

Ahlberg and McVinnie (1962) measured the number of cycles to failure for flexural beams composed of 82 percent aggregate, 14 percent fly ash, and 4 percent lime. Figure A-1 illustrates typical results which relate maximum bending stress in the beam, the estimated modulus of rupture, and the number of cycles to failure. In general, it was concluded that the repeated loads caused the mixtures of lime, fly ash, and aggregate to fracture at stress levels considerably below the static strength of the material.

Swanson and Thompson (1967) studied the flexural fatigue of four lime-soil mixtures. Optimum lime contents and moistures were used for all mixtures. Specimens were tested at stress levels ranging from 40 to 95 percent of their ultimate strength. Typical results, shown in Figure A-2, illustrate the random variation of data which is characteristic of fatigue testing of lime-treated materials.

Nguyen (1966) utilized repetitive-loading, unconfined compressive tests to study the behavior of lime-stabilized clay and concluded that the reduction in compressive strength varied with the magnitude of the load applied and the number of applications. The decrease in strength ranged from 1.3 to 18.1 percent of the ultimate static strength of the lime-stabilized Taylor Marl Clay. A small reduction in the magnitude of the applied repeated load greatly increased the number of cycles required to fracture the specimen. The ratios of the split-tensile strength to the unconfined compressive strength averaged 0.145 for specimens subjected to static loading conditions and 0.151 for specimens subjected to 10,000

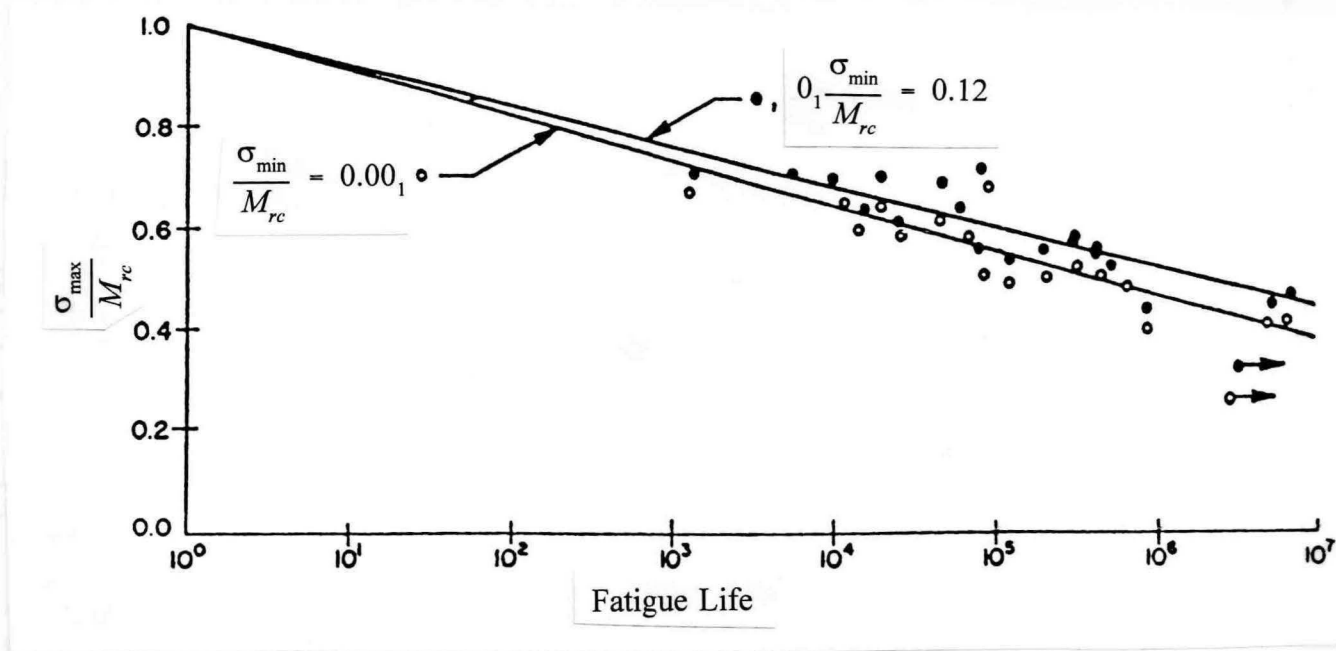


Figure A-1 Relationship between maximum bending stress and logarithm of number of cycles of failure for lime-fly ash treated materials (Ahlberg and McVinnie, 1962).

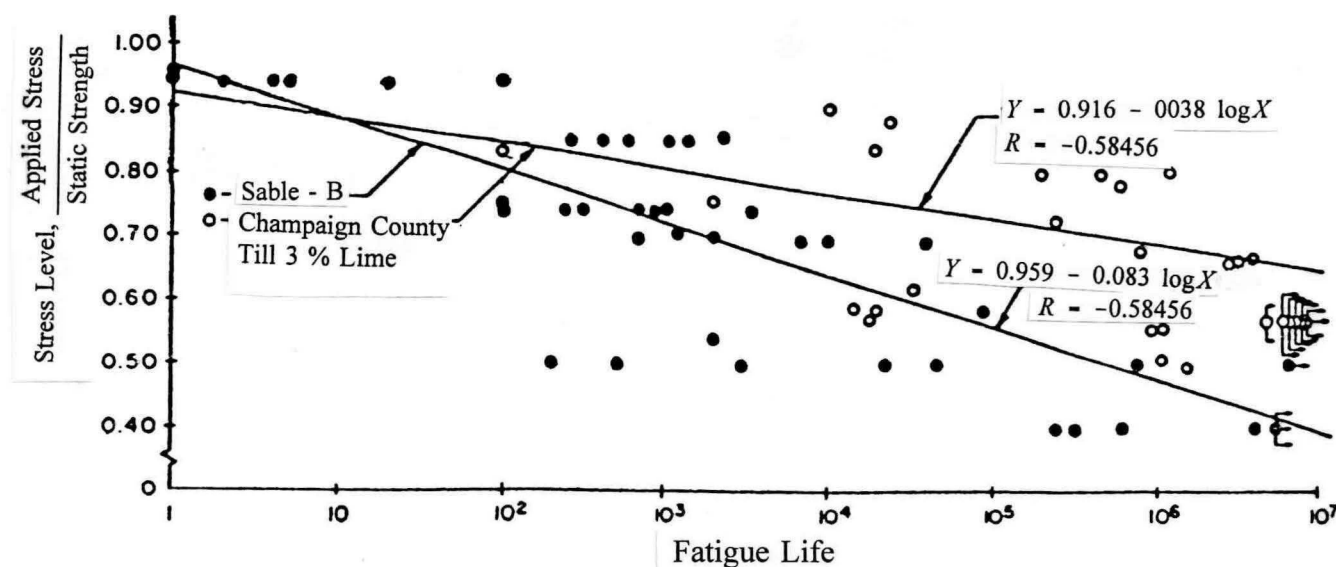


Figure A-2 Typical fatigue results for lime-treated materials (Swanson and Thompson, 1967).

and 20,000 repetitions of an unconfined compressive loading prior to testing.

In Thompson and Figueroa (1980), a mechanistic soil-lime thickness design procedure is presented. The procedure is based on a stress dependent finite element computer model (called ILLI-PAVE). The design procedure is limited to pavements constructed of a cured soil-lime layer and a non-structural (surface treatment or thin asphalt concrete) surface course. Design input data are soil-lime strength and modulus, subgrade resilient modulus, and estimated traffic.

According to Thompson (1975), soil-lime mixtures have high compressive and shear strengths, and the factor controlling layer thickness is the flexural stress at the bottom of the soil-lime layer. The design procedure is based on a limiting stress ratio (S =flexural stress/flexural strength) concept which accounts for mixture fatigue behavior. Soil-lime mixtures were considered by Thompson to be linear-elastic materials that develop significant flexural strengths and flexural moduli of elasticity when cured. A stress dependent resilient modulus behavior model was used to characterize the fine-grained subgrades. Soil-lime layer thicknesses of 15, 23 and 31 cm (6, 9, and 12 inches) were included and a wheel load of 40 KN (9,000 pounds) was used in the design. A uniform tire pressure of 560 KPa (80 psi) distributed over a circular area, was applied in 140 KPa (20 psi) increments. A summary of ILLI-PAVE soil-lime pavement responses is shown in Table A-1. Moduli-thickness-flexural stress relations for stiff, medium, and soft subgrades are shown in Figures A-3, A-4, and A-5, respectively. Although, the above mentioned figures can be used to approximate the flexural stress for various conditions, Thompson and Figueroa (1980) developed an algorithm for estimating soil-lime flexural stress as a function of layer thickness, soil-lime modulus of elasticity, and subgrade resilient modulus:

$$\sigma_r = 23.22 - 4.66t + 42.36 \log E_B - 29.11 \log E_{Ri} \quad (A-1)$$

- σ_r = Flexural stress at the bottom of the soil-lime layer, psi;
- t = Thickness of soil-lime layer, inches;
- E_B = Modulus of Elasticity of the soil-lime layer, ksi; and
- E_{Ri} = Resilient Modulus of the subgrade, ksi.
- R = Correlation coefficient = 0.95.
- S_x = Standard error of estimate = 60.1 KPa (8.3 psi).

A nomograph for solving equation A-1 is presented in Figure A-6.

The shear and compressive strengths of cured soil-lime mixtures are not the limiting factors in their use as structural layers for low volume road construction. Soil-lime layers experience repeated flexural stresses and therefore flexural strength and fatigue response are important considerations. A typical fatigue response relation for Illinois soils, obtained by averaging fatigue test results from Swanson and Thompson (1967), is shown in Figure A-7 and can be expressed as follows:

Table A-1 Data summary of Illi-PAVE soil-lime pavement responses (Thompson and Figueroa, 1980).

Soil-Lime Thickness		Soil-Lime Modulus		Subgrade	Surface Deflection		Soil-Lime Radial Strain	Soil-Lime Radial Stress		Subgrade Vertical Stress	
inches	cm	ksi	MN/m ²		mils	mm	μ strain	psi	kN/m ²	psi	kN/m ²
6	15	25	172	Stiff	31	0.78	993	9.8	68	36.6	252
		50	345		27	0.69	814	24.0	165	29.9	206
		100	690		23	0.58	607	41.7	287	23.4	161
		500	3445		13	0.33	229	88.7	611	11.4	79
9	23	25	172		23	0.58	678	10.7	74	24.2	167
		50	345		19	0.48	538	21.6	149	19.2	132
		100	690		16	0.41	388	34.5	238	14.6	101
		500	3445		9	0.23	135	65.5	452	6.7	46
12	30	25	172		18	0.46	458	7.3	50	16.9	116
		50	345		15	0.38	358	14.3	99	13.4	92
		100	690		12	0.30	254	22.3	154	10.1	70
		500	3445		7	0.18	85	40.8	281	4.6	32
6	15	25	172	Medium	43	1.09	1389	18.7	129	32.0	220
		50	345		36	0.91	1091	34.5	238	25.6	176
		100	690		29	0.74	734	53.0	365	19.7	136
		500	3445		16	0.41	252	98.8	681	9.4	65
9	23	25	172		31	0.79	906	16.9	116	21.1	145
		50	345		25	0.64	669	28.7	198	16.4	113
		100	690		20	0.51	455	41.7	287	12.3	85
		500	3445		11	0.28	146	71.6	486	5.5	38
12	30	25	172		23	0.58	597	11.0	76	14.8	102
		50	345		19	0.48	436	18.4	127	11.5	79
		100	690		15	0.38	293	26.6	183	8.5	59
		500	3445		8	0.20	91	43.9	302	3.8	26
6	15	25	172	Soft	69	1.75	2210	37.0	255	24.1	166
		50	345		54	1.37	1468	53.0	365	19.1	132
		100	690		42	1.07	934	70.5	486	14.7	101
		500	3445		22	0.56	285	113.0	779	6.9	48
9	23	25	172		46	1.17	1329	28.4	196	16.2	112
		50	345		36	0.91	879	40.0	276	12.5	86
		100	690		28	0.71	554	52.4	361	9.4	65
		500	3445		15	0.38	162	79.6	548	4.0	28
12	30	25	172		34	0.86	837	17.4	120	11.7	81
		50	345		27	0.69	557	24.9	172	8.9	61
		100	690		21	0.53	352	32.9	227	6.5	45
		500	3445		11	0.28	98	47.8	329	2.9	20

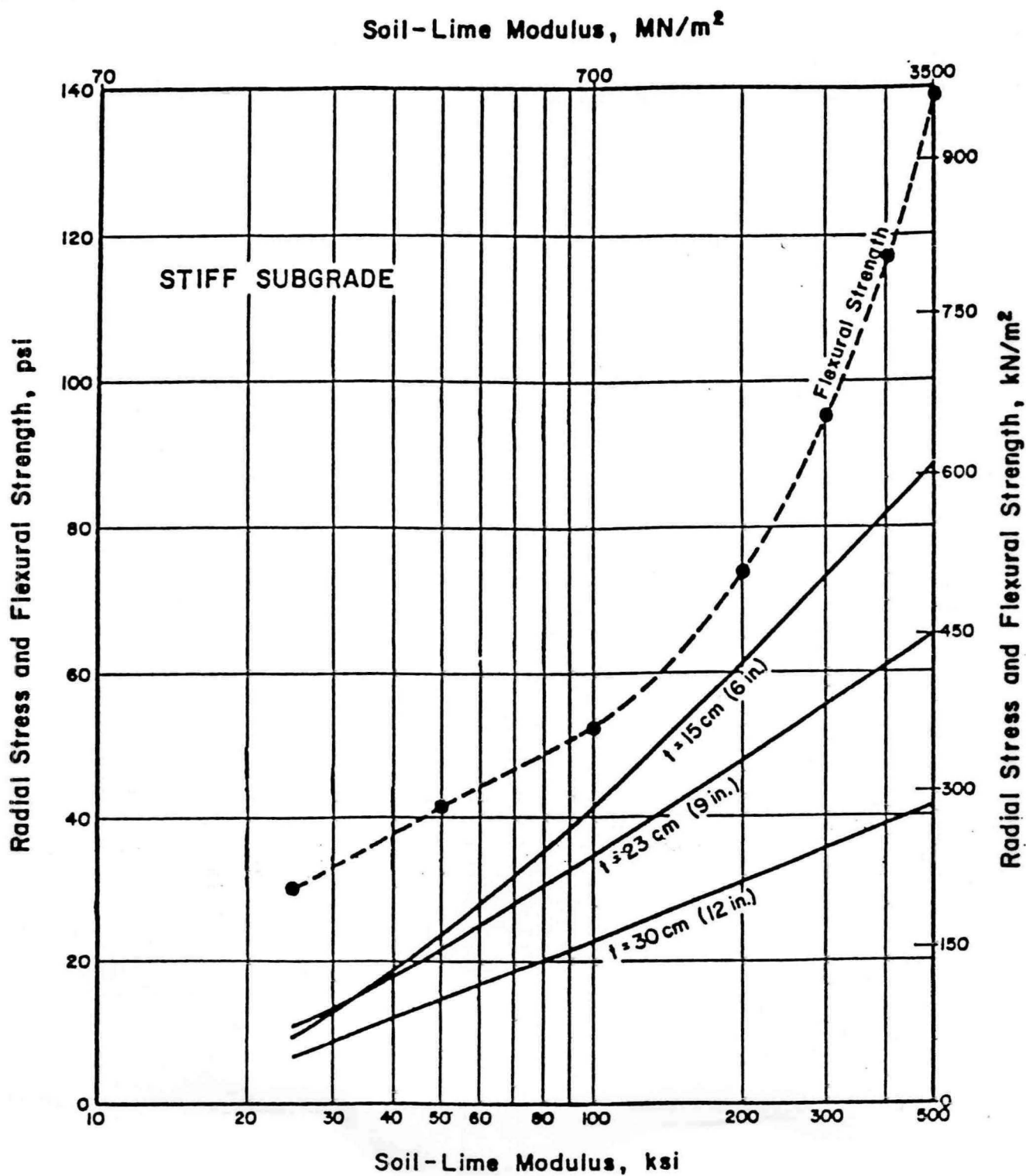


Figure A-3 Moduli-thickness-flexural stress relations for "Stiff Subgrade" (Thompson and Figueroa, 1980).

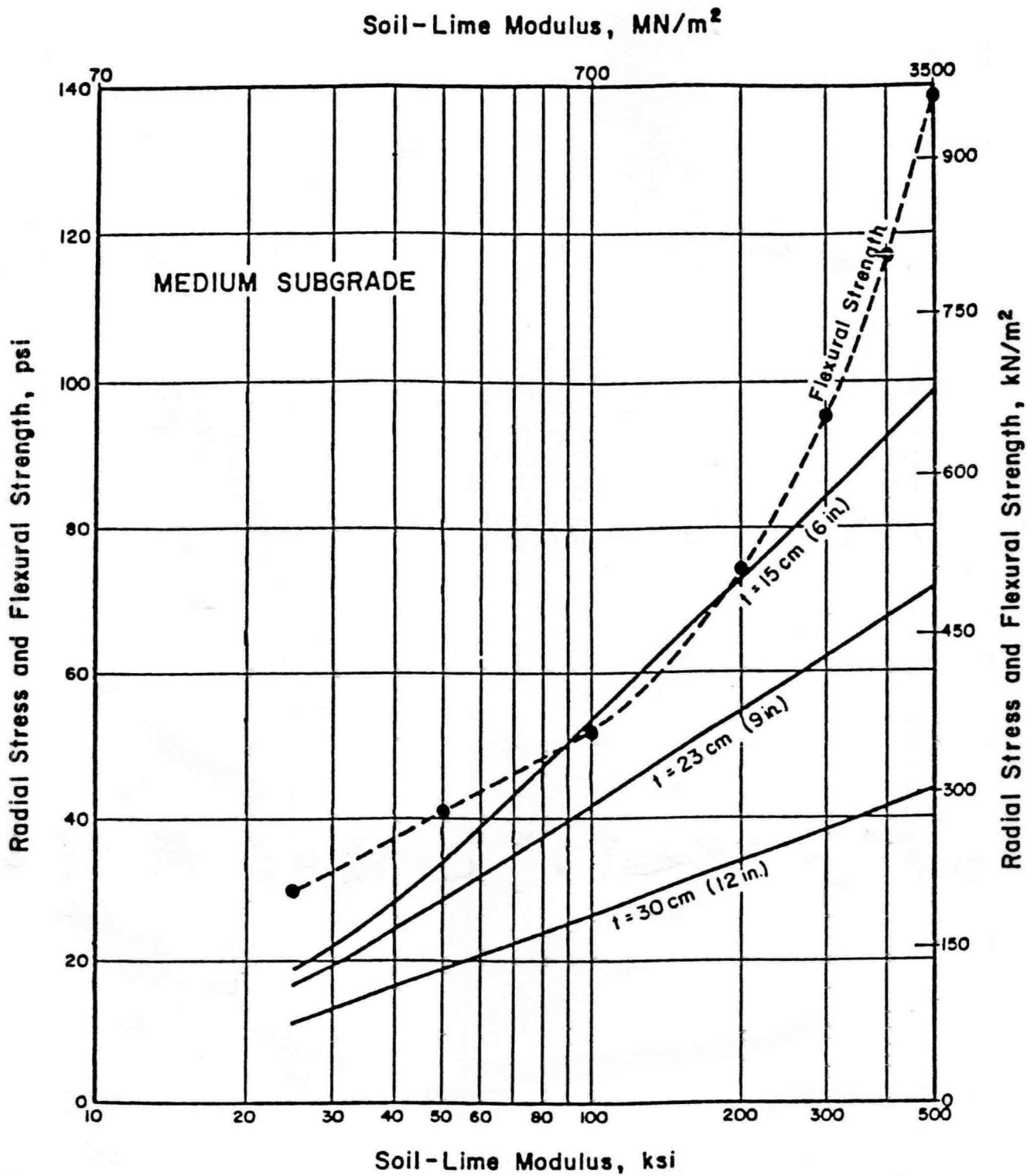


Figure A-4 Moduli-thickness-flexural stress relations for "Medium Subgrade" (Thompson and Figueroa, 1980).

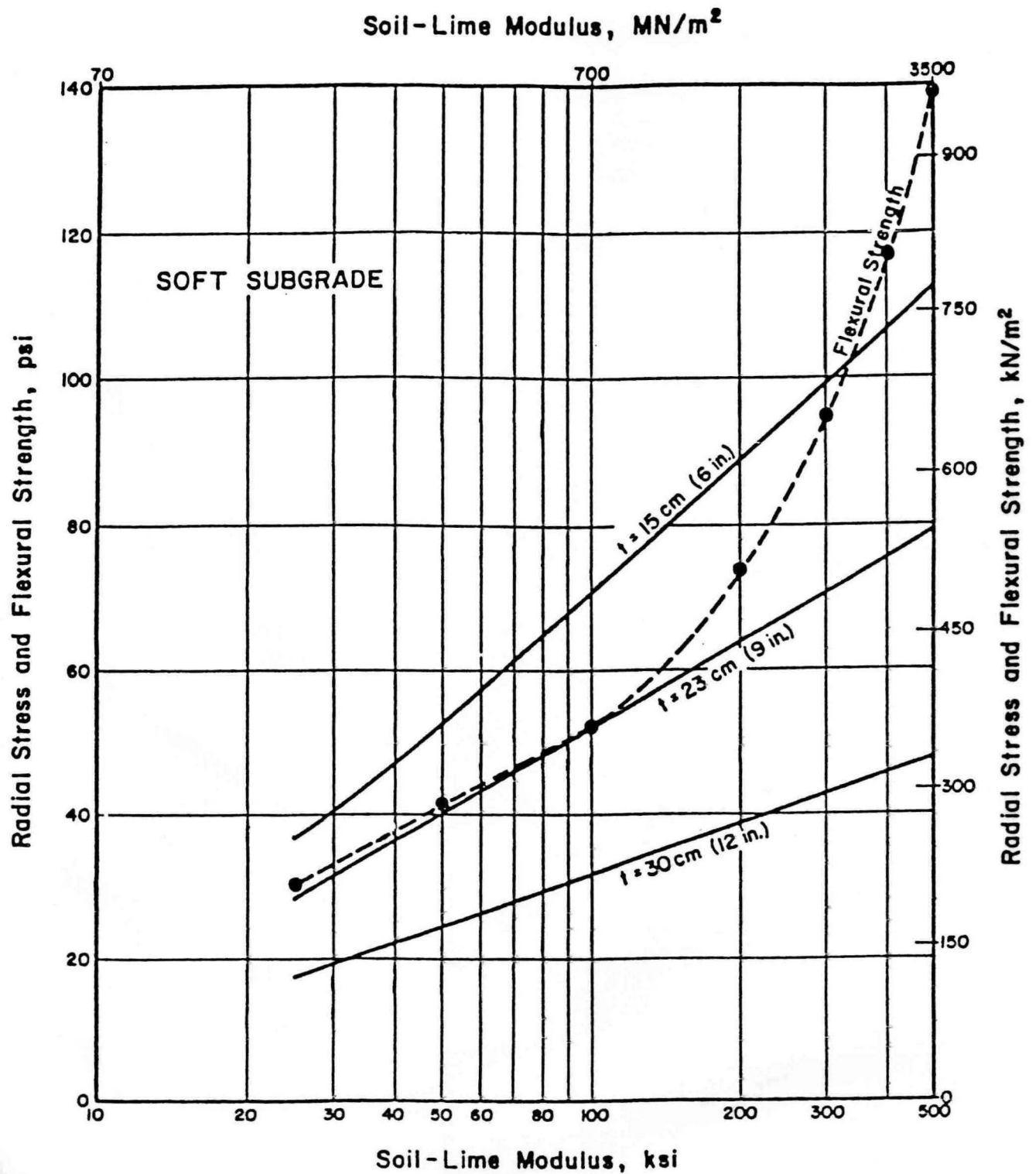


Figure A-5 Moduli-thickness-flexural stress relations for "Soft Subgrade" (Thompson and Figueroa, 1980).

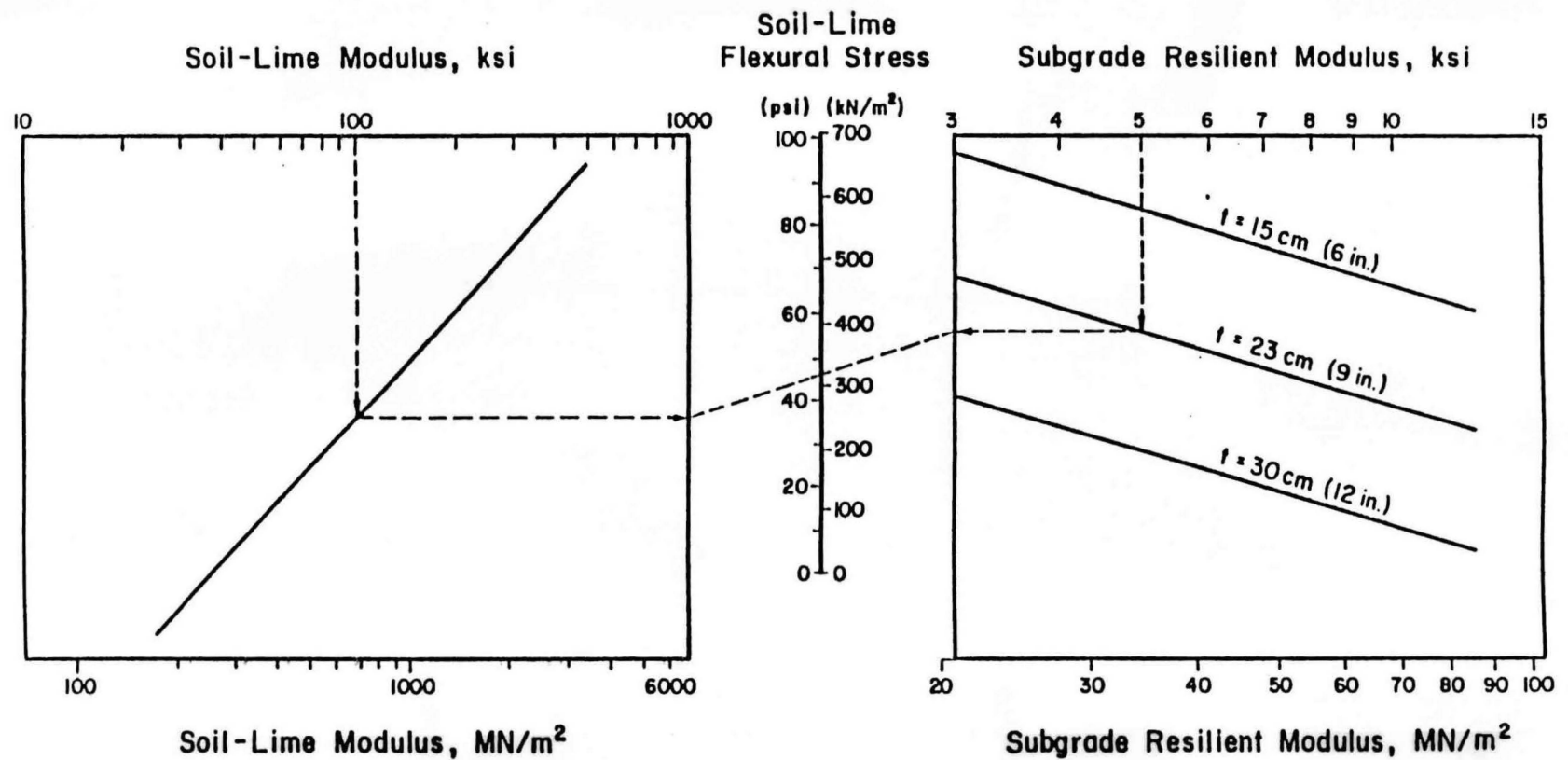


Figure A-6 Soil-lime flexural stress nomogram (Thompson and Figueroa, 1980).

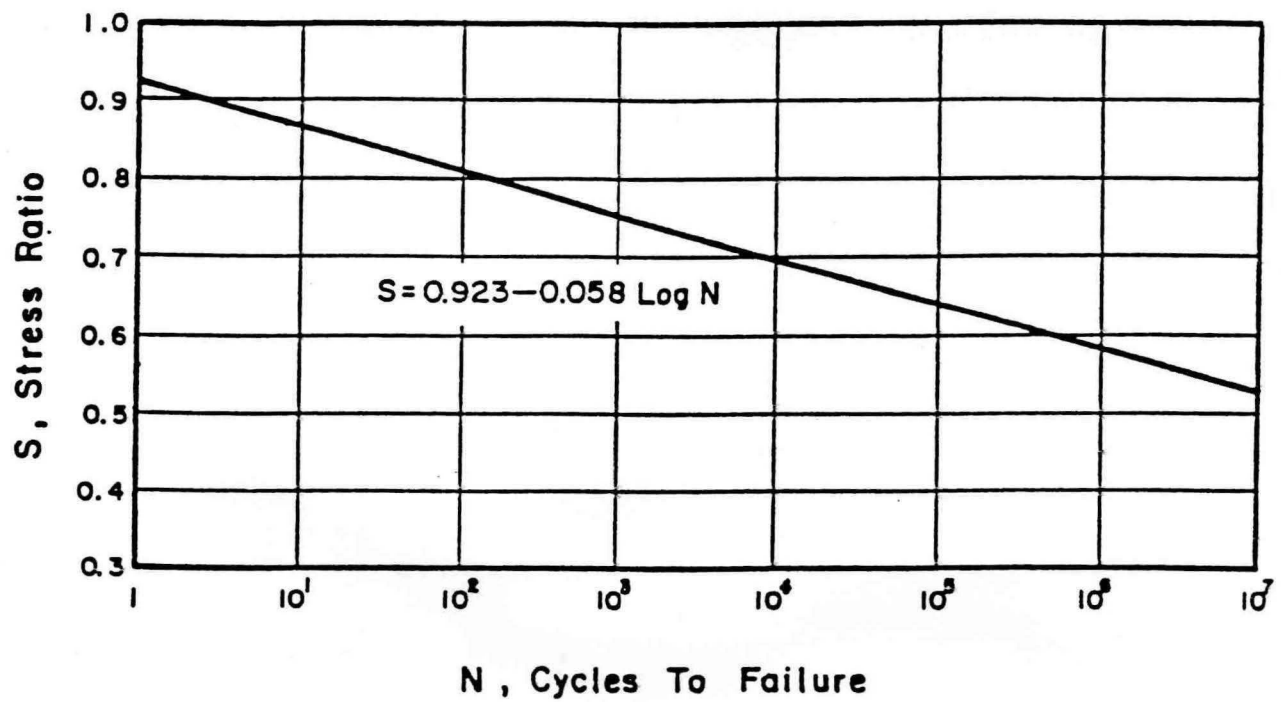


Figure A-7 Fatigue response for cured Illinois soil-lime mixtures (Swanson and Thompson, 1967).

$$S = 0.923 - 0.058 \log N \quad (A-2)$$

S = Stress ratio = repeated flexural stress/flexural strength and
N = Number of load applications to failure.

Thompson (1975) has emphasized that for many soil-lime mixtures the effects of continued strength development with increased curing tends to negate the effect of repeated loading through autogenous healing. Consideration of subgrade stresses and strength development during the pavement life should also be a part of a comprehensive pavement design approach.

According to Moore, Kennedy, and Kozuh (1971), the design procedures for lime-treated materials have often been empirical in nature and are geared to subgrade modification instead of stabilization. At the present time, design methods are based primarily on unconfined compressive strengths, plasticity characteristics of the soil or binder, or pH values. Moore et al. (1971) presented the results of a study that investigated the factors affecting the indirect tensile strength of lime-treated materials. The factors studied were clay content, lime content, molding water content, compactive effort, and curing temperature. A regression equation is presented for estimating indirect tensile strengths in terms of the factors investigated. The prediction equation derived is:

$$S_t = 228.18 - 1.647A + 3.1D - 86.375E - 2.218F - 5.234H + 0.017AF + 0.035AH + 581AE + 0.043FH + 0.137DH + 1.727EH - 0.037DF + 0.929EF - 0.261D^2 - 0.611E^2 + 0.0028F^2 - 0.008H^2 - 0.0116AEH - 0.0058AEF - 0.00348AFH - 0.0173EFH + 0.000116AEFH \quad (A-3)$$

where

- S_t = predicted value of indirect tensile strength, psi;
- A = compactive effort (high/low);
- B = compaction type (impact/gyratory shear);
- C = curing procedure (air dried/sealed);
- D = molding water content, percent by weight;
- E = lime content, percent by weight;
- F = curing temperature, °F;
- G = curing time, weeks; and
- H = clay content, percent by weight

Design Coefficients for Lime-Soil Mixtures Used as Bases

According to the research project IHR-76, "Lime Stabilization of Soils for Highway Purposes," conducted by the Department of Civil Engineering, University of Illinois, in cooperation with the Illinois Division of Highways and the Bureau of Public Roads, lime-soil mixtures can be used effectively and economically as quality highway construction materials. Report IHR-76 discusses the development of tentative strength coefficients and material requirements and limitations for inclusion of the use of lime-stabilized-soil mixtures as base and subbase in the Illinois Flexible Pavement Structural Design Procedure (Design Coefficients, 1970).

Findings of IHR-76 Study

This study addresses freeze-thaw, fatigue, shrink-swell, mix design, and several other facets of lime-soil stabilization. Key findings were as follows:

1. The critical time in the life of a lime-stabilized-soil mixture which has the potential for significant strength gain, occurs at the end of the first winter. During cold weather, the pozzolanic reaction is slowed tremendously and ceases completely at temperatures below 5°C (40°F) (Figure A-8). The pozzolanic reaction resumes when the temperature rises again and continues to increase strength for several years. Tests on lime-fly Ash mixtures, which rely on the same pozzolanic reaction, showed the same result (Figure A-9).
2. Accelerated laboratory freeze-thaw tests showed that strengths are reduced as the number of freeze-thaw cycles is increased (Figures A-10 to A-14). However, there should not be a problem as long as the design allows for this reduction in strength so that the materials do not become overstressed during the critical period.
3. Laboratory fatigue tests have indicated that the fatigue behavior of lime-soil mixtures is similar to that of Portland cement concrete (Figure A-15). Since fatigue is a long-term phenomenon, and since lime-stabilized soils gain strength for an extended period of time, fatigue should not be a critical issue when considering lime-soil stabilization in a properly designed pavement structure.
4. It is necessary to consider the detrimental effects of freeze-thaw to insure that sufficient residual strength exists during the critical "spring thaw" period. For seven freeze-thaw cycles, the lime-stabilized soils that develop unconfined compressive strengths of 1,050 KPa (150 psi) to 1,190 KPa (170 psi) prior to the onset of cold weather during the first winter will be suitable for base course construction. Lime-stabilized soils with compressive strengths of 105 KPa (75 psi) to 770 KPa (110 psi) prior to the first winter following construction will be

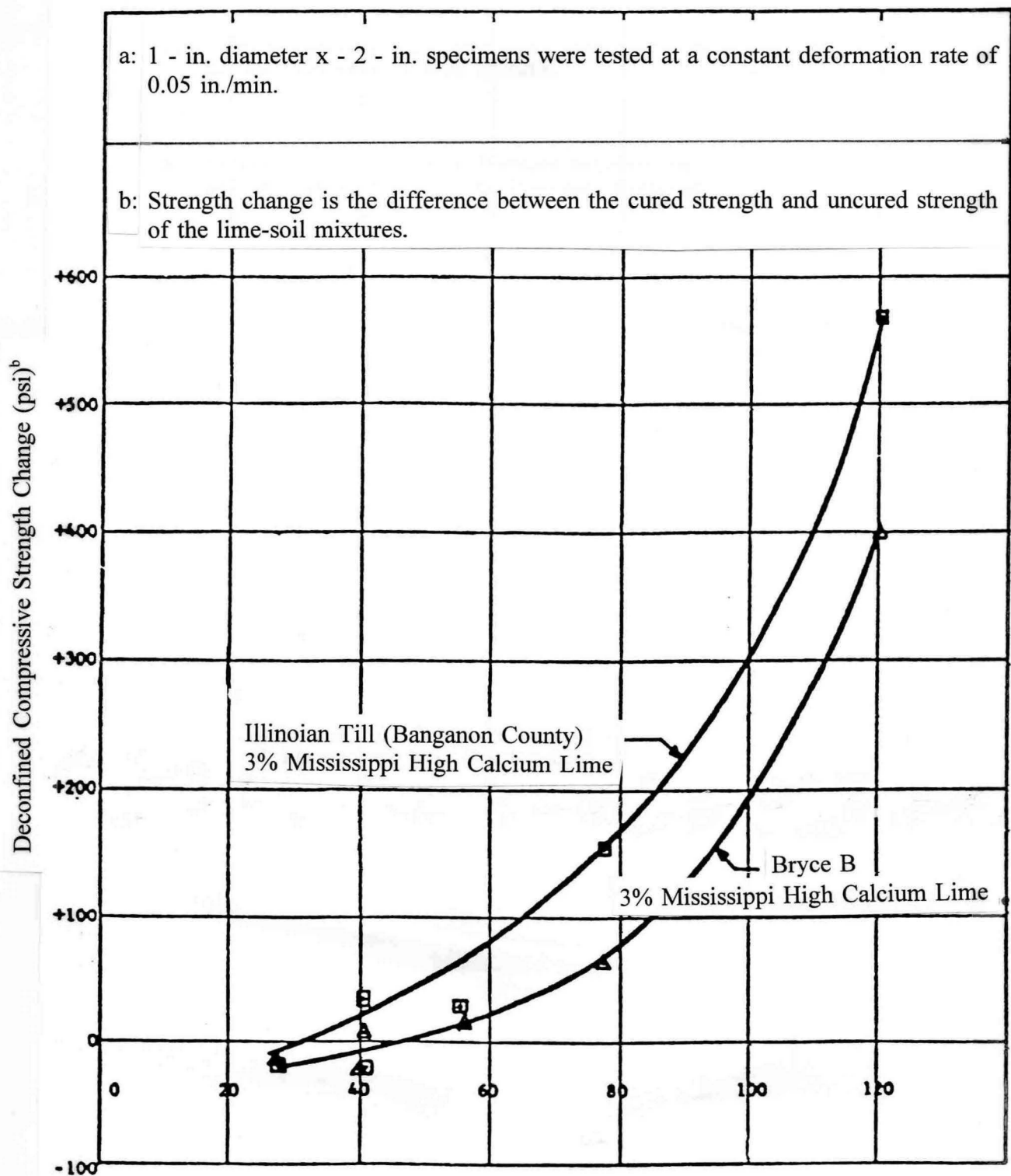


Figure A-8 Influence of curing temperature on unconfined compressive strength change (28-day curing)^a (Design Coefficients, 1970). 1 psi = 6,894 Pa 1 in = 25.4 mm

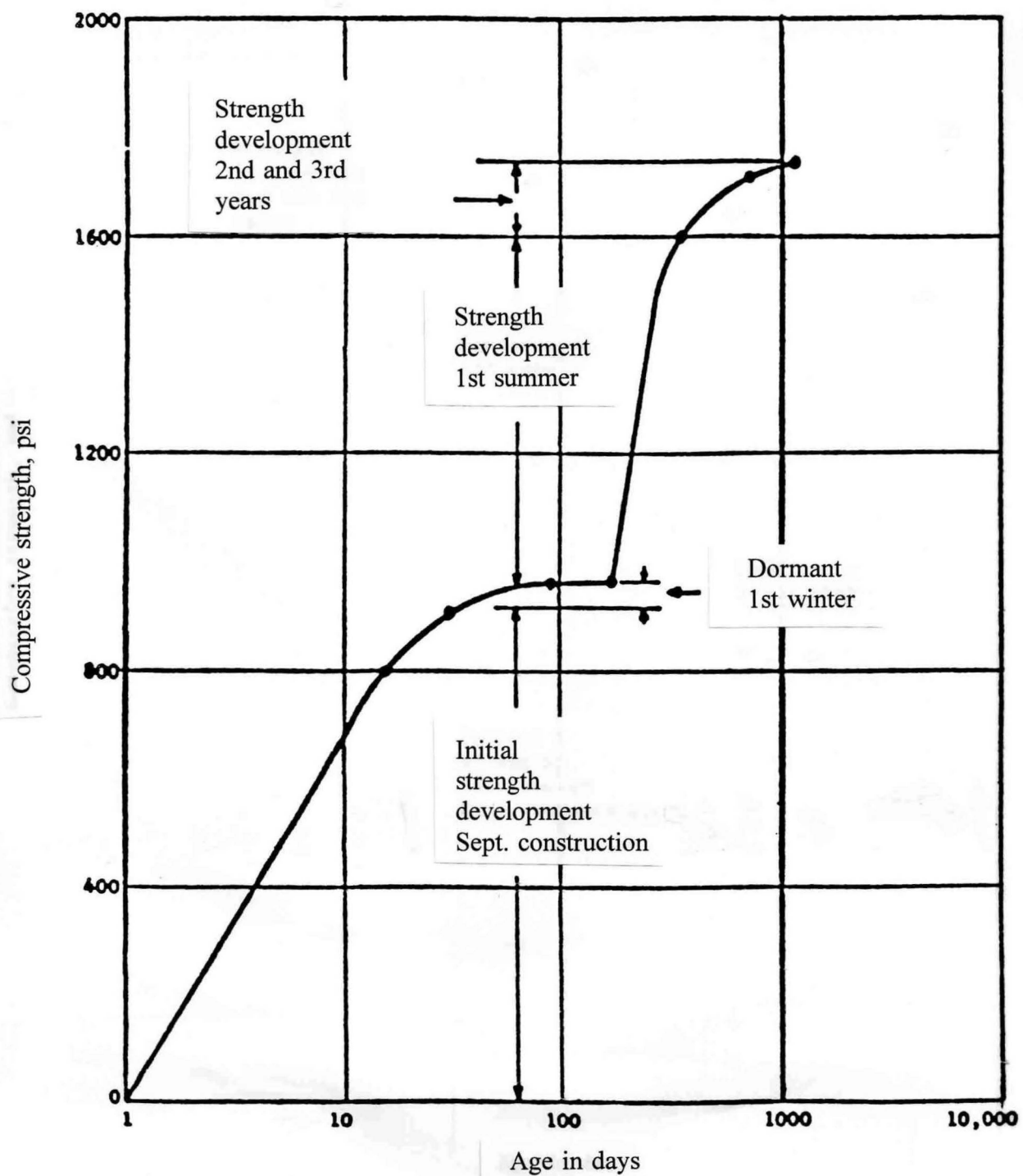


Figure A-9 Compressive strength development of in-service pavement with lime-fly ash stabilization (Design Coefficients, 1970). 1 psi = 6,894 Pa

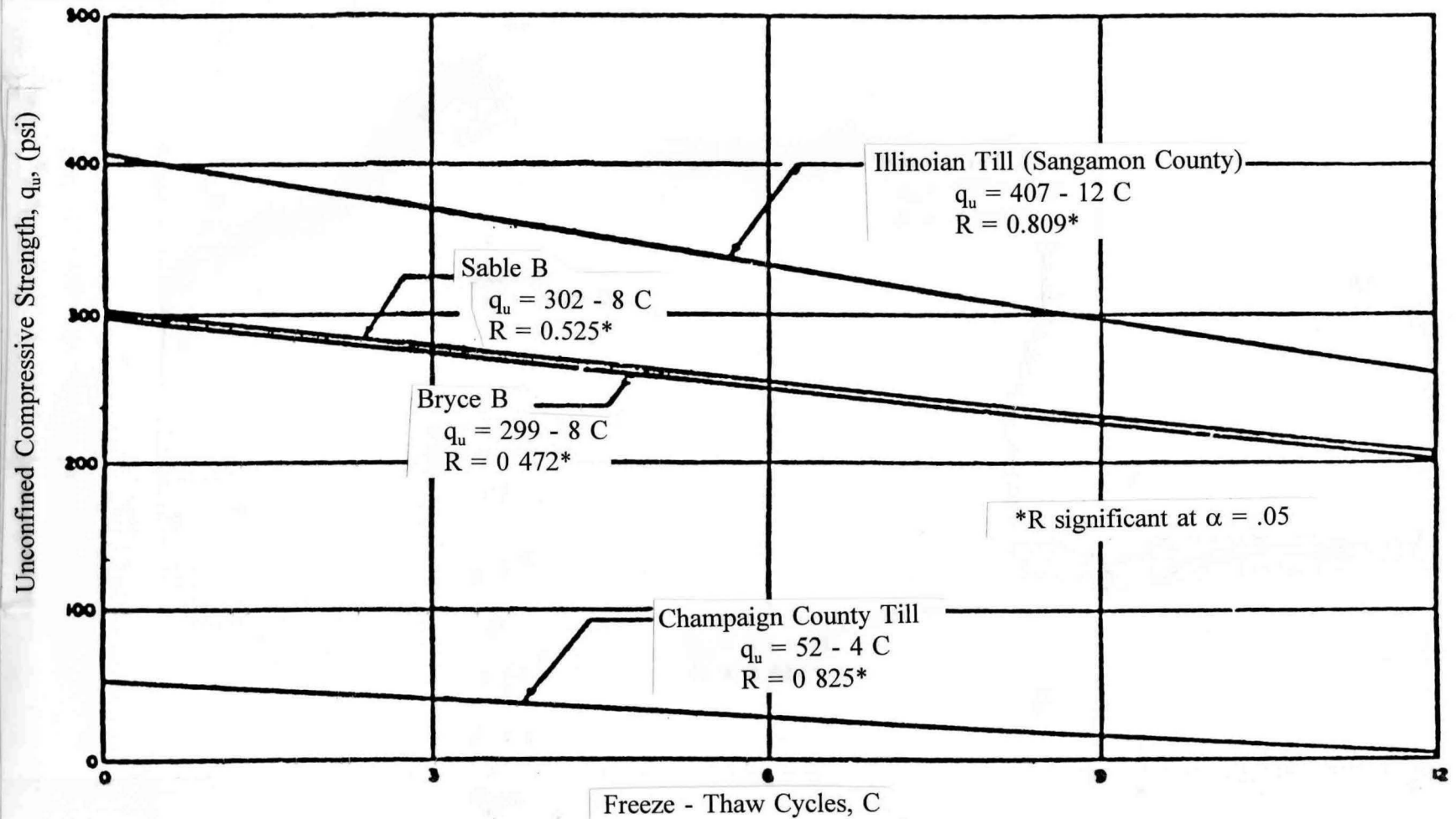


Figure A-10 Influence of freeze-thaw cycles on unconfined compressive strength (48 hour curing) (Design Coefficients, 1970).
 1 psi = 6,894 Pa

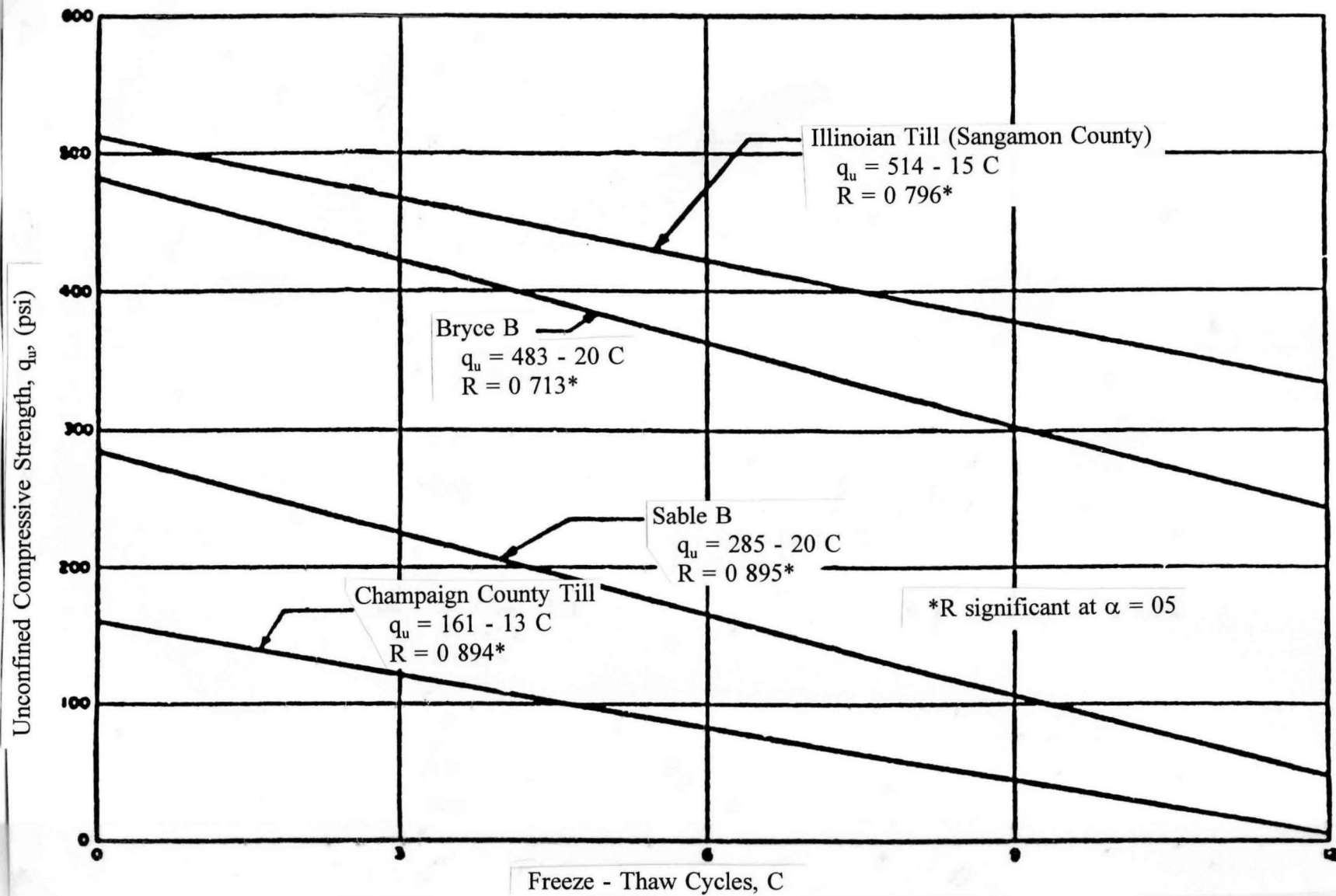


Figure A-11 Influence of freeze-thaw cycles on unconfined compressive strength (96 hour curing) (Design Coefficients, 1970).
1 psi = 6,894 Pa

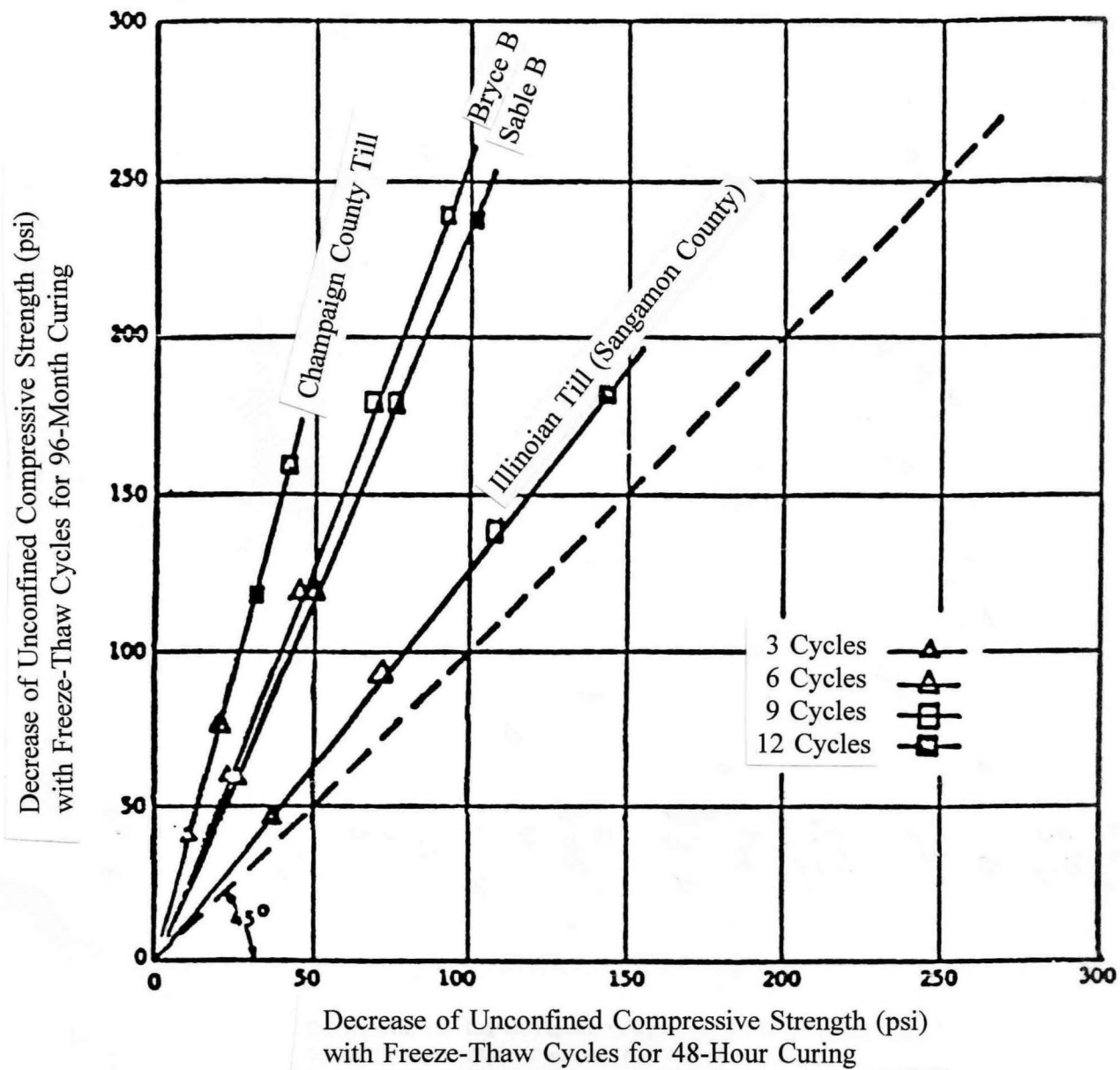


Figure A-12 Effect of curing period on decreases of unconfined compressive strength with freeze-thaw cycles (Design Coefficients, 1970). 1 psi = 6,894 Pa

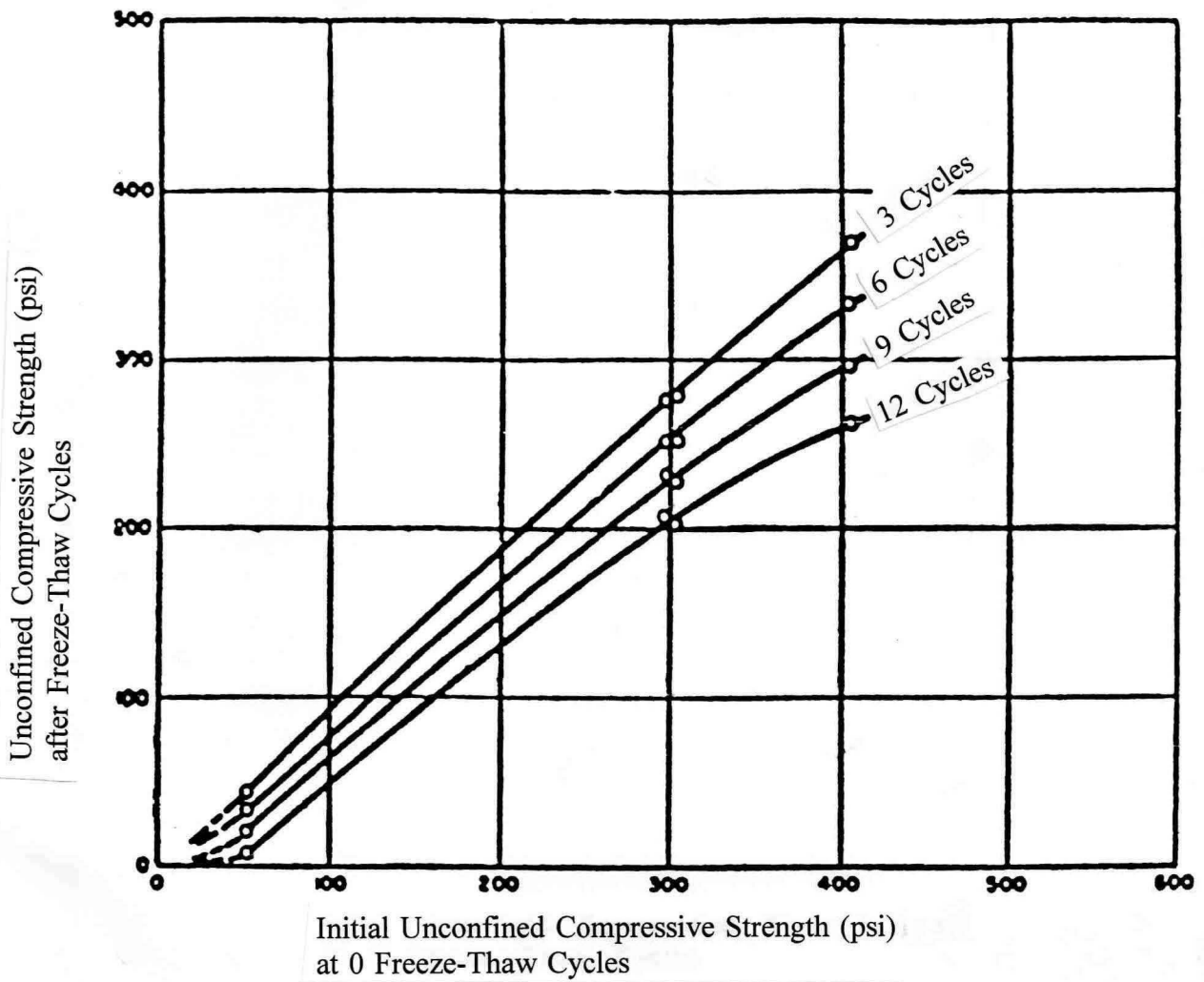


Figure A-13 Influence of initial unconfined compressive strength on the residual strength after freeze-thaw cycles (48 hour curing) (Design Coefficients, 1970).
1 psi = 6,894 Pa

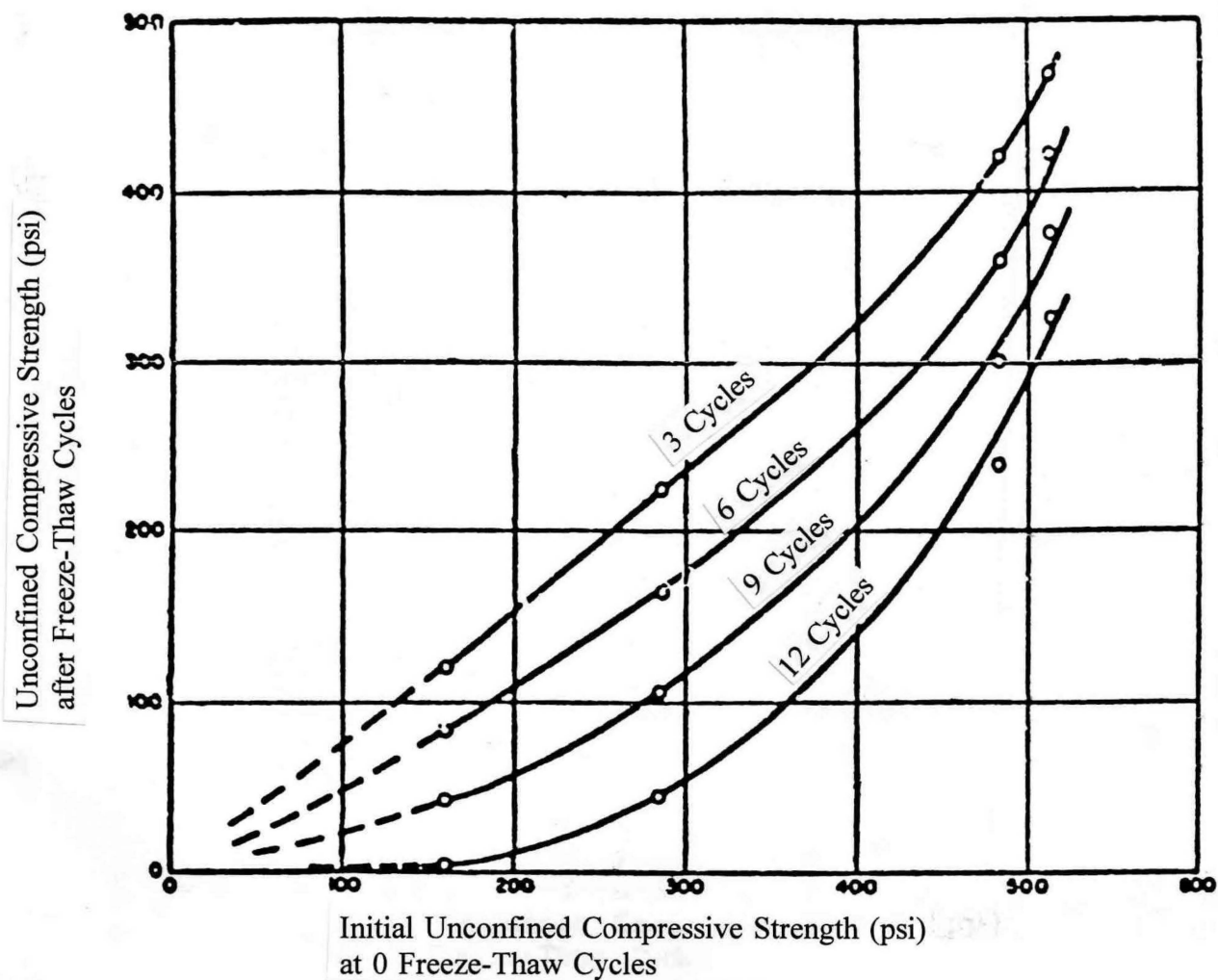


Figure A-14 Influence of initial unconfined compressive strength on the residual strength after freeze-thaw cycles (96 hour curing) (Design Coefficients, 1970).
 1 psi = 6,894 Pa

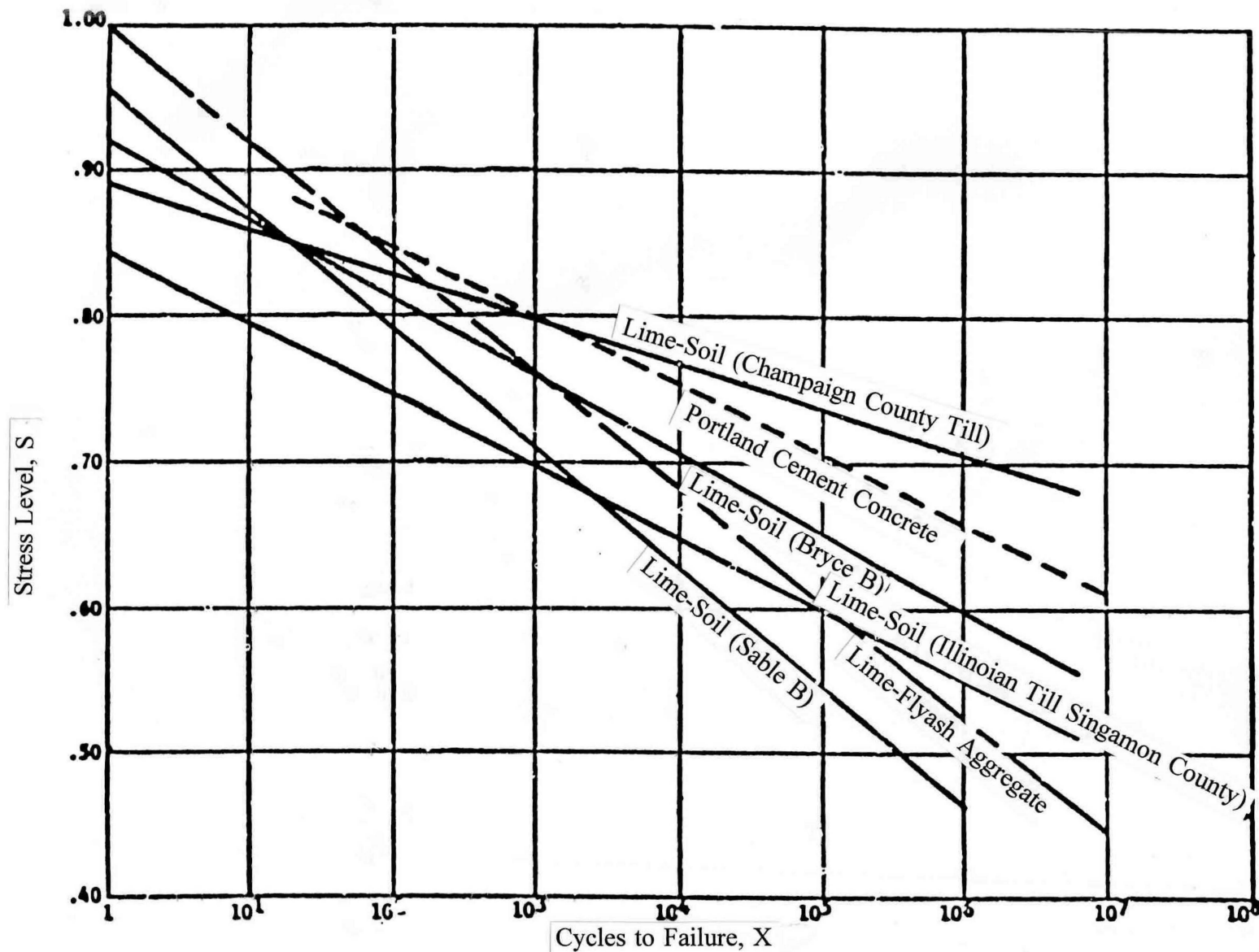


Figure A-15 Flexural fatigue response curves for lime-soil mixtures and Portland cement concrete (Design Coefficients, 1970).

suitable for subbase construction when at least eight inches of material overlies the lime-stabilized subbase. Normally, subbases and bases in Illinois will not be subjected to more than about seven freeze-thaw cycles in a well-designed pavement.

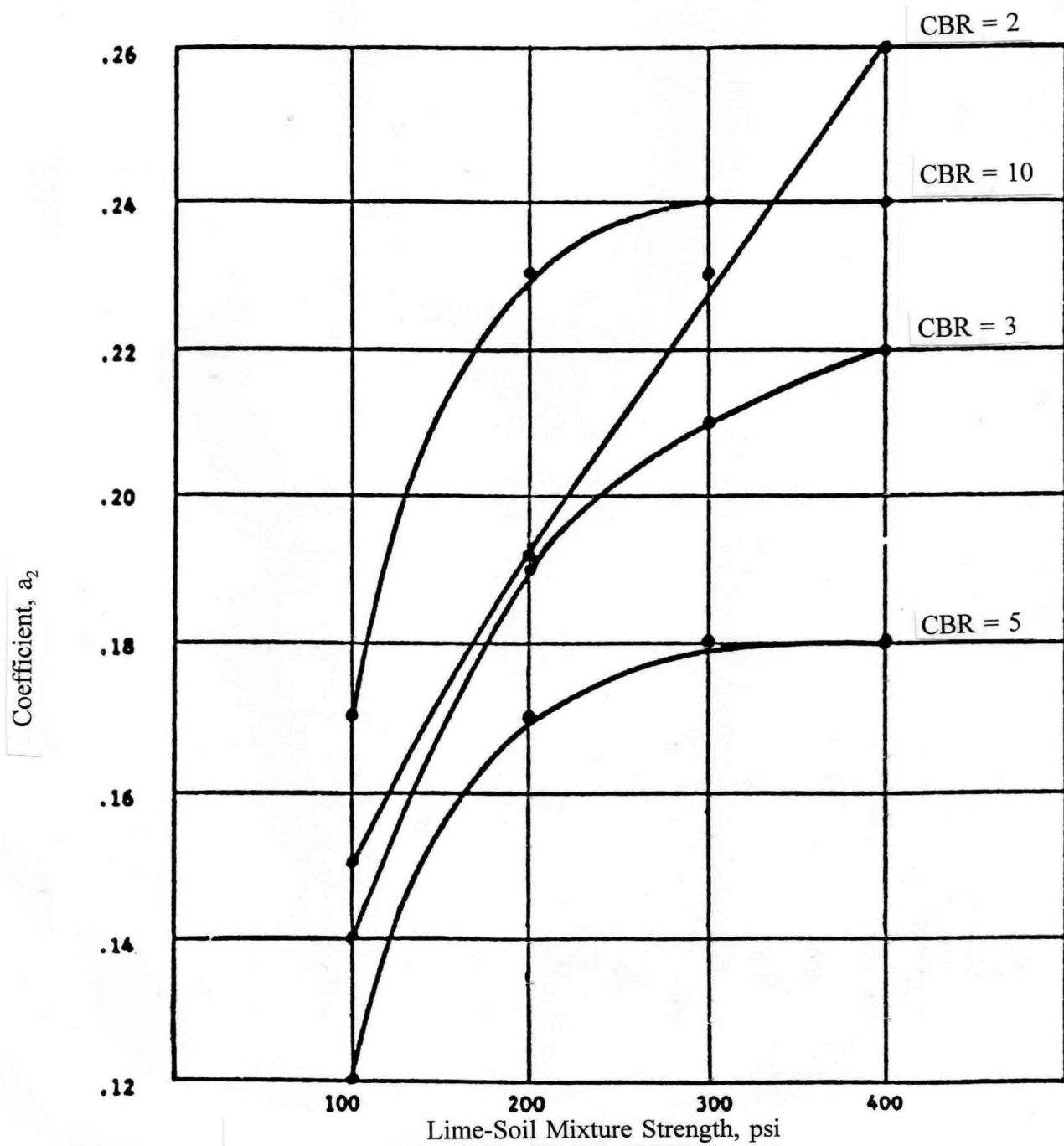
In Service Roads

A background to establish the structural adequacy of lime stabilized section (Design Coefficients, 1970) referred to Missouri experience which indicates that five inches of lime-stabilized-soil subbase with a strength of 525 KPa (75 psi) after seven days curing could be used to adequately replace an equivalent thickness of crushed stone and a 20 percent reduction in cost would be possible, with no sacrifice in service. Tests in Nebraska (Design Coefficients, 1970) indicate that lime-treated sections have performed better than an equivalent thickness of granular material. A thickness of seven inches was used for the lime-stabilized -soil subbase, and a thickness of six inches was used for the lime-stabilized-soil base. The State of Texas has built a number of miles of pavement constructed with lime-stabilized materials and satisfactory results have been obtained when a minimum unconfined compressive strength of 350 KPa (50 psi) was specified for subbase and 700 KPa (100 psi) was specified for bases (Design Coefficients, 1970).

Strength Coefficient Values for Lime-Stabilized Soils

Information from the IHR-76 study suggests that unconfined compressive strengths can be used as meaningful measures of strength or stability of lime-stabilized-soil mixtures, and that estimates of coefficient values may be made by relating these compressive strengths to those obtained for cement-aggregate mixtures. The pozzolanic reaction produces a cementing similar to that of cement-treated mixtures; and lime-stabilized and cement-stabilized plastic soils are similar in flexural strength, modulus of elasticity, failure strains, and Poisson's ratio. The major difference is that cement-stabilized soils gain strength rapidly while lime-stabilized soils increase in strength at much slower rates and over longer periods of time. According to Research Project IHR-28 report, studies of the effect of curing temperatures on strength of Illinois soils have shown that the laboratory method of curing samples at 49°C (120°F) for 48 hours produces unconfined compressive strengths approximately equivalent to those obtained on samples cured for 30 days at 21°C (70°F). This indicates that the 48 hour curing at 49°C (120°F) should provide realistic estimates of field strengths at the onset of cold weather during the first winter following construction for lime-stabilized-soil mixtures completed immediately prior to a recommended September 15 cutoff date (Design Coefficients, 1970).

It should be carefully noted, however, that accelerated curing can be misleading. Alexander and Doty (1978) found on a study of 12 California soils that 5-day accelerated cure at 38°C (100°F) was a reasonable predictor of 26-day strength at 23°C (73°F). However, the 26-day strength and the accelerated strength was often only a fraction (in



Coefficient-Strength Relations for Lime-Soil Mixture Base Courses.
(Class III - 700 ADT)

Figure A-16 Coefficient-strength relations for lime-soil mixture base courses (Design Coefficients, 1970). 1 psi = 6,894 Pa

some cases only about 25 percent), of the long-term strength of the mixture (360 day strength). In this study, strength testing with five Texas soils (Beaumont, Victoria, Burleson and Arlington (2)) has demonstrated that accelerated curing is not always as adequate a predictor of long-term curing, i.e., Beaumont clay requires long-term curing to develop the required level of pozzolanic reactivity for substantial strength gain. This pozzolanic reactivity is not demonstrated in accelerated curing.

Base Course Coefficient, a_2

In a preliminary study of lime-soil base course coefficients (Design Coefficients, 1970), relationships between a_2 and compressive strength (Figure A-16) were developed utilizing layered elastic analysis and ultimate strength considerations, and comparing crushed stone base thicknesses with equivalent lime-stabilized soil base thicknesses. This work suggests that values of a_2 for lime-stabilized soil could range from 0.12 to 0.26 for compressive strengths of 700 to 2,800 KPa (100 to 400 psi).

Information obtained from published reports on in-service roads suggests that lime-stabilized soil base courses are equivalent in performance to granular base courses. This suggests coefficient values for lime-stabilized soils ranging from 0.10 (uncrushed gravel) to 0.13 (crushed stone).

A value of $a_2 = 0.11$ is recommended (Design Coefficients, 1970) for use in the Illinois flexible pavement design procedure as the design coefficient for lime-stabilized soils as base course.

Subbase Coefficient, a_3

Following the recommendations of the IHR-76 study, a minimum unconfined compressive strength of 700 KPa (100 psi) is suggested for lime-stabilized soil when used as the subbase for flexible pavements. In Figure A-17, a lime-stabilized soil with a minimum compressive strength of 700 KPa (100 psi) when used as base course would be assigned a coefficient value, a_2 , of 0.095. From the relationships shown in the Illinois flexible pavement design procedure, a granular base course equivalent to the 700 KPa (100 psi) lime-stabilized soil ($a_2=0.095$) would have a CBR of 44. This same granular material (CBR=44) when used as a subbase would be assigned a coefficient a_3 equal to 0.12. A value of $a_3=0.12$ is recommended for lime-stabilized soil (700 KPa (100 psi) minimum compressive strength) when used as subbase. This compares favorably with the range in a_3 of 0.11 to 0.14 for granular subbase materials.

Design Limitations

The Illinois flexible pavement design procedure contains minimum thickness and material strength requirements for each layer of the pavement structure which have been established in consideration of construction and maintenance problems to avoid the

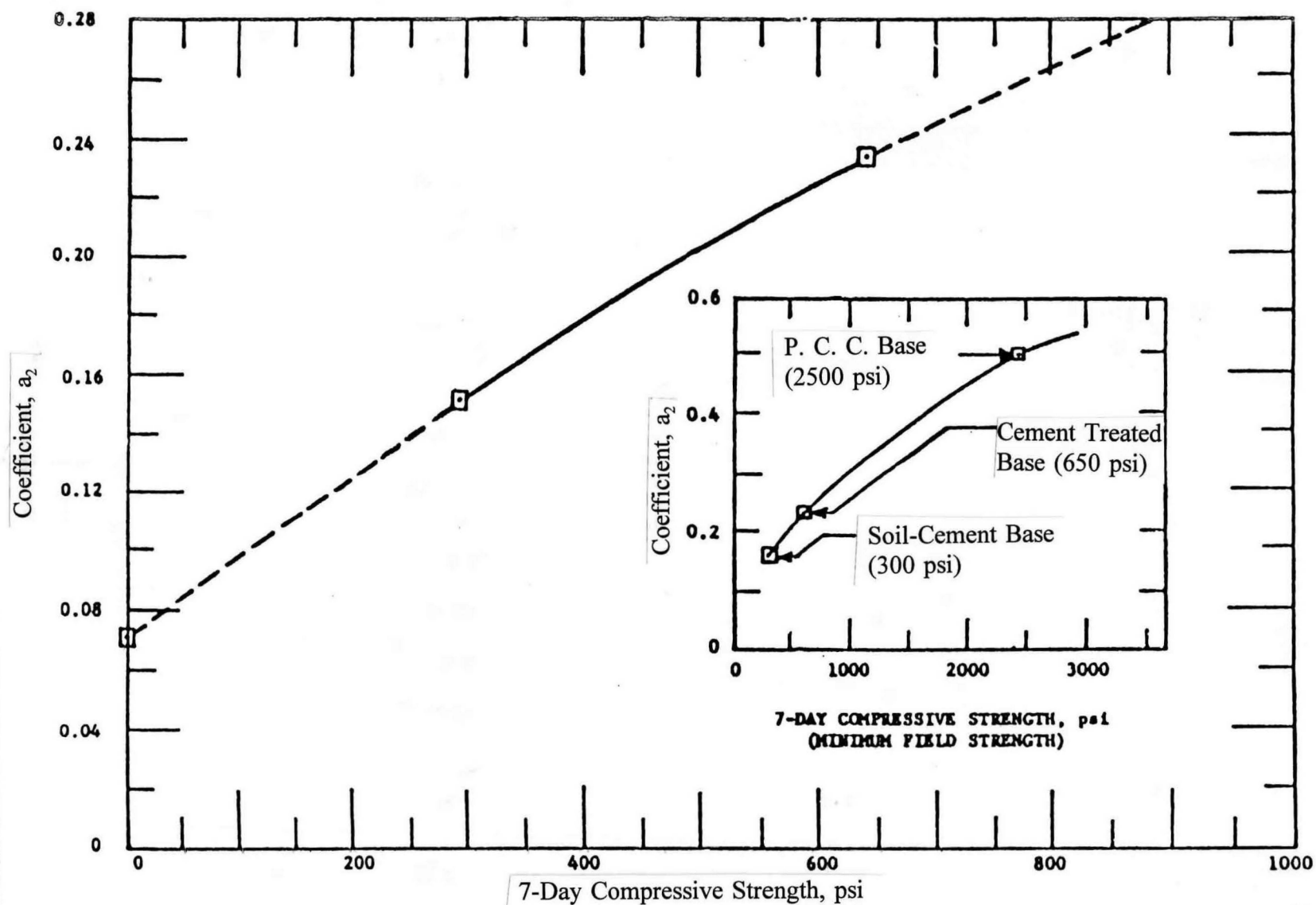


Figure A-17 Coefficient-compressive strength relations for lime-soil mixture base courses (Design Coefficients, 1970).
1 psi = 6,894 Pa

possibility of developing impractical designs. It is recommended that only lime-stabilized - soil mixtures developing at least 1,050 (150 psi) compressive strength when cured at 49°C (120°F) for 48 hours be used as base course, and only those developing at least 700 KPa (100 psi) be used as subbase. Design coefficients of $a_2 = 0.11$ and $a_3 = 0.12$ have been recommended as base course and subbase, respectively. The Illinois design manual includes a minimum of eight inches of Aggregate Base Course, Type B, for pavement designs requiring Structural Numbers less than 2.50. The assigned coefficient value of a_2 , of this material ranges from 0.10 to 0.13. The suggested value of $a_2 = 0.11$ for lime-stabilized-soil mixtures is within this range and thus, it is recommended that a minimum of 20 cm (8 in) of lime-stabilized soil be permitted as the base course for pavements requiring Structural Number less than 2.50. The Illinois flexible pavement design manual makes optional the use of a subbase for pavement designs with Structural Numbers less than 5.00. If used, however, it must be at least four inches of pit-run gravel ($a_3 = 0.11$). For pavements requiring Structural Numbers of 5.00 and greater a granular subbase is required, with the minimum being four inches of processed uncrushed gravel ($a_3 = 0.12$).

Texas Method of Designing Lime Stabilized Bases

The Flexible Pavement Design Guide (McDowell, 1972) is equally applicable for both untreated and treated (stabilized) soils and base course materials. It provides a rational design method for evaluating paving materials, permitting reduction in pavement thicknesses if comparative test results warrant it. With soils and base materials containing clay, the most effective and commonly used stabilizer is lime, which reacts both physically and chemically to yield stable paving materials. The design method discussed in this manual to determine pavement thickness involves

1. Comparison of soil strength characteristics with wheel load stress conditions at various levels;
2. Ability of material layers to support both heavy loads and repetitive loadings;
3. Reduction of thickness when tensile strengths of pavement layers are increased; and
4. Minimum thickness of bituminous surface courses.

Outline of Design Procedure

1. Determine strength of the untreated subgrade soil in terms of R-value (using AASHTO T190 or ASTM 2844), California Bearing Ratio (using AASHTO T193 or ASTM 1883), or triaxial strength design class by standard test method AASHTO T212.
2. Enter the value determined in Step 1 on Figure A-18 and convert to design value number (DVN).

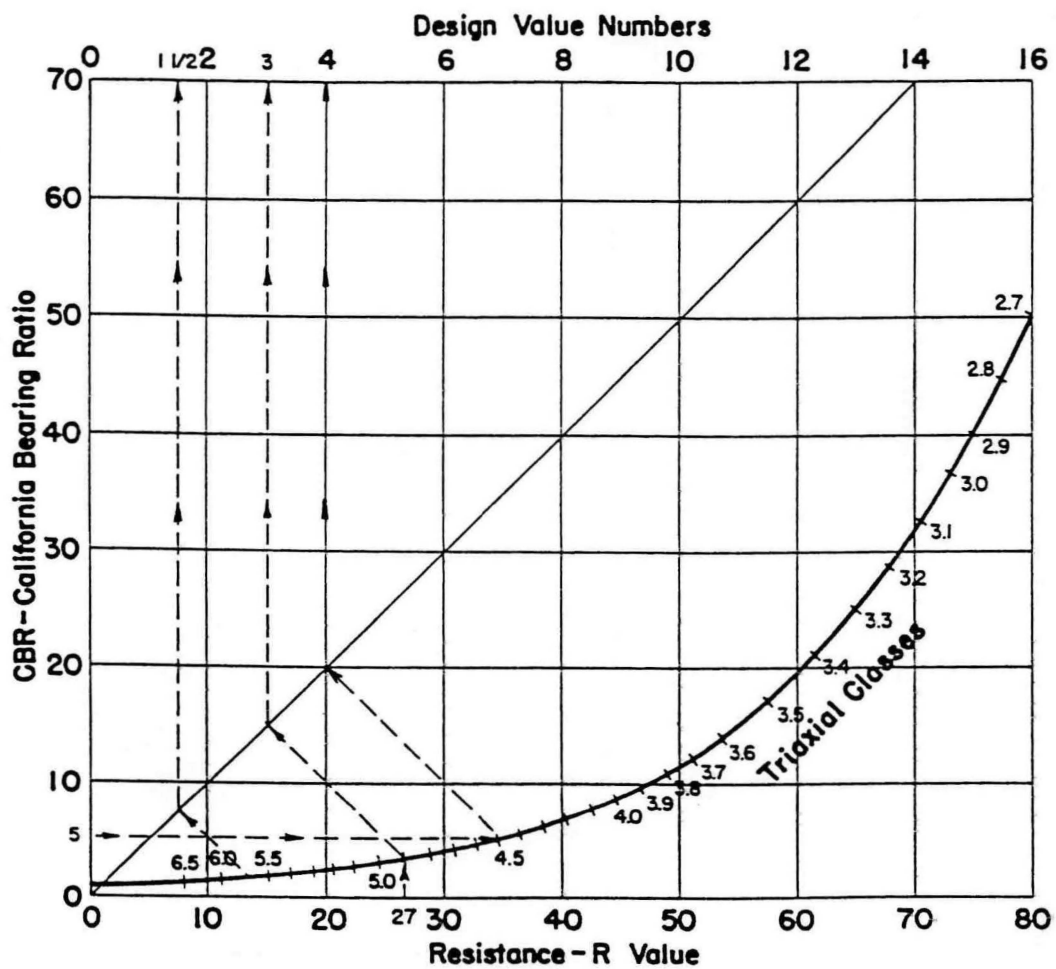


Figure A-18 Strength ratio chart (McDowell, 1972).

3. On Figure A-19, enter design value number and proceed to one of four traffic curves that corresponds most closely to given traffic conditions, then project horizontally to minimum depth of cover required.
4. If the average daily ten heaviest wheel loads (ADTHWL) for one of the curves given in Figure A-19 is similar to loads anticipated but there is a different number of load applications from those used in Figure A-19, then use the following procedure:
 - a. Divide the minimum depth value obtained in Step 3 by the load design factor (LFDF) shown in the table in Figure A-19 for the traffic curve used in Step 3.
 - b. In Figure A-20 select and enter the number of equivalent 80 KN (18 kip) single axle load applications anticipated during the life of the pavement, and read with the new LFDF on the abscissa.
 - c. To obtain the corrected thickness, multiply the depth value obtained in Step 4(a) by the LFDF obtained in Step 4(b).
5. Determine the thickness for an ADTHWL different from any of the four curves shown on Figure A-19, by selecting one design curve in Figure A-19 having the ADTHWL just below that desired for use and multiplying the obtained thickness by the square root of the ratio of the anticipated wheel load (ADTHWL) to the wheel load used for the design curve.

The above steps apply only to the use of conventional aggregates, borrow materials, and soils that have little or no tensile strength. However, the following steps should be taken to determine replacement equivalencies and/or reduction in total pavement thickness if stabilized materials are used which develop appreciable tensile strength due to the cementing and binding action imparted by the stabilizing additive.

6. Determine the tensile strength by flexural, diagonal compression (split tensile) or cohesiometer tests on properly cured specimens, or preferably from cores. In the absence of tensile strength data, unconfined compressive strengths may be used as a general guide for estimating the tensile strength by approximating tensile strength as one-tenth of the unconfined compressive strength. An 18-day curing cycle, similar to AASHTO T220-66, should be used to obtain realistic unconfined compressive strength values. In the case of lime-soil mixtures the unconfined compressive strength generally ranges from 525 to 1,750 KPa (75 to 250 psi), which would correspond to tensile strength values of 52.5 to 175 KPa (7.5 to 25 psi), respectively.

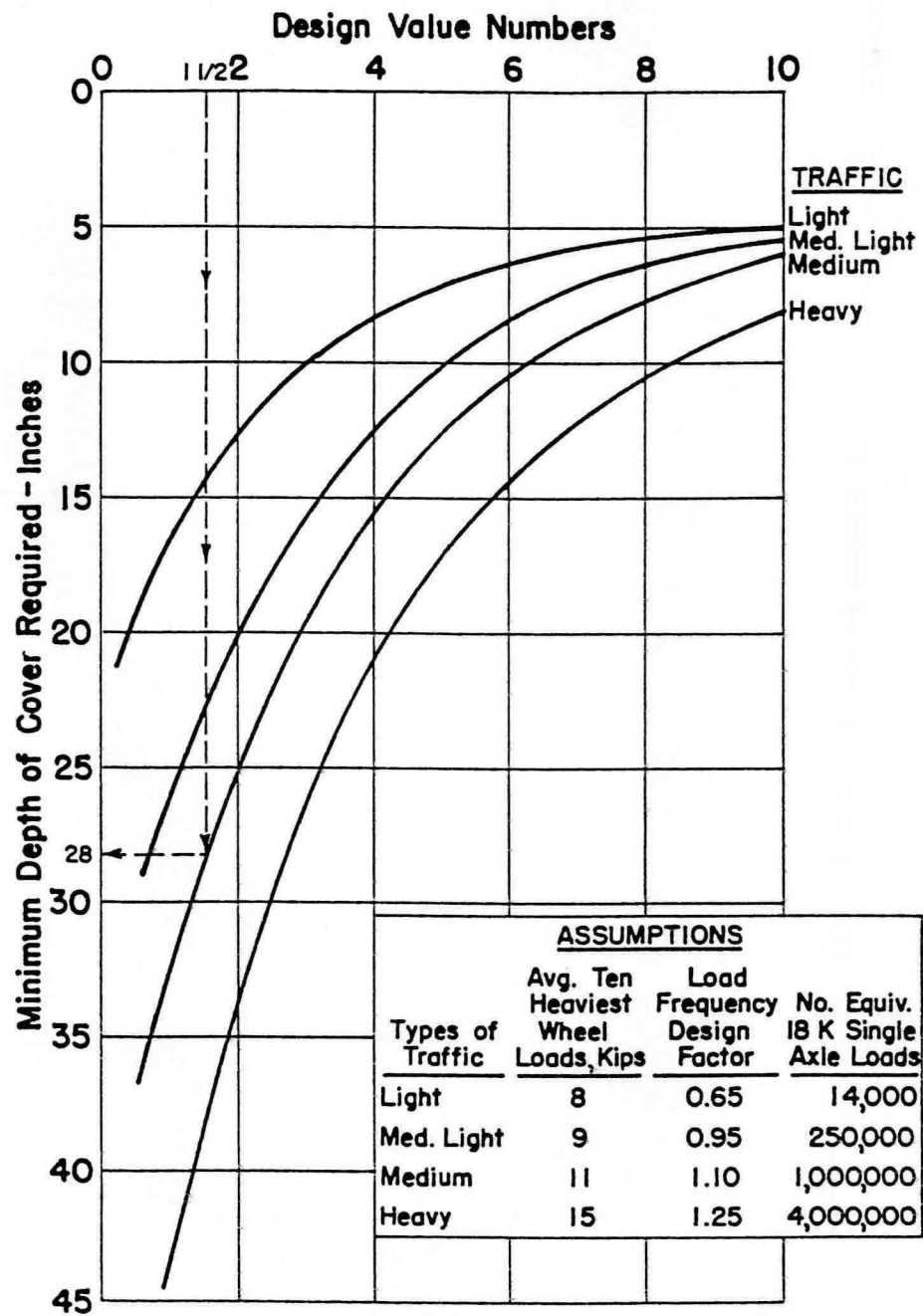


Figure A-19 Design value numbers (McDowell, 1972). 1 in = 25.4 mm

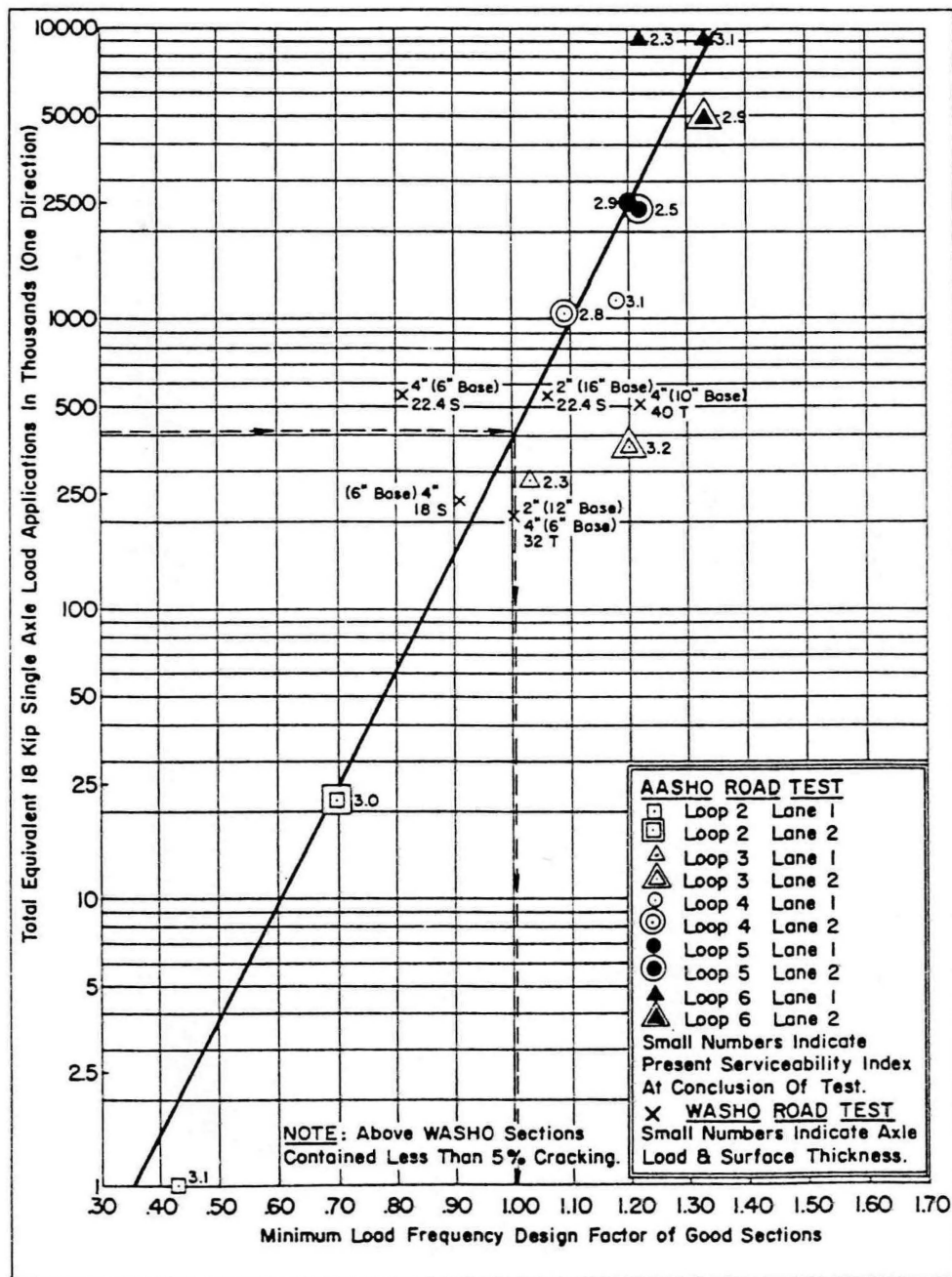


Figure A-20 Minimum load frequency design factor of pavement sections (McDowell, 1972). 18 K = 80 KN

7. Determine tensile strength modification factor (S_t) from Figure A-21 by using the thickness of surfacing, base or subbase, whichever has the greatest tensile strength. The modified tensile strength value is obtained by multiplying the tensile strength value from Step 6 by this factor.
8. Determine the maximum thickness reduction due to tensile strength from Figure A-22 by entering with the depth from Step 4 or Step 5 and the modified tensile strength from Step 7. Multiply this value by 0.75 as a safety factor.
9. Subtract the value obtained in Step 8 from the value entered in Figure A-22. This is the minimum total design thickness of subbase, base, and surfacing.
10. From Figure A-23 determine the minimum thickness of bituminous surfacing. Subtract this value from the thickness obtained in Step 9, giving the minimum thickness of base and/or subbase.

Lime Treated Subgrades

Subgrade stabilization with lime is a routine operation in the State of Texas and is often done to develop a working platform upon which to construct and compact the base layer. However, it has been observed that substantial pozzolanic reaction can occur if appropriate amounts of lime are added. The pozzolanic reaction results in increased stiffness, improved load-carrying capacity, better durability, and reduced seasonal stiffness fluctuations. Increased shear strength and hence deformational resistance offered by the lime stabilized subgrade layer could improve the cost effectiveness of pavement designs.

The behavior and performance of pavement systems are greatly affected by their subgrade support conditions. In recent years, good correlation has been found between performance and the elastic or recoverable surface deflection of flexible pavements. Because typically 60 to 70 percent of the elastic or recoverable deflection observed at the surface of a flexible pavement is accumulated in the subgrade, it is obvious that the behavior of subgrade soils subjected to repeated loads of short duration is an important consideration in pavement design (Robnett and Thompson 1976).

In Robnett and Thompson (1976), it has been shown that lime treatment of fine-grained subgrade soils has definite potential for beneficially altering subgrade softening due to high moisture content and freeze-thaw action. The effect that moisture content and freeze-thaw cycles have on the resilient response were examined on a number of treated and untreated soils; and a finite element procedure was used to evaluate the structural response of a flexible pavement on untreated and lime-treated subgrades. The analysis revealed that high moisture contents and freeze-thaw action in the subgrade have a detrimental effect on the magnitude of pavement response parameters and that lime treatment of the upper layer of the subgrade causes a substantial improvement in pavement response.

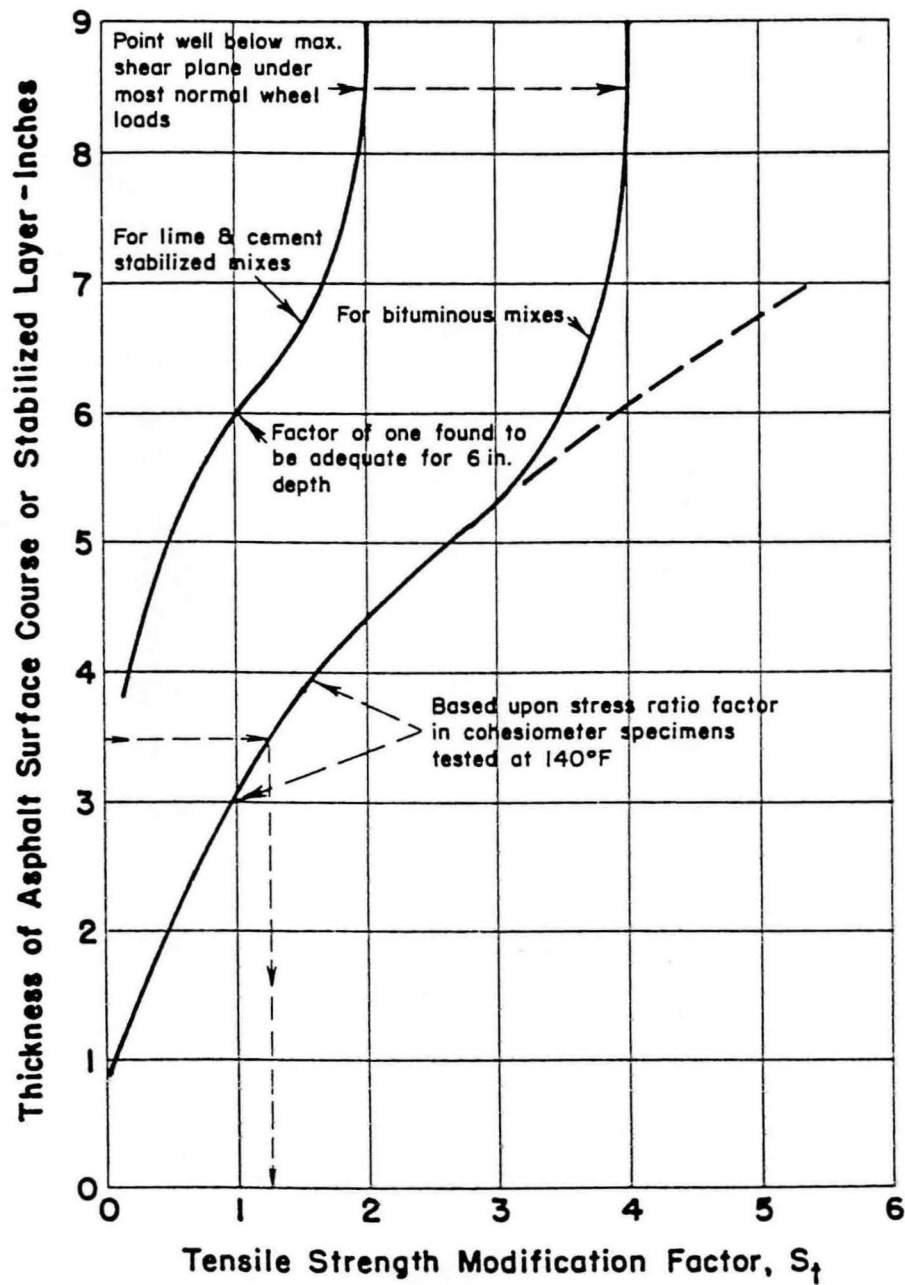


Figure A-21 Tensile strength modification factor (McDowell, 1972).
 1 in = 25.4 mm
 $1^{\circ}\text{F} = 9/5^{\circ}\text{C} + 32$

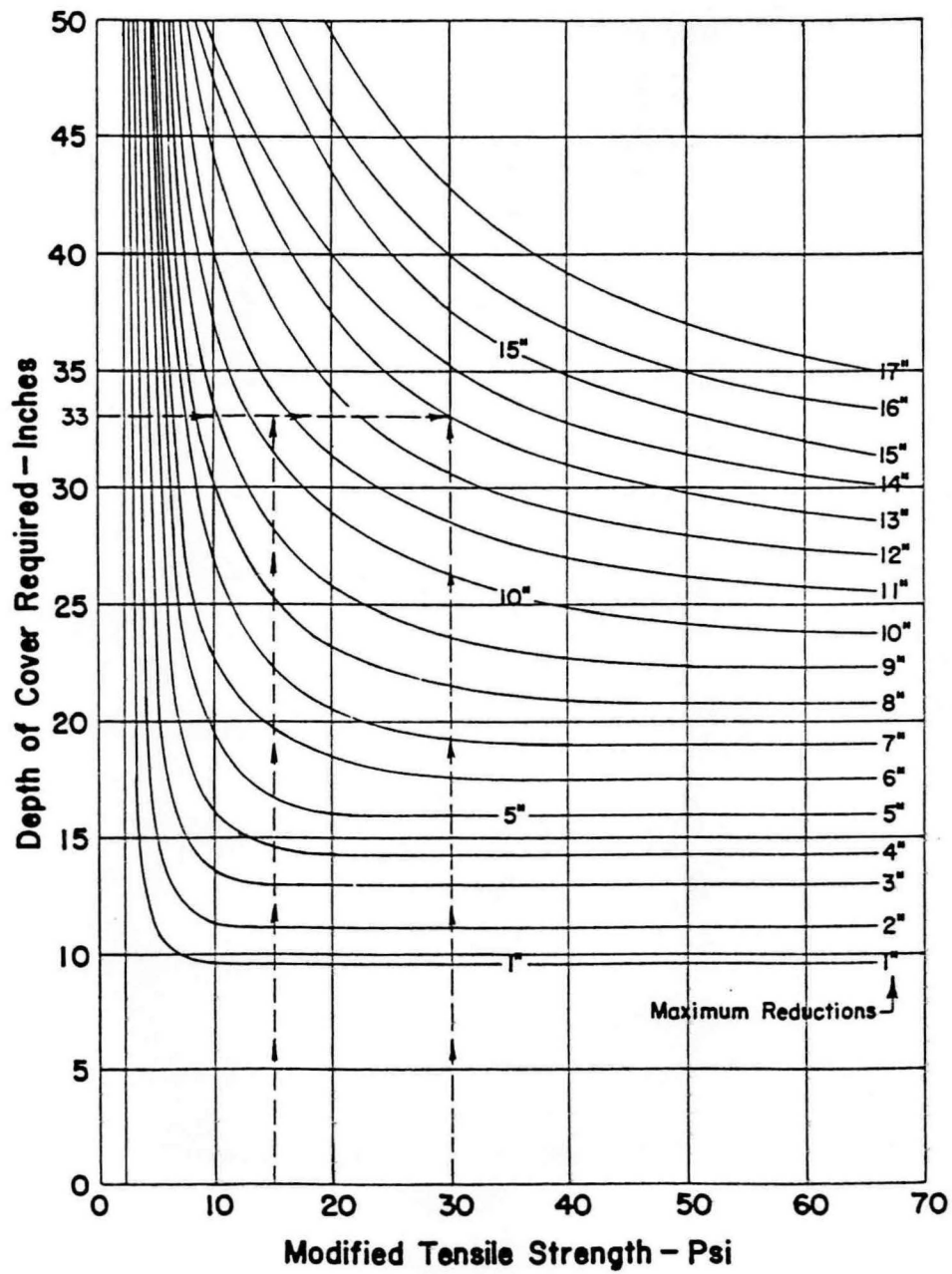


Figure A-22 Pavement thickness reduction chart (McDowell, 1972).

1 in = 25.4 mm

1 psi = 6,894 Pa

Total Equivalent
18 Kip Single Axle
Load Applications

When Tests Show Materials to be
Specifications Grades* of Base Materials

Item 248

	Grade 1	Grade 2	Grade 3**	
14,000	ST	ST	ST	
25,000	ST	ST	ST	
38,000	ST	ST	ST	
61,000	ST	ST	1-1/2	
100,000	ST	1-1/2	2	
150,000	ST	1-3/4	2-1/2	
250,000	1-1/4	2	3	} Not recommended for use except where availability of better base materials is very expensive.
400,000	1-1/2	2-1/4	3-1/2	
600,000	1-3/4	2-1/2	4	
1,000,000	2	3	4-1/2	
1,500,000	2-1/2	3-1/2	5	
2,500,000	3	4	5-1/2	
4,000,000	3-1/2	4-1/2	6	
10,000,000	4-1/2	5-1/2	7	

* It is assumed that the material in question is no better than the grade shown.
** Exclusive of Cohesionless Materials.

Notes: ST denotes surface treatments.

Stage construction of surfacing permitted if traffic studies indicate slow
development of axle load equivalencies.

Test Method Tex-117-E

Rev: June 1964

Figure A-23 Suggested thickness of surface courses (McDowell, 1972).
18 K = 80 KN
1 in = 25.4 mm

Effect of Subgrade Resilience on Pavement Structural Response

Resilient modulus is defined as applied deviator stress divided by recoverable or resilient strain. To demonstrate the influence of subgrade resilient behavior on pavement response, two identical flexible pavement sections were compared, but with each supported by a different subgrade. Two Illinois subgrade soils, one high in silt content (Fayette C) and the other high in clay content (Tama B), displaying substantially different resilient responses (Figures A-24, A-25, and A-26) were considered as supporting subgrades. Pertinent properties of these soils are given in Table A-2. The structural response of the flexible pavement subjected to a 40 KN (9-kip) wheel load was analyzed by using a finite element computer program that considers the stress-dependent or nonlinear response of the subgrade soil and the granular base course material (Robnett and Thompson, 1976).

Table A-3 summarizes the response data obtained from the analysis of the pavement on the two subgrades. It should be noted from the data presented in this table that substantial differences in pavement structural response can be effected by differences in subgrade resilient characteristics. It can be seen from that table that the surface deflection is about 60 percent greater for the pavement on the Fayette C subgrade than for the pavement on the Tama B subgrade. Similar trends are noted for the other pavement response factors (Robnett and Thompson, 1976).

Resilient Behavior of Lime-Treated Soils

Lime has been widely and successfully used as a stabilizing agent for fine-grained plastic soils. When lime is added to a fine-grained soil, several reactions are initiated. Cation exchange and agglomeration-flocculation reactions take place rapidly and produce immediate changes in soil plasticity, workability, and swell properties. Plasticity and swell are reduced and workability is substantially improved because of the low plasticity and the friable nature of the mixture. Depending on the characteristics of the soil being stabilized, a soil-lime pozzolanic reaction may commence. The cementing agents formed as a result of the pozzolanic reaction increase mixture strength and durability. The strength properties of lime-treated soil mixtures at early ages are important in certain aspects of pavement design and construction. Immediate stability increases have been noted due to lime treatment of fine-grained soils. From the standpoint of long-term pavement behavior and performance, it is desirable to have a knowledge and understanding of the resilient characteristics of lime-treated soil mixtures (Robnett and Thompson, 1976).

Effect of Lime Treatment on Resilient Behavior

It can be demonstrated that, without exception, the resilient response of uncured lime-treated soil is substantially different from the response of untreated soil. Figure A-26 shows (a) the typical stress-dependent resilient behavior of untreated and lime-treated fine-grained soils, (b) the effect that compaction moisture content has on resilient behavior, and (c) the beneficial effect that lime treatment has on resilient behavior. The immediate effects of lime

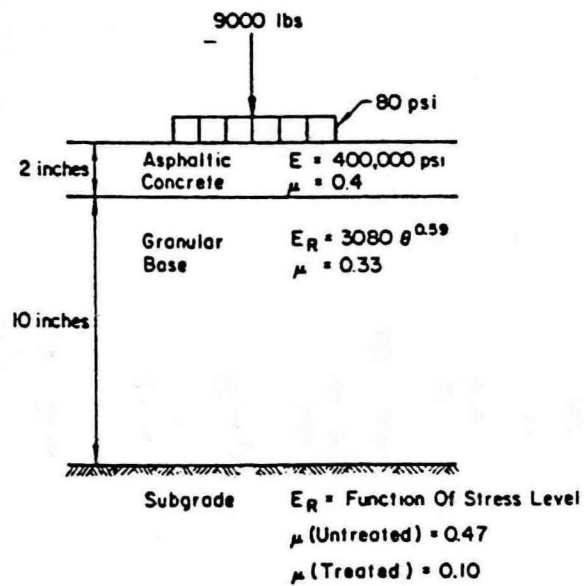


Figure A-24 Dimensions and properties of flexible pavement used in study with two Illinois subgrade soils to demonstrate the influence of subgrade resilient behavior on pavement response (Robnett and Thompson, 1976).

1 in = 25.4 mm

1 psi = 6,894 Pa

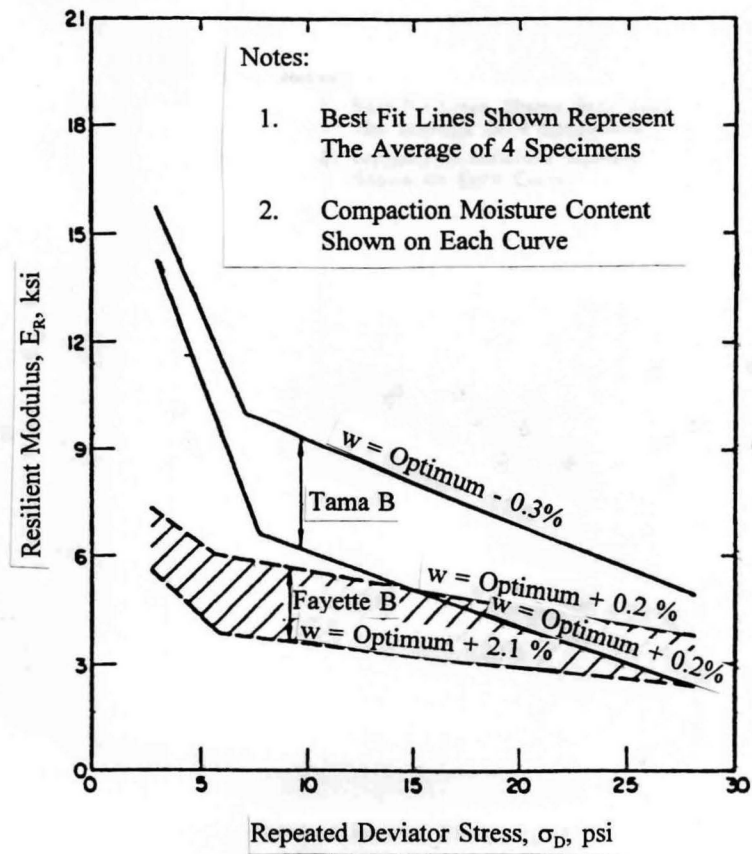


Figure A-25 Resilient behavior of Fayette C and Tama B subgrade soils (Robnett and Thompson, 1976).
 1 psi = 6,894 Pa

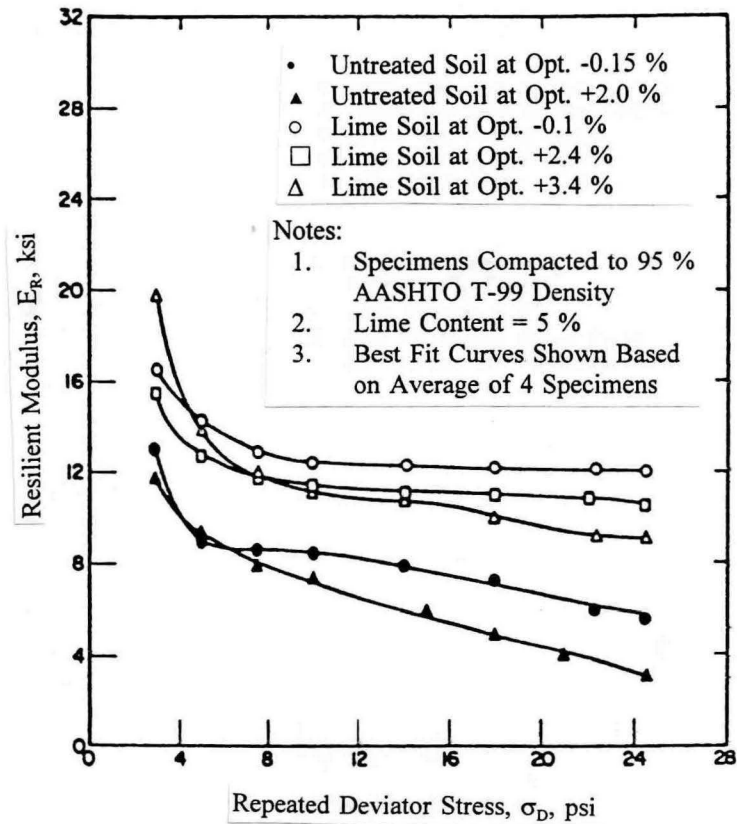


Figure A-26 Effect of lime treated and variable compaction moisture on resilient response of Flanagan B soil (Robnett and Thompson, 1976).
1 psi = 6,894 Pa

Table A-2 Summary of pertinent properties of Fayette C and Tama B soils (Robnett and Thompson, 1976).

Property	Fayette C	Tama B
Atterberg limits		
Liquid limit	32	46
Plasticity index	9	24
Grain size		
Percentage passing No. 200 sieve	98	100
Silt (0.002 to 0.050 mm), percent	75	67
Clay (< 0.002 mm), percent	18	32
AASHTO classification	A-4(9)	A-7-7(27)
Unified classification	ML	CL
Moisture-density (AASHTO T-99)		
% max, lb/ft ³	109.4	100.8
w _{opt} , percent	17.2	21.9
Soaked CBR	5.3	3.2
Compressive strength, ^a psi		
w = optimum	22	24
w = optimum + 2 percent	19	21

Note: 1 lb/ft³ = 16 kg/m³; 1 psi = 6.9 kPa

^a0 percent lime (95 percent AASHTO T.99)

Table A-3 Summary of results from analysis of pavement structural behavior on subgrades soils Fayette C and Tama B (Robnett and Thompson, 1976).
1 in = 25.4 mm
1 psi = 6,894 Pa

Subgrade Condition	Surface Deflection (in)		Radial Tensile Strain in Surface (in/in)		Compressive Strain in Subgrade (in/in)		Compressive Stress in Subgrade (psi)	
	Fayette C	Tama B	Fayette C	Tama B	Fayette C	Tama B	Fayette C	Tama B
Untreated								
Optimum moisture	0.060	0.041	0.00083	0.00065	0.00117	0.00076	10.9	13.1
Optimum + 2 percent	0.068	0.043	0.00087	0.00066	0.00161	0.00082	10.3	12.8
9-in freeze-thaw layer ^a	0.073	0.055	0.00089	0.00082	0.00297	0.00186	9.9	11.6
18-in freeze-thaw layer ^a	0.075	0.059	0.00089	0.00084	0.00271	0.00168	9.2	10.8
Lime treated								
9-in treated layer ^a	0.050	0.040	0.00065	0.00063	0.00074	0.00037	5.3	6.9
18-8in treated layer ^a	0.045	0.039	0.00063	0.00061	0.00039	0.00021	2.8	3.8

Note: 1 in = 2.5 cm; 1 psi = 6.9 kPa
For optimum + 2 percent compaction moisture condition

on the resilient behavior are evident. The resilient behavior is substantially improved (increased resilient modulus, reduced resilient deflection) when lime is added. Also, compared to the untreated soil at optimum moisture, lime treatment causes a substantial increase in resilient moduli (higher resistance to repeated loads) at moisture contents as high as 3.4 percent above optimum (Robnett and Thompson, 1976).

In Raad and Figueroa (1980), it is assumed that failure of granular and subgrade soils under repeated loads is governed by the Mohr-Coulomb theory. Thus for a given state of stress, failure occurs when

$$\sigma_1 = \sigma_3 \tan^2 \left(45 + \frac{\phi}{2} \right) + 2c \tan \left(45 + \frac{\phi}{2} \right) \quad (A-4)$$

in which σ_1 = major principal stress,
 σ_3 = minor principal stress,
 c = cohesion, and
 ϕ = friction.

This test should be performed at rates of loading similar to those induced by traffic loads. At failure the principal stress state, σ_1, σ_3 , defines a circle tangent to the Mohr-Coulomb envelope. Such a stress state, when repeated, will cause yielding of the material and a corresponding increase in permanent strain. Resilient strains, on the other hand, remain unaffected as shown in the Figure A-27, i.e., the amount of resilient strain remains the same although the amount of permanent strain increases with repeated loading. The ratio of the repeated deviator stress to the recoverable strain is defined as the resilient modulus, M_R , and is a function of applied stresses. For granular soils resilient modulus (M_R) is expressed as:

$$M_R = K\theta^n \quad (A-5)$$

where

θ = $\sigma_1 + \sigma_2 + \sigma_3$,
 σ_1, σ_2 , and σ_3 = principal stresses, and
 k and n = material constants.

For fine-grained soils compacted on the "wet side" of optimum moisture content and subjected to deviator stresses at low values of confining pressure similar to those induced by traffic loads,

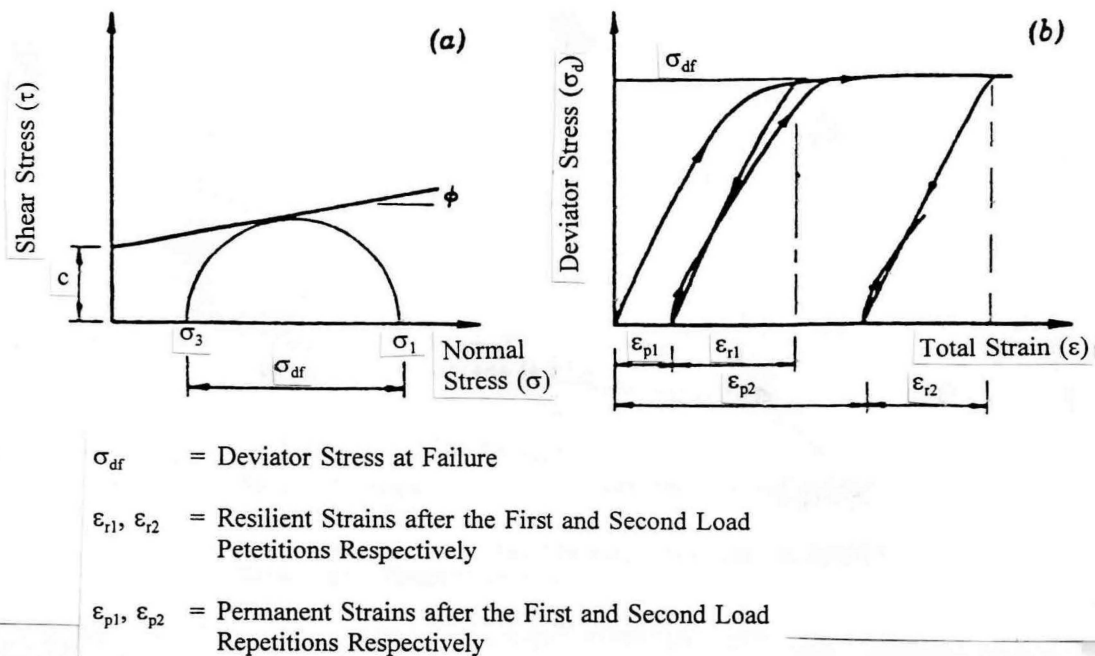


Figure A-27 Effect of repeated stress on permanent and resilient strains at failure of granular and subgrade soils (Raad and Figueroa, 1980).

$$M_R = K_2 - K_3 [K_1 - (\sigma_1 - \sigma_3)] ; K_1 > (\sigma_1 - \sigma_3) \quad (A-6)$$

$$M_R = K_2 + K_4 [(\sigma_1 - \sigma_3) - K_1] ; K_1 < (\sigma_1 - \sigma_3) \quad (A-7)$$

where

$$\begin{aligned} K_1, K_2, K_3, \text{ and } K_4 &= \text{material constants; and} \\ K_3 \text{ and } K_4 &= \text{the rate of change of } M_R \text{ with repeated deviator stress } \sigma_1 - \sigma_3. \end{aligned}$$

The finite element method can be used to determine the stresses and resilient deformation in a given pavement system. The system is discretized into a set of elements connected at their joints or nodal points. Nonlinear properties of the granular and subgrade layers are included by means of a successive iteration technique. The principal stresses in the granular and subgrade layers are modified at the end of each iteration so that they do not exceed the strength of the material as defined by the Mohr-Coulomb envelope. This is achieved by using the vertical stress, σ_v , in each element at the end of the iterative step to calculate limiting values for major and minor principal stresses $(\sigma_1)_{\max}$ and $(\sigma_3)_{\min}$, respectively, such that

$$(\sigma_1)_{\max} = \sigma_v \tan^2(45 + \frac{\phi}{2}) + 2c \tan(45 + \frac{\phi}{2}) \quad (A-8)$$

$$(\sigma_3)_{\min} = \sigma_v \tan^2(45 - \frac{\phi}{2}) - 2c \tan(45 - \frac{\phi}{2}) \quad (A-9)$$

If σ_3 and σ_1 are the minor and major principal stresses at the end of the iterative step, respectively, then σ_3 should not be smaller than $(\sigma_3)_{\min}$ and σ_1 should not exceed $(\sigma_1)_{\max}$. However, σ_1 should not assume a value greater than σ'_1 , the major principal stress associated with σ_3 at failure where

$$\sigma'_1 = \sigma_3 \tan^2(45 + \frac{\phi}{2}) + 2c \tan(45 + \frac{\phi}{2}) \quad (A-10)$$

The relation between modulus and unconfined compressive strength has been shown in Thompson and Robnett (1979). Regression equations relating E_{Ri} , and unconfined strength and E_{Ri} and static modulus are

$$E_{Ri} = 3.46 + 1.9E; R = 0.73; S_{\frac{\cdot}{x}} = 2.43 \quad (A-11)$$

$$E_{Ri} = 0.86 + 0.307q_u; R = 0.684; S_{\frac{\cdot}{x}} = 2.61 \quad (A-12)$$

where

- E = Static modulus, in kips per square inch,
- q_u = Unconfined compressive strength in psi, and
- Sx = Standard error of estimate.

CEMENT STABILIZATION

Soil Cement Reactions

Cement stabilization resembles lime stabilization in many ways, except with cement, pozzolanic material combined with calcium oxide present in the cement initially and need not be derived from the soil itself. In predominantly coarse-grained soils the cement paste bonds soil particles together by surface adhesion forces between the cement gel and particle surfaces. In fine-grained soils the clay phase may also contribute to the stabilization through solution in the high pH environment and reaction with the free lime from the cement to form additional calcium silicate hydrate (CSH). A basic difference is that the cement stabilization reaction with coarser soil occurs more quickly than does the lime-soil reaction. However, both cement and lime reactions continue with time. The crystallization structure formed by the set cement is mainly extraneous to the soil particles. This structure can be disrupted by subsequent swelling soil particle groups if an insufficient cement content is used. Disruption of the cement structure can also be caused by certain salt solutions; e.g., sulfates, although some of these salts, if present initially, may have a beneficial effect (Little et al. 1982).

Improvements of Engineering Properties

Compressive Strength

Unconfined compressive strengths can range considerably from below 1,400 KPa (200 psi) for fine-grained soil to over 14,000 KPa (2,000 psi) for coarse grained soils with higher cement contents (about 15 percent by weight). The relationship between strength and curing time for a given soil and cement mixture can be approximated by (Little et al., 1982)

$$(UC)_d = (UC)_{d_0} + K \log (d/d_0);$$

where

- $(UC)_d$ = unconfined compressive strength at an age of d days, in psi;
 $(UC)_{d_0}$ = unconfined compressive strength at an age of d days, in psi;
 K = 70 C for granular soils and 10 C for fine-grained soils and
 C = cement content, in percent by weight. (A-13)

The 28-day strength was found to be 1.4 to 1.7 times the 7-day strength by different researchers. A value of 1.5 times the 7-day strength would seem a reasonable value for estimating purposes (Little et al., 1982).

Tensile Strength

The tests used to evaluate the tensile strength are the flexural beam, direct tension, and the split tension test. The flexural strength is about one-fifth to one-third of the unconfined compressive strength. A good approximation for the flexural strength f is:

$$f = 0.51 (UC)^{0.88} \quad (A-14)$$

Griffith crack theory characterizes the strength of cement-treated soils under various combinations of major (σ_1) and minor (σ_3) principal stresses. With the normalized strength data, and a knowledge of the unconfined compressive strength, principal stress combinations causing failure can be directly estimated. These data may help to predict fracture potential for specialized or expedient design situations (Little et al., 1982).

Deformation Characteristics and Moduli

The stress-deformation behavior of cement-stabilized soils is nonlinear and stress dependent. However, for many soils and treatment levels and within limited loading ranges, the material may be assumed as linearly elastic under repeated loadings. Deformation moduli may range from about 70,000 KPa (10,000 psi) to several million psi, depending on soil type, treatment level, curing time, water content and test conditions. Cement-treated fine-grained soils have modulus values near the lower end of the range whereas granular soil-cements exhibit the higher value dependent on soil type, cement content, compaction and curing conditions, and test type. With load repetitions in the range of a few hundred to 10,000, the resilient modulus in compression M_{RC} can be expressed by (Little et al., 1982):

$$M_{RC} = K_C (\sigma_1 - \sigma_3)^{-k_1} (\sigma_3)^{k_2} (UC)^n \quad (A-15)$$

where

UC	=	unconfined compressive strength, in psi;
$(\sigma_1 - \sigma_3)$	=	deviator stress, in psi;
σ_3	=	confining pressure, in psi;
K_C	=	material constant;
k_1	=	0.2 to 0.6;
k_2	=	0.25 to 0.7;
n	=	$1.0 + 0.18 C$; and
C	=	cement content in percent by weight.

Determination of k_1 , and k_2 and K_C requires separate measurements of M_{RC} under at least two values of σ_3 and two values of $(\sigma_1 - \sigma_3)$. If it is assumed that confining pressure has no effect on resilient modulus in flexure, M_{RF} , then, from the results of beam tests (Little et al., 1982):

$$M_{RF} = K_F (10)^m UC \quad (A-16)$$

where

K_F	=	material content;
UC	=	unconfined compressive strength, in psi;
m	=	$0.04(10)^{-0.186C}$; and
C	=	cement content in percent by weight.

At working stress levels for pavement bases and treated subgrades, Poisson's ratio is in the range of 0.1 to 0.2 for treated granular soils. Treated fine-grained soils exhibit somewhat higher values, with a typical range of 0.15 to 0.35 (Little et al., 1982).

Fatigue Behavior

These are some observations pertaining to the fatigue behavior of cement-treated soils. Fatigue life is shorter under repeated direct tensile stresses than in compression. Flexural fatigue is unlikely for repeated stress levels less than 50 percent of the flexural strength. The flexural fatigue of soil-cement can be related to radius of curvature according to (Little et al., 1982)

$$R_c/R = aN^{-b} \quad (A-17)$$

where

- R_c = critical radius of curvature, i.e., the radius of curvature causing failure under static loading;
- R = radius of curvature leading to failure under N load applications;
- a = $h^{3/2} / 2.1(h-1)$;
- h = slab thickness, inches;
- b = 0.025 for granular soil-cements and 0.050 for fine-grained soil cements; and
- N = number of load applications.

From its initial value T_i , the tensile strength progressively decreases from repeated tensile stresses, and when the strength drops to F , cracking failure is initiated.

Shrinkage

Cement-treated soils demonstrate shrinkage on curing and drying in an amount that depends on cement content, soil type, water content, degree of compaction, and curing conditions. Observations show the cracks to be from 1/8 to 1/4 inch wide at spacings of 10 to 20 feet. It is important to consider edge loading conditions in thickness design and to provide surface sealing so that water is prevented from entering the subgrade with consequent loss of support (Little et al., 1982).

Models of the Fatigue Behavior of Cement-Treated Bases

Griffith Model as Developed by Raad

Raad, et al.(1977) used the Griffith failure theory (1924) to develop an analytical model of the fatigue behavior of cement-treated materials subjected to triaxial stress pulses. The model can be used to establish an analytical approach for the design of cement-stabilized layers in pavement sections that accounts for both crack initiation and crack propagation in the layers. Griffith (1924) assumed that the fracture is caused by stress concentrations at the tips of minute Griffith cracks or starter flaws that are presumed to occur in the material, and that it is initiated when the maximum stress near the tip of the most favorably oriented crack reaches a value characteristic of the material. The Griffith criterion for failure can be written as

$$(\sigma_1 - \sigma_3)^2 / (\sigma_1 + \sigma_3) = 8 T_0 = \sigma_c \quad (\sigma_1 + 3 \sigma_3 \geq 0)$$

and

$$\sigma_3 = - T_0 = - \sigma_c / 8 \quad (\sigma_1 + 3 \sigma_3 \leq 0) \quad (A-18)$$

where

- σ_1 = major principal stress,
- σ_3 = minor principal stress,
- T_0 = tensile strength, and
- σ_c = unconfined compressive strength.

In his derivation, Griffith assumed that the cracks were open and elliptical in shape. Under compressive conditions ($\sigma_1 > 0$, $\sigma_2 > 0$) the cracks may close and the modified Griffith theory will be more applicable. Experimental data for failure of cement-treated soils as presented by many investigators are plotted in Figure A-28. The major and minor principal stresses are normalized in terms of the unconfined compressive strength σ_c . The Griffith failure criterion seems to apply for values of σ_3/σ_c less than 0.1, whereas for values of σ_3/σ_c greater than 0.1 the modified Griffith criterion is more appropriate to use. In this case, the modified criterion can be expressed as

$$\sigma_1/\sigma_c = 5 (\sigma_3/\sigma_c) + 1 \quad (A-19)$$

Analytical Fatigue Model

At any point in the base, the stress state generated by a moving wheel load can be represented by the principal stresses (σ_1 , σ_2 ,and σ_3). Because these stresses are repeatedly applied under the action of traffic loads, the strength of the cement-treated material will decrease until failure occurs. Let F be a stress factor defined as

$$\begin{aligned} F &= (\sigma_1 - \sigma_3)^2 / 8 (\sigma_1 + \sigma_3) \quad (\sigma_1 + 3\sigma_3 \geq 0) \\ F &= -\sigma_3 (\sigma_1 + 3\sigma_3 \leq 0) \end{aligned} \quad (A-20)$$

Failure will take place when the tensile strength of the material decreases from an initial value (T_i) to a value of (T') equal to the maximum value of the stress factor (F_{max}), which is defined by the σ_1 and σ_3 pulses. The variation of tensile strength with the number of repetitions of stress applications for a given F_{max} is shown in Figure A-29. The strength decrease is defined in terms of a rate "a" given by

$$\begin{aligned} a &= (\log T_i - \log T') / (\log N_f - \log 1) \\ &= (\log T_i - \log F_{max}) / \log N_f \\ &= \log [1 / (F_{max} / T_i)] / \log N_f \end{aligned} \quad (A-21)$$

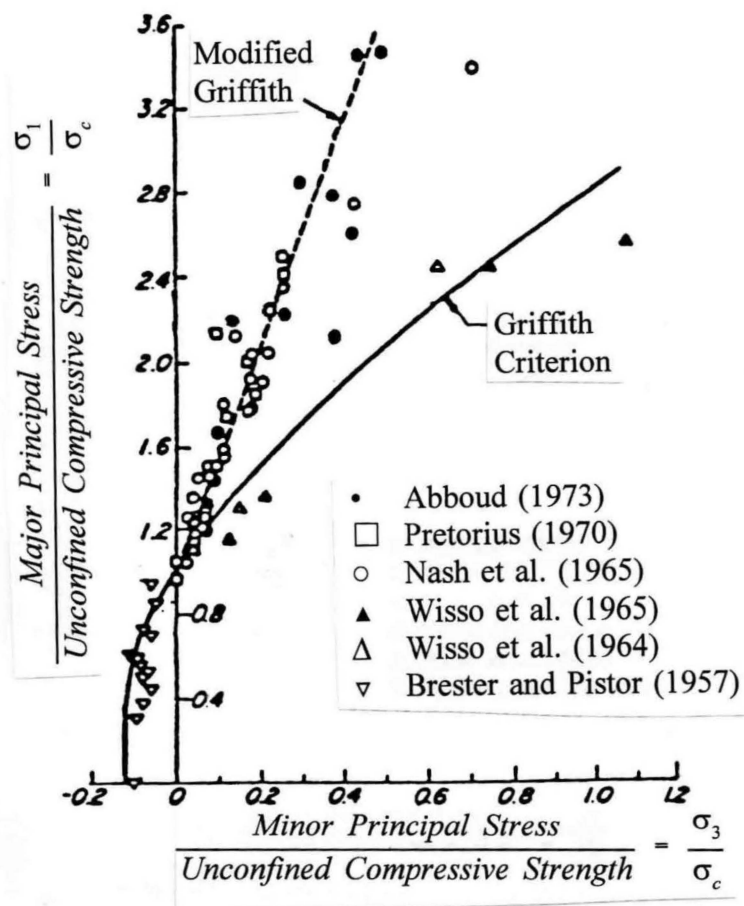


Figure A-28 Failure envelope for cement-treated soils (Raad et al., 1977).

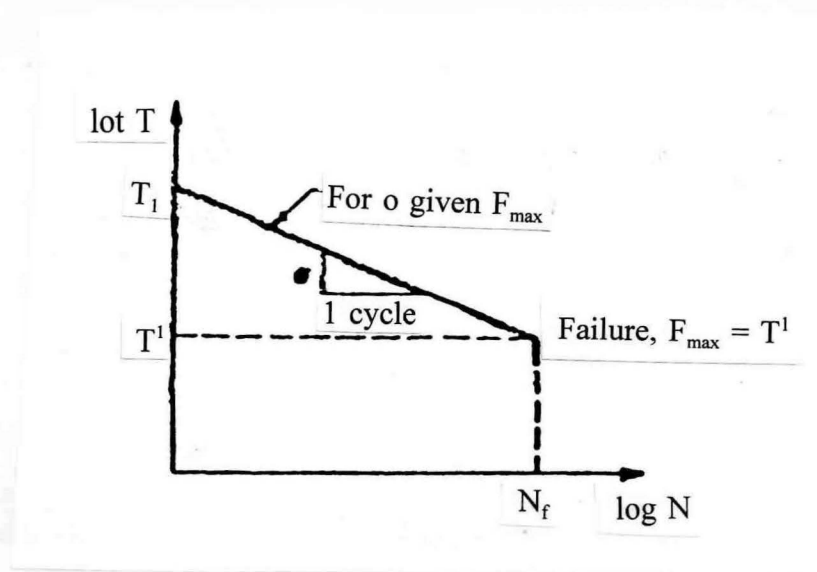


Figure A-29 Variation of tensile strength with number of stress applications for a given F_{max} (Raad et al., 1977).

where N_f = number of repetitions to failure. From the definition of a , the number of stress repetitions to failure (N_f) can be written as

$$\log N_f = \log[1/(F_{\max}/T_i)^a] \quad (A-22)$$

Therefore, the number of stress repetitions to failure can be determined for a given " a " and F_{\max}/T_i . The relation that describes the variation of F_{\max}/T_i with N_f defines the fatigue-failure criterion for a cement-treated material. The values for a and F_{\max}/T_i are obtained from Figure A-30 and are used in equation A-22 to establish a relationship between F_{\max}/T_i and N_f as shown in Figure A-31.

Crockford and Little AFOSR Model

According to Crockford and Little (1987) and Kim and Little (1987), rate of crack propagation and critical stress intensity factors which control fracture propagation can be determined in soil cement material by using (1) bending beam fracture testing (ASTM D813), (2) compact tensile testing, and/or a simple system of creep tests performed at various levels of relative humidity. Bendana (1988), describes a mechanistic design methodology that permits a rational computation of equivalent wheel load factors (EWLFs) for airfield pavements with stabilized layers. Bendana (1988) used fracture mechanic constants for cement stabilized soil that developed by Crockford (1924). The acquisition of these data in conjunction with the fracture mechanic theory discussed by Crockford and Little (1987) permitted the development of a mechanistic design methodology to estimate EWLF. Also, a finite element computer program was studied, verified, and modified to compute stress intensity factors. The Bendana program can be used to compute EWLF's for any vehicle. This approach also determines the number of equivalent strain repetitions of the standard vehicle. The equivalent strain repetitions are a function of the EWLF, the actual number of passages of the j -aircraft and the maximum transverse distribution factor ($\max f_j$) for each aircraft under consideration. The f_j factor converts the number of passages of the j -aircraft to the number of times the j -aircraft actually stresses a particular point on the pavement. The EWLF value indicates the unit damage caused by the j -aircraft relative to the unit damage caused by the standard aircraft. This program and analytical technique can easily be modified to consider highway type traffic and loading considerations.

Kim and Little Fracture Model

Kim and Little (1987) proved that excellent estimates of the fracture properties can be calculated based on tensile creep and indirect tensile strength testing. According to Kim, Schapery's crack velocity equation based on the generalized power law can be used to predict the tendency of compacted soil-cement to fatigue. Predicted values of $\log A$ and n (the intercept and slope, respectively, of the crack speed versus change in stress intensity

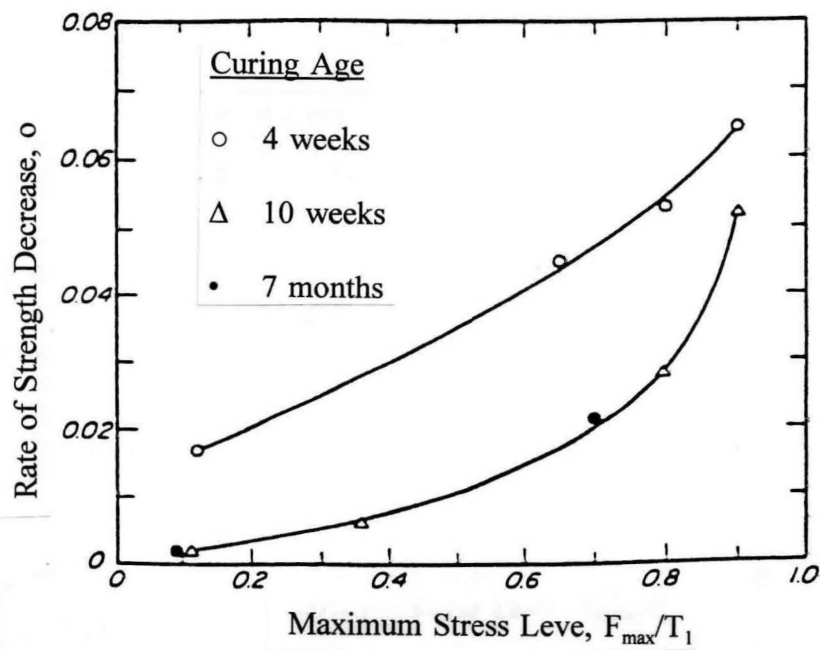


Figure A-30 Variation of "a" with $(F_{\max})/T_i$ (Raad et al., 1977).

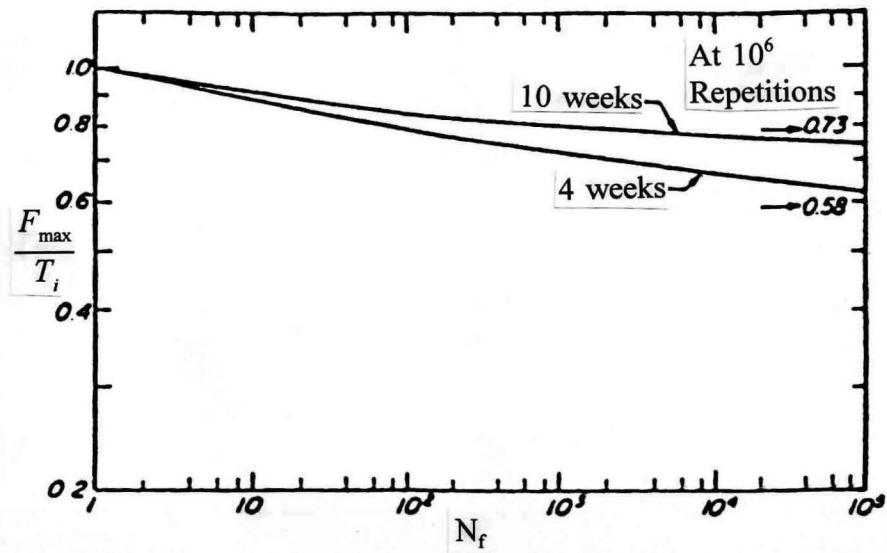


Figure A-31 Suggested fatigue failure criteria for cement-treated soils (Raad et al., 1977).

factor relationship, based on the Schapery model) are very strong linear functions of $1/m$ (the reciprocal of the log-log slope of the tensile compliance curve). The regression equation relating $\log A$ and m and n are as follows:

$$\begin{aligned}\log A &= -4.956 - 7.463 * 1/m, \text{ with } R^2 = 0.955 \text{ and} \\ n &= 1.727 + 1/m, \text{ with } R^2 = 0.998.\end{aligned}\tag{A-23}$$

The crack growth parameters of the soil cement, A and n , can be predicted from the viscoelastic exponent of the creep test, m , and the regression equations.

Incorporation of bi-modularity as developed by Raad

Raad (1985) offered an improved approach to the analysis of pavements with stabilized layers. The method incorporates the bimodular properties (i.e., tensile modulus different than compressive modulus) of the stabilized layer and the stress-dependent behavior of granular and subgrade soils. The proposed method could be used to predict stresses, resilient strains, and deformations using a finite element representation of the pavement structure. The proposed method has been used to study the behavior of stabilized layers under repeated loads. A limited number of split tension and flexure tests conducted on a cement treated silty clay show that the material exhibits bimodular behavior and that modulus values computed for similar specimens are generally different and depend on testing procedure and method of computation. On the basis of laboratory results, it has been proposed to characterize the stabilized layer in terms of its split tensile strength. This method of characterization was incorporated in the analysis to study the behavior of stabilized layers in pavements. Specifically, the influence of material characteristics on response prediction and the fracture of stabilized layers under repeated loads have been investigated. Results of the analysis show that an increase in bimodular ratio tends to increase the tensile strains and decrease the tensile stresses on the underside of the stabilized layer. Fracture of stabilized layer, on the other hand, depends on stiffness, strength, and bimodular properties of stabilized material and on stiffness of underlying subgrade.

Selection of Best Model

Among all the fatigue models, the Griffith model as developed by Raad (1977) is easily and directly applicable to pavement design and analysis. The Griffith crack approach appears applicable to the description of cement-treated soils under the various combinations of σ_1 and σ_3 that are likely to be encountered in a treated layer. It also offers the advantage of requiring knowledge of only the unconfined compressive strength of the material. The model can be used to establish an analytical approach for the design of cement-stabilized layers in pavement sections that accounts for both crack initiation and crack propagation in the layers.

Raad, et al. (1977) used the fatigue data shown in Table A-4 to compare experimental fatigue data and the fatigue-failure criteria. The variables used in the comparison were (a) type of stabilized material, (b) cement content, (c) frequency of applied stress pulses, and (d) curing age. Comparisons of the experimental and analytical results are shown in Figures A-32 through A-36. The ratio of the applied stress to the initial strength (i.e., the maximum stress level) is plotted versus the number of repetitions to failure. Analysis of the data shown in Figures A-32 through A-36 leads to the following conclusions (Raad et al., 1977).

1. The fatigue-failure criteria are appropriate for the prediction of the fatigue failure of cement-treated soils independent of the loading frequency.
2. The fatigue criteria for a curing age of 4 weeks agree well with the fatigue data for cement-treated materials that have a curing age of up to 4 weeks (Figures A-32 to A-36), and the criteria corresponding to a curing age of 10 weeks agree with the data for a curing age of 10 or more weeks (Figure A-36).
3. There is reasonable agreement between the experimental values and those that correspond to the suggested analytical criteria, independent of the type of stabilized soil and the cement content (Figures A-32 through A-36).

Thus, the suggested criteria fit the available fatigue data for cement-treated soils, for different curing ages, independent of type of material, cement content, and frequency of applied loads, which indicates the possible applicability of these criteria for cement-treated soils in general.

Work done in South Africa

The analysis of pavements with semi-rigid cement treated base (CTB) layers have traditionally presented engineers with problems concerning accurate predictions of expected behavior and hence of the remaining life of the pavement. The analysis of the pavement structure of Main Road MR27 in the Western Cape of South Africa, which contains a cement treated base course showed that a weak layer (± 40 mm thick) formed at the top of the CTB layer just below the asphalt surfacing and that the behavior of the pavement is controlled mainly by this layer (Jordaan, 1992).

Cement Structure and Observed Behavior

Main Road is a dual carriageway in the Western Cape in South Africa which was opened to traffic in 1971. The pavement structure is typical of a large number of roads constructed in South Africa during the late 1960's and consists of a 35 mm wearing course, a 230 mm strongly cemented base course (constructed in two layers) and a 200 mm laterite subbase on in-situ sand. The cement treated layers were constructed using crushed stone and

Table A-4 Design criteria for soil-cement bases using present analytical approaches (Raad et al., 1977).

Material	Cement Content (%)	Water Content (%)	Curing Age (d)	Dry Density (Mg/m ³)	Repeated Load Test	Reference
Well graded sand	6 to 14	9 to 11	7 to 28	1.99	Rotating cantilever	Symons
Uniformly grade sand	12 to 16	13	7	1.65	Rotating cantilever	Symons
Silty clay	6 to 14	19	7	1.68	Rotating cantilever	Symons
Crushed rock A-2-4, A-4, A-3,	4 to 8	8	7	2.03	Rotating cantilever	Symons
A-1-6	6.5 to 8.5	7 to 11	365	1.78 to 2.18	Flexural beam	Scott
A-2-4, A-4	6.7 to 8.4	10.7 to 12.4	28	1.78 to 1.89	Flexural beam	Scott
Lean clay	10	15.7	14 to 28	1.73	Flexural beam	Irwin
Gravelly sand	6	6.2	21	2.15	Flexural beam	Irwin
Clayey gravel	5.5	7.5	90	2.19	Flexural beam	Pretorius
Silty clay	8 to 16	38	14	1.39	Flexural beam	Bofinger
Uniform sand	6	9	2 to 14	1.84	Direct compression	Gregg

Note: 1 Mg/m³ = 62.4 lb/ft³

Mixing content

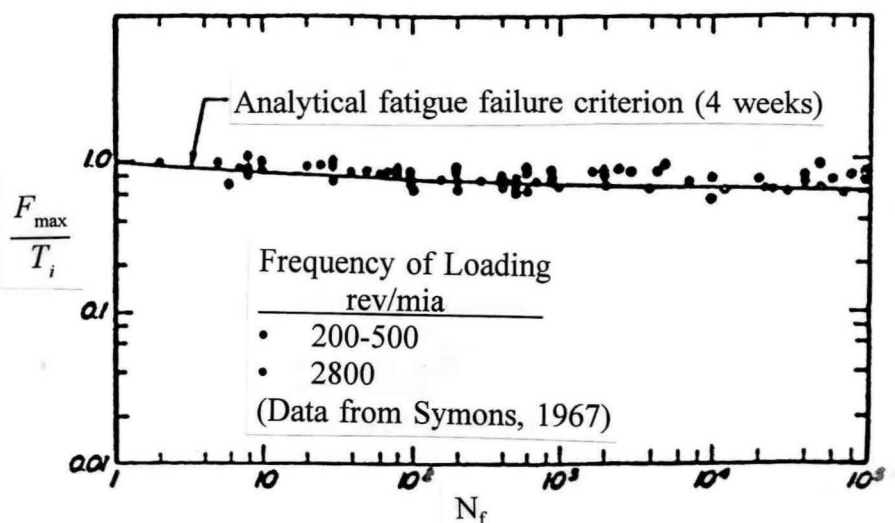


Figure A-32 Comparison of fatigue data for cement-treated (6 to 14 percent cement) well grades and (7 and 28 day curing) at different loading frequencies with suggested fatigue-failure criterion (Raad et al., 1977).

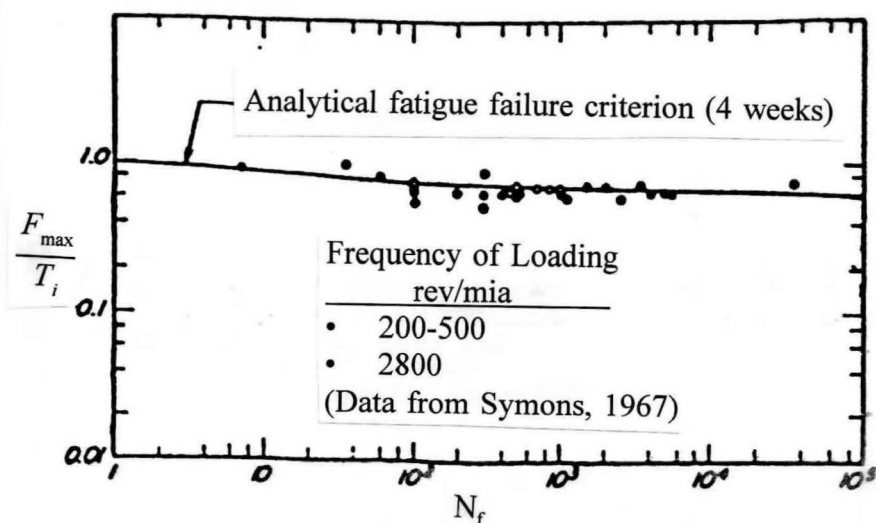


Figure A-33 Comparison of fatigue data for cement-treated (12 to 16 percent cement) uniformly graded sand (7 day curing) at different loading frequencies with suggested fatigue-failure criterion (Raad et al., 1977).

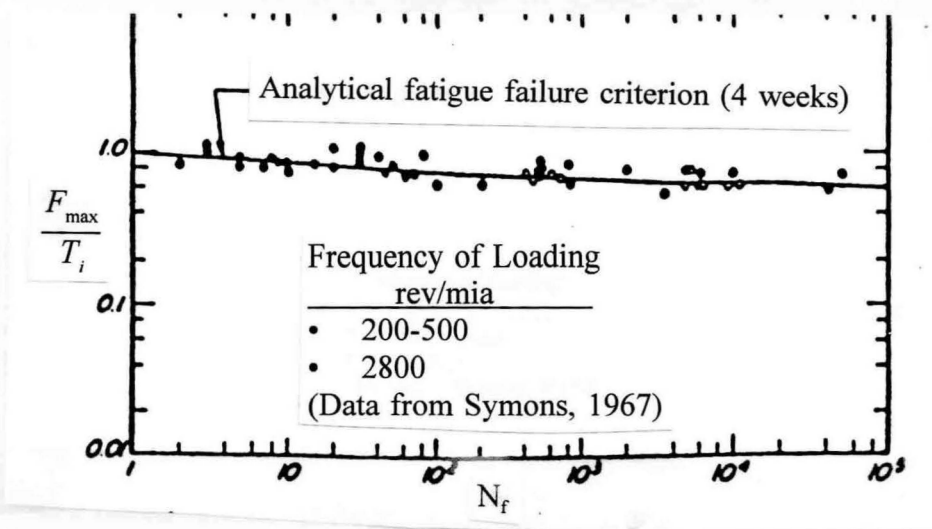


Figure A-34 Comparison of fatigue data for cement-treated (6 to 14 percent cement) silty clay (7 day curing) at different loading frequencies with suggested fatigue-failure criterion (Raad et al., 1977).

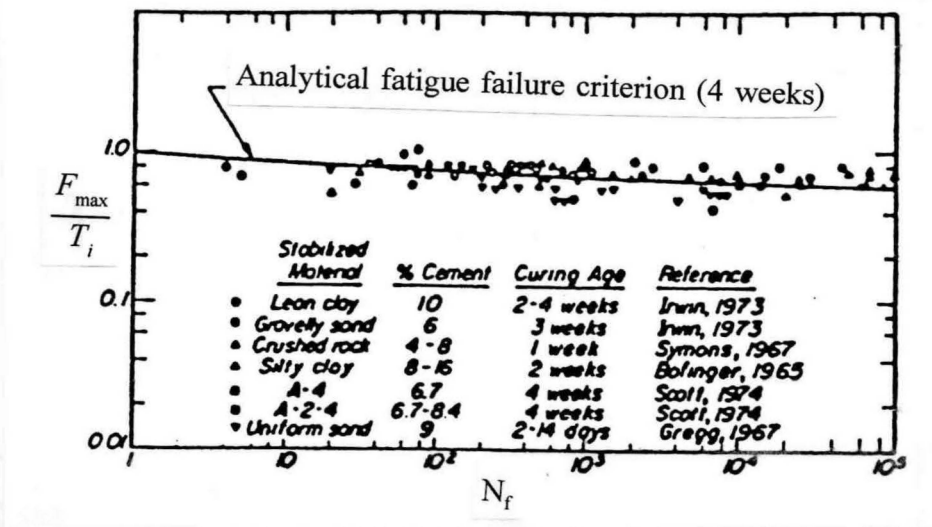


Figure A-35 Comparison of fatigue data for cement-treated soils (<4 weeks curing) with suggested fatigue-failure criterion (Raad et al., 1977).

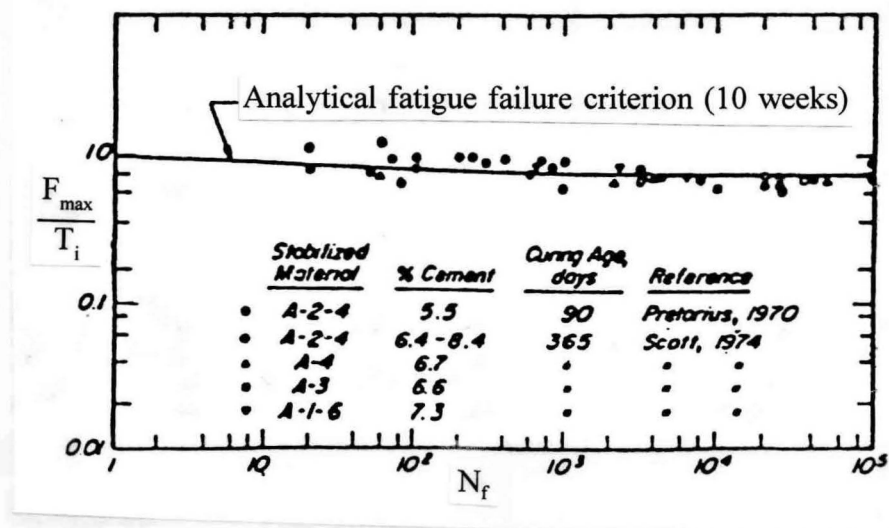


Figure A-36 Comparison of fatigue data for cement-treated soils (>10 weeks curing) with suggested fatigue-failure criterion (Raad et al., 1977).

a sand/soil filler in a 4:1 ratio and between 4 and 5 per cent cement by weight, added as a stabilizer. Shrinkage cracking (block cracking) typical of a pavement containing a strongly cement-treated base course developed early in the life of the road. An investigation showed that the distress was limited mainly to the top of the pavement, i.e. the wearing course and the top 40 mm of the CTB layer.

Modeling of the Behavior of CTB Layers

Elastic moduli in excess of 3000 MPa are generally considered applicable for the modeling of CTB layers in the mechanistic analysis of pavements in South Africa. However, in-depth deflection measurements often show that the effective elastic moduli are much lower. In the case of the road MR27 (2), the use of in-depth deflection measurements also resulted in the calculation of a relatively low effective moduli (500 to 600 MPa) for the "intact" CTB layer. The pavement was modeled using an effective modulus of 4000 MPa for the CTB layer and moduli for the other layers as derived from in-depth deflections measured at the beginning of the accelerated pavement test. Under these circumstances relatively low horizontal tensile strains develop under loading at the bottom of the CTB layer as shown in the Figure A-37. Hence, in this case, the recommended analysis procedure based on the maximum horizontal tensile strain at the bottom of the treated layer, gives no apparent reason for distress development (fatigue) in the CTB layer.

An analysis of the pavement using the low effective moduli of 500 to 600 MPa, calculated from in-depth deflections, give a horizontal strain profile through the CTB layer as shown in Figure A-38. Again, relatively low tensile strains develop at the bottom of the CTB layer. In order to explain the observed behavior, two factors are important in the modelling of the MR27.

1. The effective elastic moduli of apparently intact cement treated layers are much lower than the recommended values of more than 3000 MPa,
2. The maximum horizontal tensile strain is not always a maximum at the bottom of cement treated layers and can be used as a basis to explain the formation of distress as observed on the MR27.

Elastic Moduli of Cement Treated Pavement Layers

Fundamental to the explanation of the behavior of the distress observed on the MR27 is the modeling of the cement treated layer using an effective elastic modulus of between 500 MPa and 600 MPa. It is postulated that the effective linear elastic modulus of a good cement treated pavement layer is relatively high (>4000 MPa) directly after the construction of the pavement. Under these circumstances relatively low horizontal tensile strains develop at the bottom of the layer, when a load is applied to the pavement. However, in many cases,

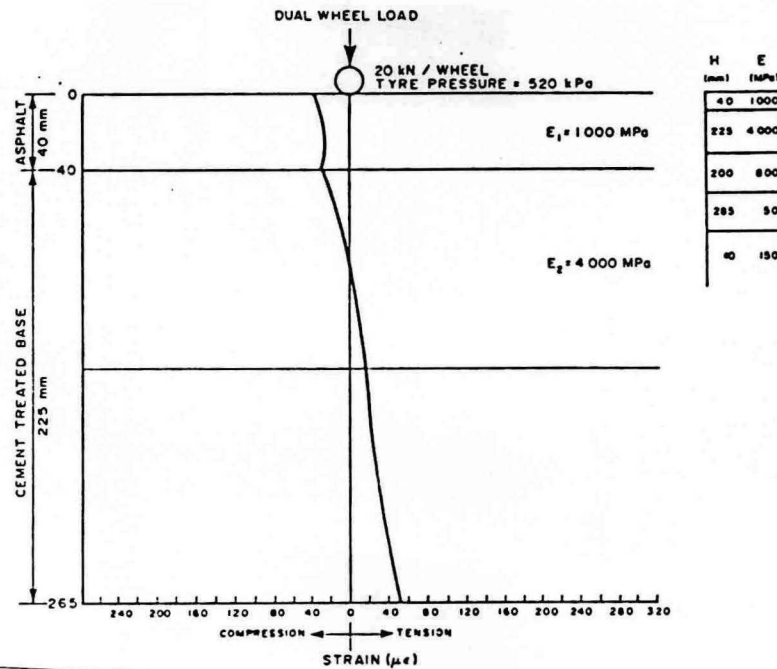


Figure A-37 Horizontal tensile strain in the CTB layer of the MR27 assuming a high effective modulus for the CTB layer (Jordaan, 1992).

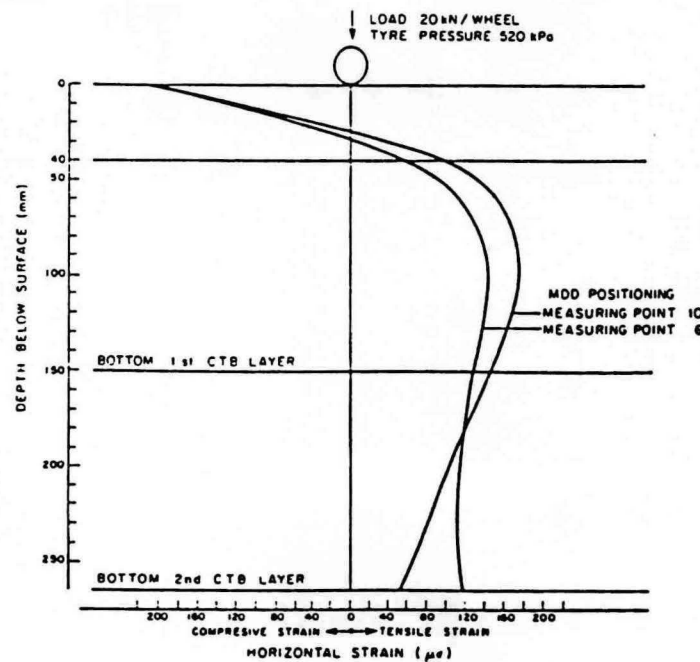


Figure A-38 Horizontal tensile strain in the CTB layer of the MR27 using effective elastic moduli calculated from measured in-depth deflections (Jordaan, 1992).

these low tensile strains are adequate to initiate the development of micro cracks. Above a certain critical loading condition, which is about 35 per cent of the strength and about 25 per cent of the strain at break, micro cracking starts as a loss of bond between the aggregate and the matrix of fine material and cement. Despite the case of micro-cracks, the cemented layer will still appear intact. If tested, the layer will also show a relatively high comprehensive strength ($UCS > 3 \text{ MPa}$). However, the tensile strength of the cement treated materials is much lower than the compressive strength and this weak link- the tensile strength must be evaluated and not the compressive strength. It follows that, under these circumstances, a CTB layer should ideally be modeled using an anisotropic modulus- high vertically in compression and low horizontally in tension. In the case of the assessment of the fatigue life of the layer in terms of its tensile strength, using the linear elastic theory which assumes isotropic behavior, it is appropriate to model the layer using an effective elastic modulus associated with the tensile strength of the layers.

The Development of Distress in the MR27

Assuming the accuracy of the above postulation for the use of relatively low effective moduli for CTB layers, the rapid reduction of the elastic properties of the CTB layer in the MR27 would have resulted in a horizontal tensile strain distribution as shown in the Figure A-39. It is seen that the maximum horizontal tensile strain develops close to the surfacing of the CTB layer and would cause the layer to break at that point. The life of the pavement up to the development of the break is considered to be Phase I in the behavior of the cemented layer. The break in the layer would result in a dramatic change in the strain distribution through the cemented layer as is shown in Figure A-40 (Phase II). It is expected that the sub-layer will break up further and develop into a "weak" inter-layer due to the very high horizontal tensile strains at the bottom of the sub-layer. It is also seen that the horizontal tensile strain in the remainder of the layer is relatively low and this part of the layer is expected to remain visibly intact for much longer.

Development of Procedures for the Analysis of Cement Treated Layers in Pavements

The MR27 pavement composition was used to investigate the influence of the various pavement and pavement layer characteristics on the position of the maximum horizontal strain within the layer. The results of the investigations were used to establish the balance (Be) between the critical pavement characteristics at which the maximum horizontal tensile strain shifts from a position at the bottom of the layer to a position within the cemented layer. It was found that the position at which the maximum horizontal tensile strain occurs is a function of the elastic moduli of the asphalt layer (E_1), the cemented layer (E_2), and the supportive layer (E_3) and the thickness of the asphalt layer (h_1) and the cemented layer (h_2). In fact it was found that:

$$Be = f(E_3, E_1, 1/E_2, h_1, h_2) \quad (A-24)$$

It was established that the maximum horizontal tensile strain will occur at the bottom of the layer if

$$(E_3/E_2)(h_1 (E_1/E_3)^{1/3} + h_2 (E_2/E_3)^{1/3}) < k \text{ (mm)}$$

where

- E_1 = elastic modulus of the asphalt layer (MPa),
- E_2 = elastic modulus of the cement treated base layer (MPa),
- E_3 = elastic modulus of the supportive layer (MPa),
- h_1 = thickness of the asphalt layer (mm),
- h_2 = thickness of the cement treated base layer (mm), and
- k = constant.

Preliminary findings from the analysis of a limited number of pavement structures indicate that $k = 128$.

Fatigue Life of CTB Layers in Pavements

The fatigue life of CTB layers to crack initiation, according to the South African mechanistic design method, is given by

$$N_f = 10^{9.1(1 - \frac{\epsilon_s}{\epsilon_b})} \quad (\text{A-25})$$

where

- N_f = number of repetitions at ϵ_s to crack initiation,
- ϵ_s = tensile strain in cemented pavement layer and
- ϵ_b = tensile strain of cemented material at break.

The above equation was derived in the laboratory and its applicability for use for the prediction of the life to the initiation of the visible cracking of pavement layers, is questionable. Experience in South Africa has shown that the field fatigue life of CTB layers is, in many cases, underestimated by the use of the above equation, and that some adjustment, to allow to field performance, may be required. This can be achieved by increasing the strain at break by a factor "m."

$$N_f = 10^{9.1(1 - \frac{\epsilon_s}{m\epsilon_b})} \quad (\text{A-26})$$

where

- N_f = number of 80 kN equivalent dual wheel axle loads at e_s to crack initiation,
- e_s = maximum horizontal tensile strain in the cement treated layer,
- e_b = tensile strain of the cement treated layer at break, and
- m = adjustment for in-situ pavement conditions (for MR27, the factor $m = 4.7$ was obtained).

Shrinkage/Reflection Cracking In Pavements

A part of the goal of project 1287 is to study the ability to modify existing reflection cracking algorithms based on fracture mechanics. The severity of reflection cracking above cracked stabilized layers will be highly sensitive to the cracking pattern existing in the stabilized layer. The following research needs exist regarding reflection cracking:

1. Available reflection cracking algorithms need to be studied as to their applicability to the problem of predicting reflection cracking above cracked stabilized base layers. Mechanistic-empirical design procedures which address reflective cracks in asphalt concrete pavements on cracked pavements have been developed and are available for use. The procedure developed for FHWA has been developed for use with asphalt concrete overlays on asphalt concrete pavements and asphalt overlays on Portland cement concrete pavements and is an example of the type of approach which needs to be followed.
2. TTI must evaluate available approaches and recommend an approach to TxDoT based on expected accuracy, availability or required data, and ease of use. Most of the available procedures address reflective cracking of asphalt concrete overlays on existing flexible or rigid pavements. Some modifications to the procedure to model movements of cracks in a stabilized layer would probably be needed.
3. The pertinent properties of the base materials and asphalts concrete influencing reflection cracking must be identified and verified.
4. Regression equations should be used to develop the relationship between the mechanistic model results and observed performance for each of the environmental zones.

Reflection cracking may be described as the appearance of cracks at the surface of an asphaltic concrete layer that mirror those in a lower pavement layer. The pre-existing crack or discontinuity in the lower pavement layers is most commonly due to the effects of temperature and shrinkage on a cement treated layer. Reflection cracking is usually non-structural in that it does not in and of itself reduce the life of the pavement but the

combined effects of traffic and the environment can often lead to premature distress and failure (Caltabiano and Rawlings, 1992).

For various reasons, stabilizers, especially Portland cement and lime, are being used widely in Texas for treating bases, subbases, and subgrades when the pavements are generally surfaced with asphaltic concrete (AC). Transverse cracking of these cemented pavements often occurs soon after construction, and this in turn results in reflection cracking in the overlying asphaltic layer. These cracks are a source of moisture entry and this can lead to premature severe distress in the form of block and alligator cracking. This is usually accompanied by pumping of fines from within the pavement structure and often occurs early in the service life of the pavement (Caltabiano and Rawlings, 1992).

Jayawickrama and Lytton (1987) developed a new design methodology for the prediction of the reflection cracking life of asphalt concrete overlays on flexible pavements. A mechanistic-empirical approach was used in developing this design method. The variables used and the form of the design equations were chosen based upon a mechanistic model that simulates the actual process of reflection crack propagation. This model can probably be used for reflection cracks occurring in pavements having cement treated bases.

Mechanics of Reflection Cracking

The basic mechanisms generally assumed to lead to reflection cracking are the vertical and horizontal movements of the underlying pavement layers. These damaging movements may be caused by traffic loading, thermally induced contractions and expansions, or a combination of these mechanisms. Figure A-41 shows the three pluses of high stress concentrations occurring at the tip of the crack as the wheel load passes over it: one due to bending stresses and two due to shearing stresses. Contraction and expansion of pavement and underlying layers can also contribute the growth of reflection cracks.

Use of Fracture Mechanics Principle

The rate of crack propagation in asphalt concrete can be predicted by using the empirical power law relation developed by Paris (1963).

$$\frac{dC}{dN} = A (\Delta K)^n \quad (A-27)$$

where

- k = stress intensity factor amplitude,
- A,n = fractural parameters of the material, and
- N = number of loading cycles.

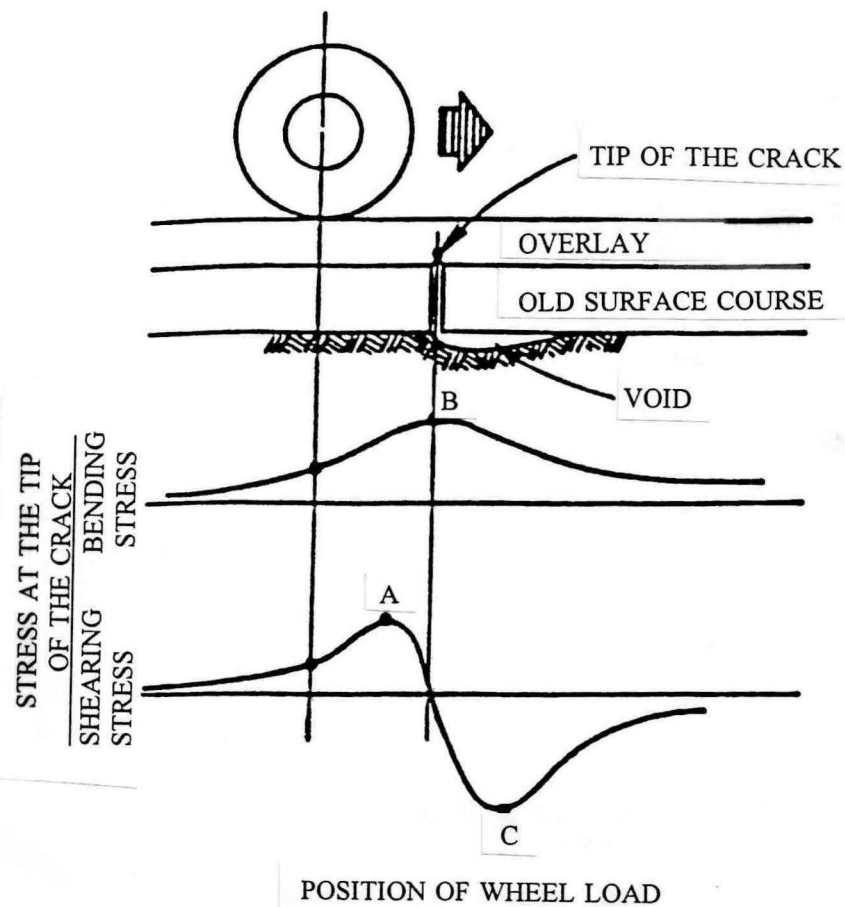


Figure A-41 Stresses induced at the cracked section due to a moving wheel load (Jayawickrama and Lytton, 1987).

Theoretical justification for the use of Paris' crack growth law to nonlinear viscoelastic composite materials was presented by Schapery (1981,1983). He assumed a nonlinear behavior for the material which can be described by

$$\sigma/\sigma_0 = b_0 \epsilon^{b_1} \quad (A-28)$$

where

$$\begin{aligned} \sigma &= \text{applied stress,} \\ \sigma_0 &= \text{yield stress, and} \\ b_0, b_1 &= \text{constants.} \end{aligned}$$

When the length of the failure zone at the crack tip, α and Γ are assumed to be constant, $n = 2/m$, where m is the slope of the log stiffness vs. log loading time curve. A linear relationship exists between $\log A$ and n :

$$\begin{aligned} n &= -1.558 - 0.401 \log A \quad (\text{for traffic associated cracking}) \\ n &= -0.653 - 0.608 \log A \quad (\text{for thermal cracking}) \end{aligned} \quad (A-29)$$

Development of the mechanistic model

The use of Paris' law to predict the crack growth rate in overlays requires a knowledge of the stress intensity factors induced within the overlay under the wheel load. This has been accomplished by following the two-step analysis procedure. In the first step, beam on elastic foundation theory is used to establish the form of the expressions for stress intensity factors of both the opening and shearing modes. The pavement layers consisting of both the original surface layer and the overlay are represented in the model as a beam (Jayawickrama and Lytton, 1987).

In Figure A-42, by representing the cracked section as a hinge with partial moment restraint the following expression was derived for the maximum bending moment.

$$\begin{aligned} M_{\max} &= qf/2\beta^2 e^{-\beta d/2} \sin(\beta d/2) \\ \text{and } \beta &= (k/4EI)^{1/4} \end{aligned} \quad (A-30)$$

where

$$\begin{aligned} q &= \text{pressure exerted on the pavement by wheel load,} \\ f &= \text{bending efficiency factor (i.e. the ratio between the bending moment carried by a cracked pavement and uncracked continuous pavement),} \\ d &= \text{loaded area dimension,} \\ k &= \text{modulus of subgrade reaction for the supporting medium,} \\ E &= \text{elastic modulus of the overlay and} \\ I &= \text{moment of inertia per unit width of the transformed section of the asphalt layers including both the existing asphalt layer and the overlay.} \end{aligned}$$

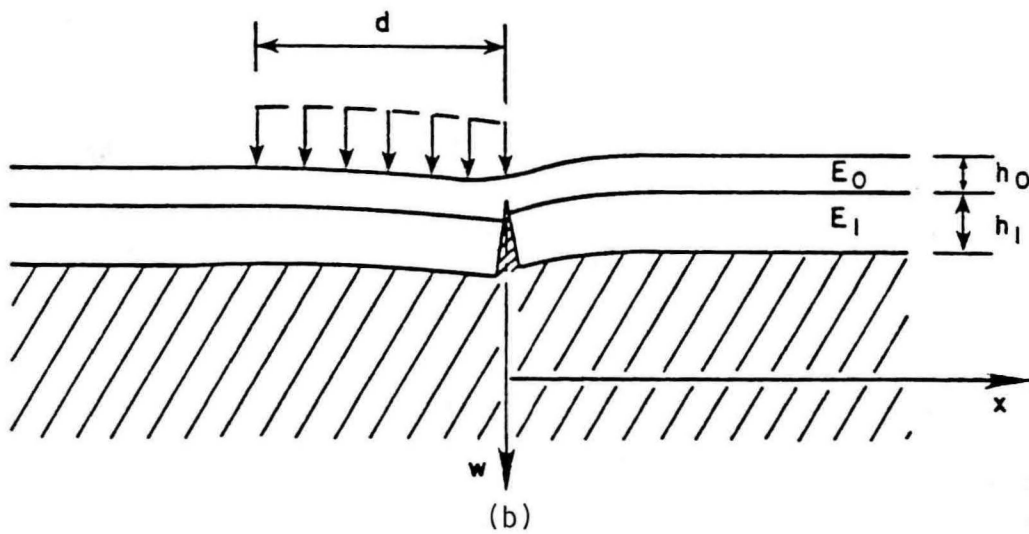
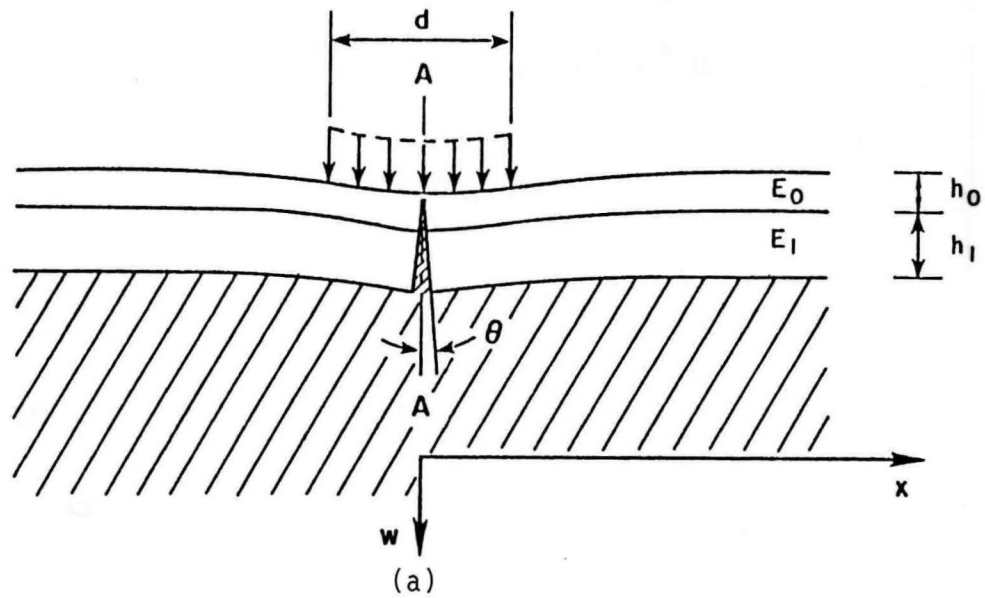


Figure A-42 Wheel load positions that cause maximum stresses at the cracked section (Jayawickrama and Lytton, 1987).

The bending efficiency factor, f , of the cracked pavement depends on the level of aggregate interlock and the length of the crack. The bending action due to the wheel load tends to create tensile stresses at the cracktip causing the crack to open. The bending moment can be related to the resulting opening mode stress intensity factor by using the following formula.

$$K_b = \sigma M \sqrt{\pi c / h^2} F_1(c/h) \quad (A-31)$$

Therefore,

$$K_b \sim q e^{-\beta d/2} / \beta^2 h^{3/2} \sin(\beta d/2) \{f \sqrt{c/h} F_1(c/h)\} \quad (A-32)$$

where

- c = crack length, and
- h = sum of the transformed thicknesses of the existing pavement layer and the overlay.

By defining,

$$\begin{aligned} K_{b0} &= q e^{-\beta d/2} / \beta^2 h^{3/2} \sin(\beta d/2) \\ K_b &\sim K_{b0} \{f \sqrt{c/h} F_1(c/h)\} \\ K_b &= K_b / K_{b0} \sim f \sqrt{c/h} F_1(c/h) \end{aligned} \quad (A-33)$$

K_b = non-dimensionalized stress intensity factor for the opening mode.

The shear force Q at the cracked section under this loading condition is given by,

$$Q = q/4\beta [1 + e^{-\beta d} (\sin \beta d - \cos \beta d)] \quad (A-34)$$

The stress intensity factor for the shearing mode, k_s can be written as $K_s = Q/\sqrt{\pi h} \{ \sqrt{c/h} F_2(c/h) \}$ (A-35)

Therefore,

$$K_s \sim q/4\beta \sqrt{h} [1 + e^{-\beta d} (\sin \beta d - \cos \beta d)] \sqrt{c/h} F_2(c/h) \quad (A-36)$$

By defining,

$$K_{s0} = q/4\beta \sqrt{h} [1 + e^{-\beta d} (\sin \beta d - \cos \beta d)] \quad (A-37)$$

Hence,

$$K_s \sim K_{s0} \sqrt{c/h} F_2 (c/h)$$

$$K_s = K_s / K_{s0} \sim \sqrt{c/h} F_2 (c/h) \quad (A-38)$$

The stress intensity factors resulting from the horizontal movements of the underlying pavement layers were determined in the following manner.

$$K_t = 2E_o / h(1 - \nu) \sqrt{\pi c} F_3 (c/h) V_o \quad (A-39)$$

k_t = stress intensity factor due to temperature damage
 E_o = modulus of the overlay, and
 V_o = maximum crack opening.

$$\text{If } V_o = s \alpha (\Delta T) \quad (A-40)$$

where

s = crack spacing,
 α = coefficient of thermal expansion, and
 ΔT = change in temperature.

$$\text{Thus } K_t \sim E_o / \sqrt{h} (1 - \nu_2) \{(s\alpha\Delta T) \sqrt{c/h} F_3 (c/h)\} \quad (A-41)$$

Defining, as before

$$K_{t0} = E_o / \sqrt{h(1 - \nu^2)} \{(s\alpha\Delta T) \quad (A-42)$$

$$\text{gives } K_t = K_t / K_{t0} \sim \sqrt{c/h} F_3 (c/h) \quad (A-43)$$

Finite Element Computation of Stress Intensity Factor

The magnitude of K_b , K_s , and K_t in the above equations can be determined using finite element technique. A two dimensional plane stress/plane strain finite element code (CRACKTIP) was used for this purpose (Jayawickrama and Lytton, 1987).

The number of load cycles to failure of the overlay can be computed by integrating Paris' crack growth law. First, the equation can be re written as (Jayawickrama and Lytton, 1987)

$$\frac{dC}{dN} = A (K_{\max} - K_{\min})^n \quad (A-44)$$

where

$$\begin{aligned} k_{\min} &= 0, \text{ and} \\ k_{\max} &= k, \text{ which is determined by beam-on-elastic foundation and FEM analysis described previously} \end{aligned}$$

Thus we have,

$$\frac{dC}{dN} = AK^n \quad (A-45)$$

Integrating,

$$N_f = \int_{C_o}^{C_f} \frac{dC}{AK^n} \quad (A-46)$$

$$\begin{aligned} N_f &= \text{number of the load cycles to failure,} \\ C_o &= \text{initial crack length, and} \\ C_f &= \text{final crack length.} \end{aligned}$$

The original pavement and the overlay are treated as a composite in this analysis. Therefore, the initial and final crack lengths depend on the thicknesses of these layers (Jayawickrama and Lytton, 1987).

From the expressions of k_b, k_s , and k_t , the integrals corresponding to the first stage crack growth can be written as follows (Jayawickrama and Lytton, 1987):

Bending:

$$(N_{fb})_1 = \frac{1}{AK_{b0}^n} \int_{C_o}^{C_f} \frac{dC}{\left[F \sqrt{\left(\frac{C}{h} \right)} F_1 \left(\frac{C}{h} \right) \right]^n} \quad (A-47)$$

Shearing:

$$(N_{fs})_1 = \frac{1}{AK_{s0}^n} \int_{c_0}^{c_s} \frac{dC}{\left[\left(\frac{C}{h} \right) F_2 \left(\frac{C}{h} \right) \right]^n} \quad (A-47)$$

Thermal:

$$(N_{ft})_1 = \frac{1}{AK_{t0}^n} \int_{c_0}^{c_s} \frac{dC}{\left[\left(\frac{C}{h} \right) F_3 \left(\frac{C}{h} \right) \right]^n} \quad (A-48)$$

The expressions for the number of load passes corresponding to the second stage of crack growth are obtained as below:

The number of load applications to failure due to bending and shearing mechanisms were reduced to an equivalent number of days using the average daily traffic (in terms of 18-kip ESAL's) for each pavement section (Jayawickrama and Lytton, 1987).

$$(N_{ft})_2 = \frac{1}{AK_{s0}^n} \int_{c_c}^{c_r} \frac{dC}{\left[\left(\frac{C}{h} \right) F_2 \left(\frac{C}{h} \right) \right]^n} \quad (A-49)$$

$$(N_{ft})_2 = \frac{1}{AK_{t0}^n} \int_{c_c}^{c_r} \frac{dC}{\left[\left(\frac{C}{h} \right) F_3 \left(\frac{C}{h} \right) \right]^n} \quad (A-50)$$

Analysis of Pavement Evaluation Data

The condition survey evaluations of reflection cracking were used to develop a mathematical equation that describes the growth of pavement distress with increasing time or an increasing number of load passes (Jayawikrama and Lytton, 1987).

$$g = e^{-(p/N)\beta} \quad (A-51)$$

where

- g = the damage rating of the pavement, a number that ranges between 0 and 1,
- N = the number of load applications in 18-kip ESAL's, and
- p, B = characteristics parameters.

Curves of this form may be developed for a particular pavement section by determining the characteristic parameters ρ and β that provides the best fit to the data recorded. The curves thus developed were then used to determine the number of load applications, N_i that were required to bring the overlaid pavement to a specific damage rating. This process is illustrated in Figure A-43.

Regression Analysis

The final equation for predicting the overlay life was established by performing regression analysis on the mechanically computed N_i values against field data. The form of the regression equation used in the present analysis is given as follows (Jayawickrama and Lytton, 1987):

$$N_{obs} = (N_{dt})_1 \left[\alpha_1 - \alpha_2 \frac{(N_{dt})_1}{(N_{db})_1} - \alpha_3 \frac{(N_{dt})_1}{(N_{ds})_1} \right] + (N_{dt})_2 \left[\alpha_4 - \alpha_5 \frac{(N_{dt})_2}{(N_{ds})_2} \right] \quad (A-52)$$

where

- $\alpha_i (i=1,5)$ = regression coefficients and
- N_{obs} = observed reflective cracking life, in days.

Comments on Reflection Cracking Model

The above described model can probably be used with slight modifications for reflection cracking in asphalt layer on cement treated base. In this case, the treated base layer will be considered as a part of the beam system instead of the existing cracked pavement in the above model. The cracks occurring in the treated base course will be mostly due to shrinkage and have almost the same characteristics as the shrinkage cracking in PCC pavements. The crack spacings in cement treated layers, however, will be smaller than that of PCC pavements. If the coefficient of thermal expansion for PCC and treated base are assumed to be the same, the crack lengths in treated bases will be shorter than those of PCC pavements and the crack initiation and crack propagation in the asphalt layer will probably be controlled by shearing movement of the cracked treated base as opposed to bending. This mechanistic-empirical approach provides an excellent means to develop design equations for reflection cracking in pavements having treated layers. This mechanistic

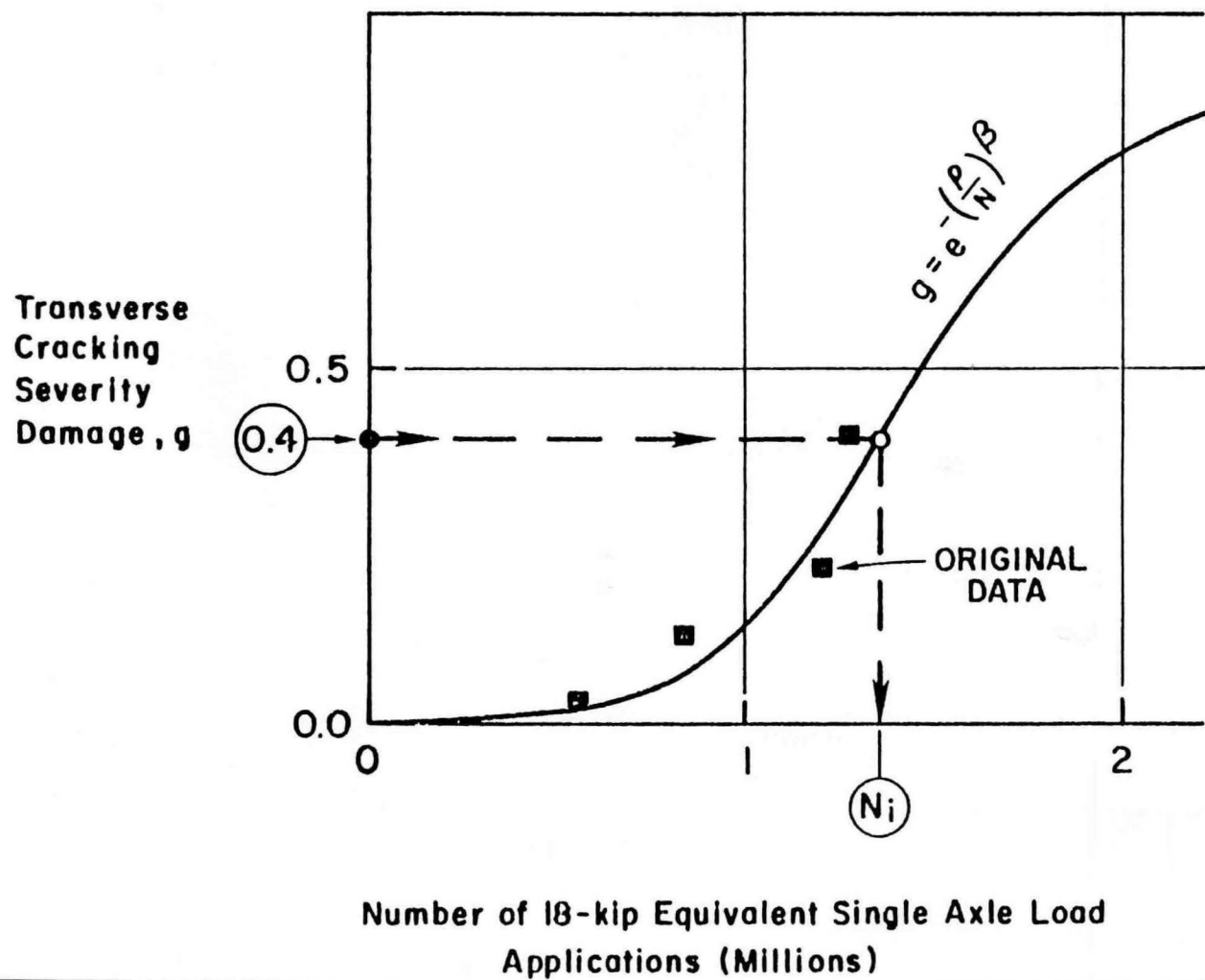


Figure A-43 Determination of N_i using the structural performance curve (Jayawickrama and Lytton, 1987).

concept has a limited amount of parameters. However, they will have to be calibrated using sufficient data from the pavements with stabilized layers.

Work Done in Australia

Pavements containing cement treated bases or subbases have become increasingly more popular for heavily trafficked roads along the eastern coastline in Australia. The Department of Transport, Queensland, Australia, has been actively involved for several years in research work and field trials relating to reflection cracking problem. This work has been predominantly in relation to cracking associated with cement treated bases (Caltabiano and Rawlings, 1992).

According to Caltabiano and Rawlings (1992), the mechanisms associated with the development of reflection cracks in an asphaltic concrete overlay can be directly attributed to the increase in tensile stress within the overlay. This tensile stress is affected by one or more of the following factors:

- Traffic loading,
- Drying shrinkage of cement treated bases,
- Temperature changes and gradients,
- Moisture loss in the subgrade,
- Settlement of differential swelling of the subgrade,
- Compaction of the pavement after construction, and
- Loss of volatiles in the surface of the overlay.

The result of these factors acting on the pavement structure is that a crack develops in the overlay and propagates through it, reflecting lower-level discontinuities. The crack displacement or propagation can follow one or more of the three fracture modes previously discussed depending on the loading configuration.

Research into the problem of reflective cracking focussed initially on the cement treated material itself, by trying to minimize or eliminate the cracking that occurs and thereby eliminating the reflection cracking problem. Later on, when it was realized that it is practically impossible to prevent the formation of cracks in the base due to the traffic and environmental effects, laboratory studies and field trials were undertaken in an attempt to identify and quantify the success or otherwise of various treatments aimed at preventing or reducing reflection cracking through an AC surfacing or overlay (Caltabiano and Rawlings, 1992).

The need to address both the reflection cracking problem and the premature distress and failure of CTB pavements were recognized by the Department of

Transportation, Queensland (DoTQ). These issues were approached from a number of research fronts:

- characterization studies,
- laboratory tests on drying shrinkage,
- accelerated load testing of full scale pavement,
- crack control products, and
- laboratory tests on reflection cracking.

Characterization Studies

The Australian study (Caltabiano and Rawlings, 1992) included an investigation into appropriate relationships for modulus-unconfined compressive strength(UCS), modulus-dry density and modulus-curing time for cement treated materials, and a literature review into fatigue characteristics of these materials. Other characteristics of these materials, such as the development of strength with age and the effect of cement content on UCS, were also examined. The findings of the laboratory experimentation facilitated a comparison with the Department of Transportation, Queensland (DoTQ) strength/stiffness criteria. The work also included an evaluation of the use of commercially available retarders to retard the set of freshly mixed cement treated material. A number of additives were also evaluated in the experimental work including type A (normal Portland) cement, type C (slow-setting) cement, and type FA (normal Portland cement/25% flyash(PFA) blend). The work proved that type C cement was most effective, with the flyash blend and set-retarder displaying similar setting characteristics (Caltabiano and Rawlings, 1992).

Dry Shrinkage Research

As part of the Australian study (Caltabiano and Rawlings, 1992) a technique for measuring the drying shrinkage of cement treated materials in the laboratory was developed. Specimens of CTB were dynamically compacted into molds, and, following curing, the shrinkage was measured in a plane normal to the direction of compactive effort. The magnitude and rate of drying shrinkage is affected by several factors including plasticity of fines, cement content, molding moisture content, cement/additive type, paving material characteristics and curing conditions. The laboratory test procedure was then used to determine the relative influence of these factors on drying shrinkage.

An important finding from the research work was the influence of the plasticity of fines on drying shrinkage potential. The Linear Shrinkage (LS) of the untreated material, determined on the fraction passing the 425 um sieve, was found to be a good indicator of the drying shrinkage potential of the material following its treatment with cement (Caltabiano and Rawlings, 1992).

Overall, this laboratory experimental work on cement treated materials provided some important findings:

1. The plasticity of clay fines present influences the drying shrinkage potential.
2. The type of clay mineral present influences the drying shrinkage potential, with the smectite group exerting the most pronounced influence.
3. Cement content influences the shrinkage potential, however, its influence appears to diminish as material quality improves.
4. The use of relatively low cement contents with poor quality materials is likely to result in significant drying shrinkage.
5. Linear shrinkage, LS, was identified as being a very good indicator of the drying shrinkage potential of a cemented treated material (Caltabiano and Rawlings, 1992).

A considerable volume of research in shrinkage and shrinkage cracking of Portland cement stabilized soils is presented in the literature, i.e., Norling (1973), Pretorius (1970), and George (1971). A review of this literature involves construction technologies to reduce shrinkage cracking and is not within the scope of his research.

Asphaltic Concrete Research

Experiments were conducted using three treatments commonly employed to inhibit reflection cracking in asphaltic concrete overlays. These treatments were geotextile, geogrid and polymer modified asphaltic concrete. The primary objective of these tests was to assess the relative performance of interlayers to delay the propagation of reflection cracks addition made here. The testing program consisted of three series of tests as outlined below with a minimum of three specimens tested for each interlayer type in each series.

Series A: beam thickness 100 mm, and applied load 810 kpa

Series B: beam thickness 75 mm, applied load 810 kpa

Series C: beam thickness 75 mm, applied load 555 kpa

All testing was conducted at 20 °C. The results summarized in Table A-5, show that there is a clear improvement in the reduction of reflection cracks in asphaltic concrete overlays when interlayer treatments are used or modification to the asphaltic concrete is made (Caltabiano and Rawlings, 1992).

Table A-5 Performance relative to a control beam for all three test series (Caltabianok and Rawlings, 1992).

Treatment Type	Increase in Control Life		
	Series C	Series B	Series A
Polymer Modified AC	2.6	2.0	3.0
Geotextile	5.0	15.0	N/A
Geogrid	10.0	31.0	N/A

Research By Portland Cement Association

Fatigue of Soil-Cement

Repetitive and static tests were made on 296 soil-cement beam specimens on end supports with a neoprene subgrade between supports (Larsen and Nussbaum, 1967). Fatigue curves were established in plots of fatigue ratio, R_c/R , versus number of load repetitions to produce failure, N (Figure A-44). From these tests, in which it was shown that soil type and section depth affected fatigue life, an expression for radius of curvature that will assure 1 million load repetitions was derived. The general fatigue equation was expressed as

$$R_c/R = a N^{-b} \text{ for } 10 < N < 10^6 \quad (\text{A-53})$$

The coefficient "a" is dependent on the thickness of the specimen and

$$a = 1.05 - 0.042h \quad (\text{A-54})$$

Replacing the value of "a" into the above equation,

$$R_c/R = (1.05 - 0.042h) N^{-b} \quad (\text{A-55})$$

Solving for the allowable radius of curvature, R

$$R = \frac{R_c N^b}{1.05 - 0.042h} \quad (\text{A-56})$$

where

- R_c = critical radius of curvature, in. defined as the radius of curvature at failure,
- R = radius of curvature, in. developed for given load and number of load repetitions,
- N = number of load repetitions,
- a = dimensionless coefficient in fatigue equation,
- b = dimensionless exponent in fatigue equation, and
- h = thickness of specimen (depth of beam), in.

Load-Deflection Characteristics of Soil-Cement Pavements

Nussbaum and Larsen (1965) developed a relationship between load and deflection for soil-cement. An equation was derived which predicts load capacity as a function of deflection, thickness of soil cement, radius of bearing area, and modulus of subgrade reaction.

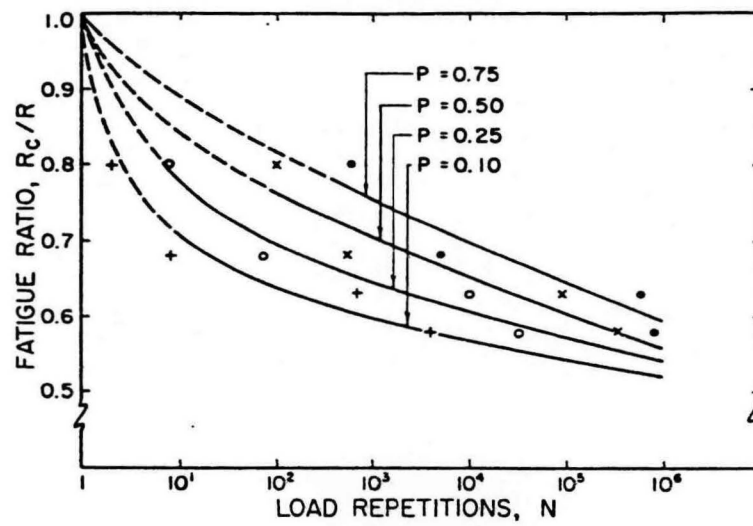


Figure A-44 Relationships for probability of fatigue failure to soil-cement (Larsen and Nussbaum, 1967).

Soil-Cement Bases

Load response of soil-cement bases is described in terms of the significant variables. A nondimensional logarithmic plot of the test data is shown in Figure A-45. Deflection w , multiplied by the modulus of subgrade reaction, k , and divided by the intensity of applied load, p , is plotted along the ordinate. The ratio of bearing area radius, a , to soil-cement thickness, h , is given along the abscissa. The relationship in equation form is:

$$\frac{wk}{p} = \alpha \left(\frac{a}{h} \right)^\beta \quad (\text{A-57})$$

where, α is the ordinate at a point on the best-fit line corresponding to an abscissa of $a/h = 1$; and β is the slope of the regression line. It is recognized that a curvilinear best-fit line would better describe the test data at an a/h of 3 or larger. However, the straight line is used for the range of a/h from 0.5 to 2.0, which covers most of the conditions of load area and pavement thickness encountered in pavement design. It is seen that $\alpha = 0.058$ and $\beta = 1.52$. Thus, the specific expression describing the load response of soil-cement is

$$\frac{wk}{p} = 0.058 \left(\frac{a}{h} \right)^{1.52} \quad (\text{A-58})$$

The above best-fit equation may be solved explicitly for thickness of soil cement, h .

Thickness Design for Soil-Cement Pavements

Larsen and Nussbaum (1969), combined the fatigue of soil-cement and the previous findings from laboratory investigations of a load-deflection relationship with an experimentally determined deflection function to develop a rational thickness design procedure for soil-cement pavements. The design method distinguishes between soil-cement made from granular and fine-grained soils.

Fatigue Consumption Concept

Traffic generally consists of repeated applications of loads of different magnitude. It may be considered that each load application consumes a portion of the fatigue resistance of the pavement. The steps involved in developing the concept of fatigue consumption are as follows:

The radius of curvature for a given condition of loading is computed from the equation (Larsen and Nussbaum, 1969)

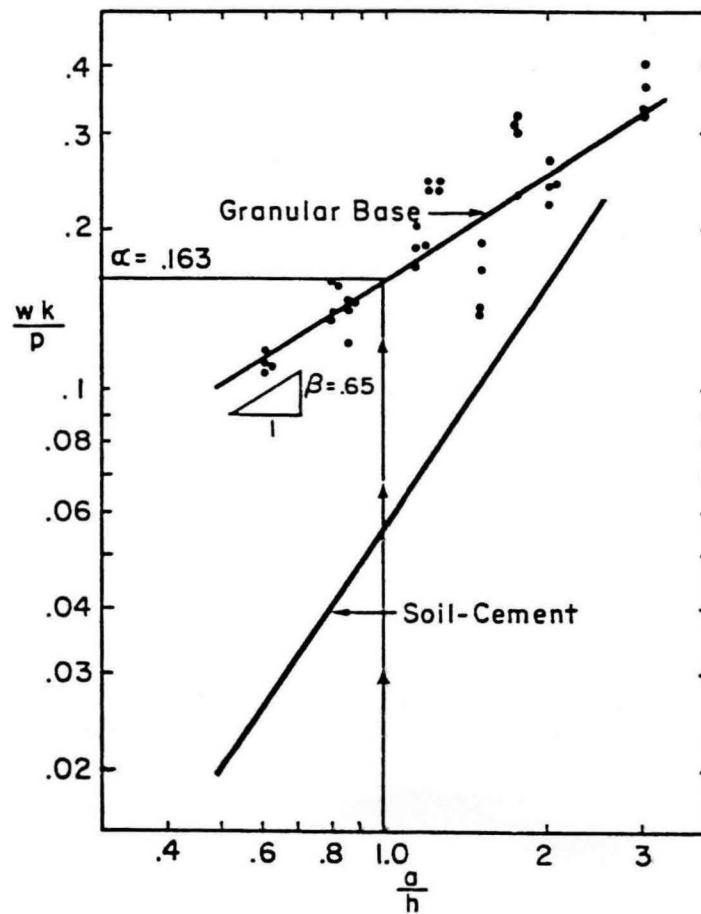


Figure A-45 Best-fit line in a nondimensional logarithmic plot for granular and soil-cement bases (Nussbaum and Larsen, 1965).

$$R = \frac{Ck\pi a^{\frac{1}{2}} h^{1.5}}{P\alpha} \quad (A-59)$$

Then, the applied fatigue ratio can be determined from the equation

$$\frac{R_c}{R_{\text{applied}}} = \frac{R'_c \alpha}{(2.1h-1) k\pi C} \left[\frac{P^{\frac{1}{2}}}{a} \right] \quad (A-60)$$

The permissible fatigue ratio is computed from the relationship

$$\frac{R_c}{R_{\text{permissible}}} = \frac{(2.1h-1)}{h^{\frac{3}{2}} N^{\delta}} \quad (A-61)$$

Equating the applied fatigue ratio to the permissible fatigue ratio and solving for the number of loads to failure gives

$$N = \left[\frac{(2.1h-1)^2 Ck\pi}{R'_c \alpha h^{\frac{3}{2}}} \right]^{\frac{1}{\delta}} \left[\frac{a^{\frac{1}{2}}}{P} \right]^{\frac{1}{\delta}} \quad (A-62)$$

where

- a = radius of loaded area, in;
- C = experimentally established deflection function;
- k = elastic modulus of subgrade reaction. psi;
- R_c = critical radius of curvature, in;
- R_{c/} = basic radius of curvature, in;
- α = dimensionless coefficient;
- h = pavement thickness, in;
- P = wheel load, kips; and
- δ = dimensionless exponent.

LIME-FLY ASH-STABILIZED BASES AND SUBBASES

Fly ash is a pozzolan and is defined by the American Society for Testing and Materials (ASTM) as "a siliceous or siliceous and aluminous material, which in itself possesses little or no cementitious value but which will, in finely divided form and in the presence of moisture, chemically react with calcium hydroxide at ordinary temperatures to form compounds possessing cementitious properties."

Use of LFA materials has increased in recent years because of energy resources and the environment. Fly ash is "the finely divided residue that results from the combustion of ground or powdered coal and is transported from the boilers by flue gases" (ASTM Specification C 593). Fly ash is collected from the flue gases by either mechanical or electrostatic precipitation devices (Lime-Fly Ash, 1976).

Lime-Fly Ash Reactions

The reactions that occur in the lime-fly ash-water system to form cementitious materials are complex. Several types of chemical reactions take place when lime is mixed with reactive fly ash and aggregates in the presence of water. Probably the most important reaction, with respect to paving applications, is the reaction which produces a cementitious gel, binding the mineral aggregate particles together. Apparently, the critical reaction is the reaction of the calcium in the lime with certain aluminous and siliceous minerals present in the fly ash, to produce a gel which is a compound of calcium or calcium aluminate. Pozzolanic reactions, required for the development of cementitious compounds, will not take place unless sufficient moisture is present in the mixture. These desirable reactions are also retarded by low temperatures and almost completely stop at temperatures below about 40° F (Little et al., 1982).

Engineering Properties of Lime-Fly Ash-Stabilized Materials

Many properties must be considered in lime-fly ash mixture proportioning characterization, and pavement structural analysis. Lime-fly ash mixture properties vary depending on lime and fly ash characteristics, mixture proportions, stabilized material, density, and curing conditions (Lime-Fly Ash, 1976).

Compressive Strength

Unconfined compressive strength is frequently used to evaluate the quality of cured LFA mixtures. A general range of typical strengths for various LFA mixtures is given in Table A-6. ASTM Procedure C 593-69 requires a minimum compressive strength of 400 psi for lime-fly ash used in paving-type mixtures. Compressive strength development continues in LFA mixtures for a substantial period following placement as shown in Figure A-46 (Lime-Fly Ash, 1976).

Shear Strength

The shear strength of LFA mixtures has not been extensively considered. Unconfined compressive strength data for typical mixtures indicate that shear strength failures are not likely for normal pavement applications (Lime-Fly Ash, 1976).

Table A-6 Ranges of compressive strength for the lime-fly ash-stabilized materials
(Lime-Fly Ash, 1976).

**RANGES OF COMPRESSIVE STRENGTH FOR THE LIME-FLY ASH-
STABILIZED MATERIALS**

Material	28 Day Immersed Compressive Strength	
	psi	(kPa)
Gravels	400-1300	(2800-9000)
Sands	300-700	(2100-4800)
Silts	300-700	(2100-4800)
Clays	200-500	(1400-3400)
Crushed Stones and Slag	1400-2000	(10,000-14,000)

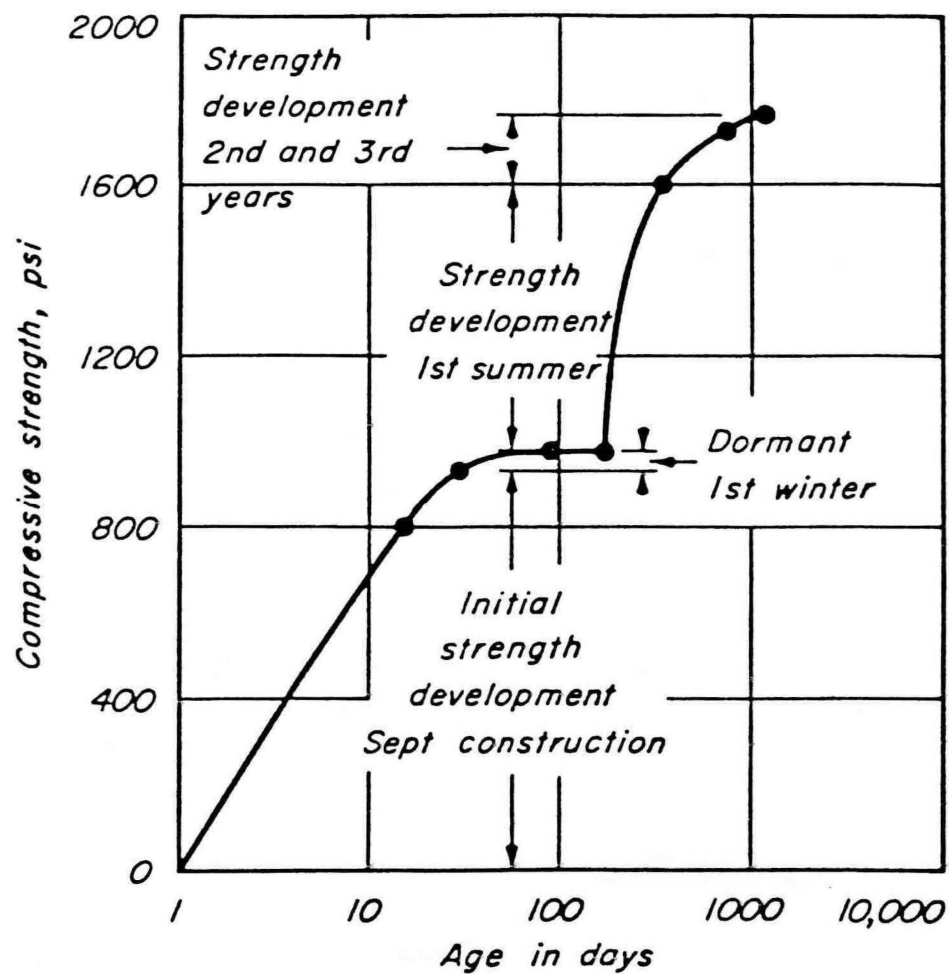


Figure A-46 Compressive strength development of lime-fly ash-stabilized mixture in Chicago area (Lime-Fly Ash, 1976). 1 psi = 6,894 Pa

Flexural Strength

The flexural strength of LFA mixtures is substantially lower than the corresponding compressive strengths. Laboratory test procedures similar to ASTM D 1635-63 can be used to evaluate the flexural strength of LFA mixtures. Typical flexural strength-cure time relations for two mixtures has been illustrated in Figure A-47. The ratio of flexural strength to compressive strength for most LFA mixtures is between 0.18 and 0.25. A value of 20 percent of the compressive strength is a conservative engineering estimate of the flexural strength of LFA mixtures (Lime-Fly Ash, 1976).

Modulus of Elasticity

The elastic moduli for LFA mixtures are different depending on whether the modulus is determined from compressive or flexural testing procedures (Lime-Fly Ash, 1976). Normally, flexural modulus is somewhat lower than the compressive modulus. LFA mixture moduli values increase as mixture strength increases (Lime-Fly Ash, 1976).

Fatigue Properties

The fatigue properties of LFA mixtures are important in pavement design analysis. Since the compressive stresses developed in most pavements with LFA mixture layers are small compared to LFA mixture compressive strength, compressive fatigue behavior is not considered to be of any consequence but flexural fatigue is considered very important. A relationship between the ratio of applied stress to the modulus of rupture of the material and the number of load applications to failure has been shown in Figure A-48 (Lime-Fly Ash, 1976). The data came from a test conducted on beam specimens with loads applied continuously at a rate of approximately 450 applications per minute. In analyzing the fatigue properties of LFA mixtures, the influence of the strength gain with time must be recognized. Because flexural strength increases with time, the stress level decreases. Thus, as the time required to accumulate the number of load applications to failure becomes longer, the number of load applications to failure becomes greater (Lime-Fly Ash, 1976).

Thickness Design Approaches

Barenberg and Thompson (1982) describe a pavement that consists of a 254 mm (10 in) thick lime and fly ash aggregate base and a 75 mm (3 in) thick asphalt concrete surface built in 1976 to serve heavy coal trucks that haul to a power plant. The structural capacity of the pavement has not decreased since construction although transverse and longitudinal cracking and very limited fatigue cracking have occurred.

According to Barenberg and Thompson (1982), thickness design of pavements with LFA mixes can be accomplished by using the AASHTO procedures and assigning an equivalency value (a_2) to the LFA mix. The LFA pavement can also be considered as a slab and the Westergaard elastic slab theory or the Meyerhof ultimate load theory can be used

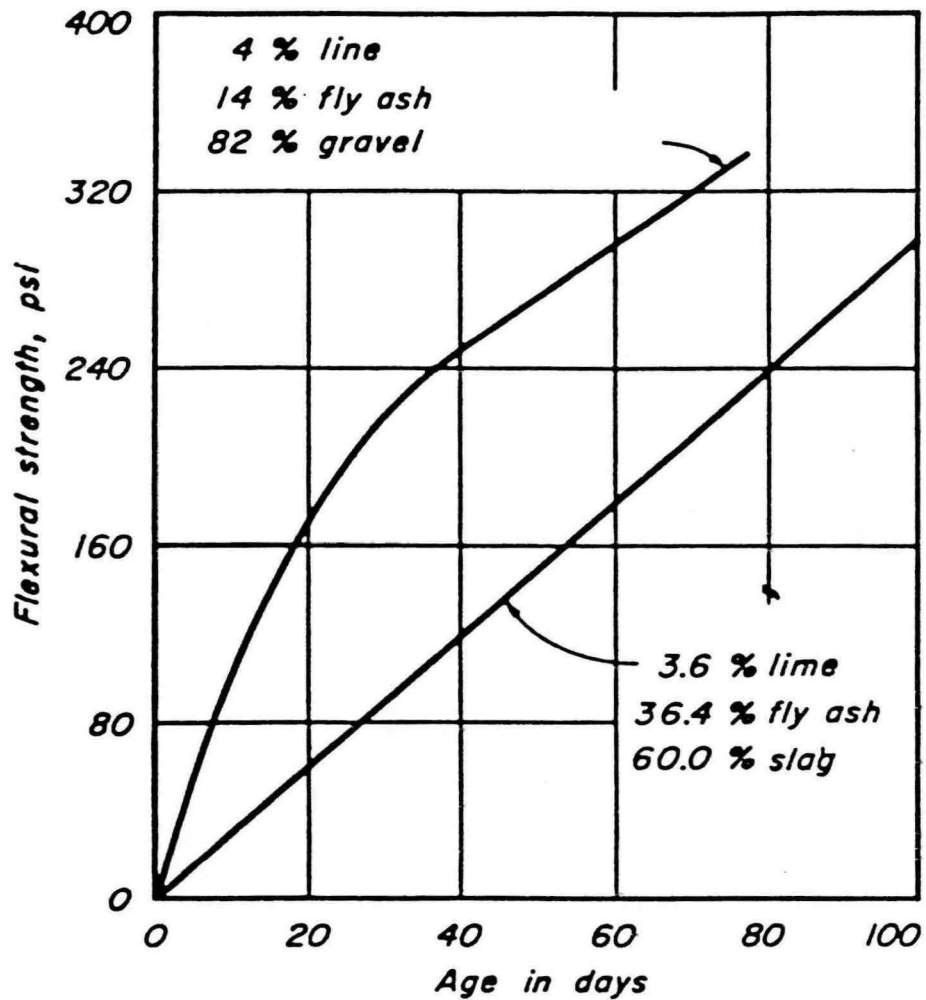


Figure A-47 Flexural strength development of typical lime-fly ash-stabilized mixtures (Lime-Fly Ash, 1976). 1 psi = 25.4 mm

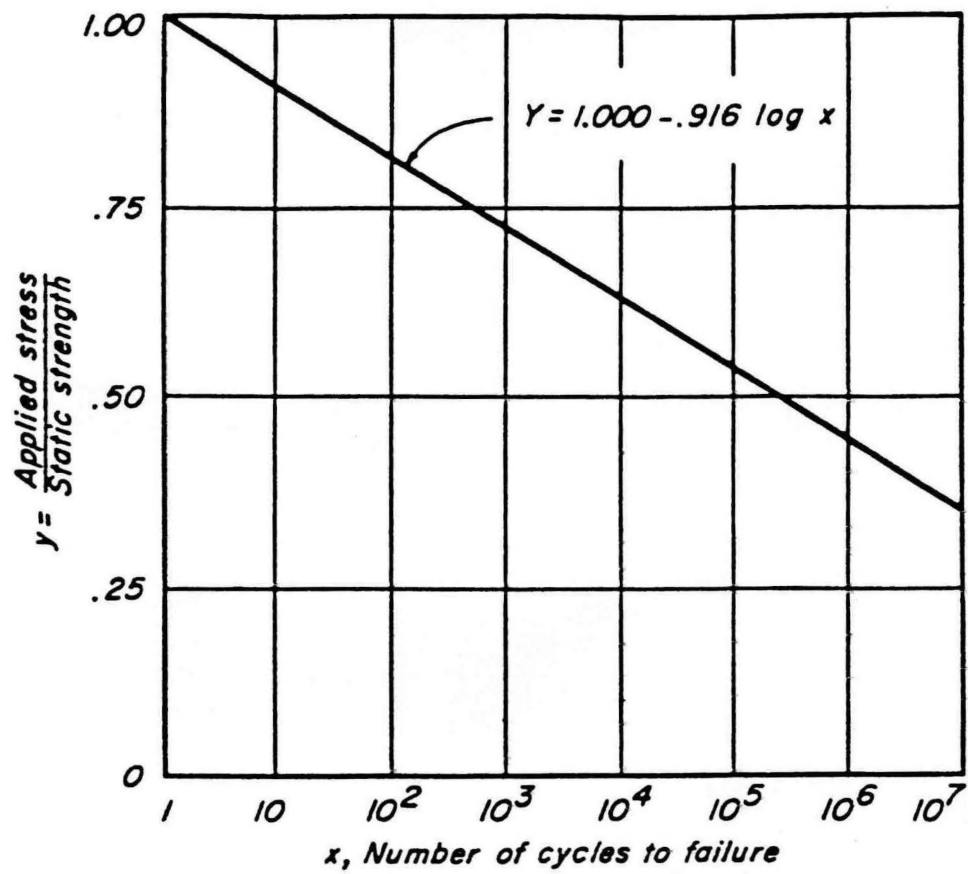


Figure A-48 Flexural fatigue behavior of lime-fly ash-aggregate mixture (Flexible Pavement Manual, 1991).

for design. According to the IDOT design procedure for flexible pavements, the structural value for the pavement is given by the equation:

$$D_t = a_1 D_1 + a_2 D_2 + a_3 D_3 \quad (A-63)$$

where D_1 , D_2 , and D_3 are the thicknesses in inches of the surface, base, and subbase layers, respectively, and a_1 , a_2 , a_3 are coefficients that are a function of material type and properties. The material coefficient value (a_2) assigned by IDOT for LFA mixes was 0.28.

The pavement was analyzed by using the Westergaard model for flexural stresses and fatigue failure in the LFA base and for ultimate load capacity by using the Meyerhof theory. The pavement was considered adequate by using all three thickness design criteria.

In the **Flexible Pavement Manual** of the American Coal Ash Association, thickness design methods for flexible pavement systems having coal fly ash bases are discussed. Pozzolanic stabilized mixtures (PSM) with coal fly ash may develop elastic moduli values in excess of 2 million psi; and with elastic moduli values of this magnitude, a PSM layer behaves essentially as a slab. A characteristic of PSM base layers is their continued strength development because of long-term pozzolanic reactions. PSM's continue to gain strength over a period of several years, except when temperatures are below 4°C (40°F). Once the temperature again exceeds 4°C (40°F), the strength gain resumes. A PSM base layer is, therefore, better able to withstand fatigue damage because even as wheel loads are applied the PSM continues to gain strength. The thickness of a PSM base layer for a flexible pavement system can be determined by one of three design methods (Flexible Pavement Manual, 1991):

1. AASHTO flexible pavement design procedures - using structural layer coefficients.
2. Mechanistic pavement design procedures - using resilient modulus values for the pavement layers.
3. A combination of the above two methods - using mechanistic design concepts to determine pavement layer coefficients.

AASHTO Thickness Design of Flexible Pavements

The original AASHTO Road Test equation was modified in the 1986 AASHTO design guide as follows:

$$SN = a_1 D_1 + a_2 D_2 m_2 + a_3 D_3 m_3 \quad (A-64)$$

where m_2 and m_3 are drainage coefficients for base and subbase layers, respectively. For a PSM base layer, the drainage coefficient m_2 is 1.0. The main factors influencing the variation in the structural layer coefficient for thickness design method are the modulus of elasticity and the compressive strength of the PSM. The field design compressive strength, determined after 56 days of moist curing at 23°C (73°F) is the compressive strength value used to determine the structural layer coefficient for PSMs. The relationship between modulus of elasticity (E_{psm}) and field design compressive strength (CS), can be estimated as (Flexible Pavement Manual, 1991)

$$E_{psm} = 500 + CS \quad (A-65)$$

where

$$\begin{aligned} E_{psm} &= \text{elastic modulus (ksi), and} \\ CS &= \text{field design compressive strength (psi).} \end{aligned}$$

The normal range of structural layer coefficients in the AASHTO design guide is from 0.20 to 0.28, where the lower limit value of 0.20 for a_2 corresponds to a minimum CS value of 2,800 KPa (400 psi), the absolute minimum CS value for assignment of a structural layer coefficient (Flexible Pavement Manual, 1991).

Mechanistic Design Procedure

The design criterion is known as flexural fatigue consumption. Flexural fatigue consumption is related to the number of load applications and the stress ratio, SR, which is calculated for PSM layers as:

$$SR = (\text{PSM Design Flexural Stress}) / (\text{PSM Flexural Strength}) \quad (A-66)$$

Figure A-49 shows permissible SR values for various design reliabilities and traffic conditions. For a given wheel load, PSM strength and pavement thickness are the primary factors that control the PSM design flexural stress. The pavement thickness factor is quantified by the equivalent thickness, T_{EQ} , which is defined as:

$$T_{EQ} = 0.5 T_{AC} + T_{PSM} \quad (A-67)$$

where

$$\begin{aligned} T_{AC} &= \text{asphalt wearing course thickness, inches; and} \\ T_{PSM} &= \text{thickness of the PSM base layer, inches.} \end{aligned}$$

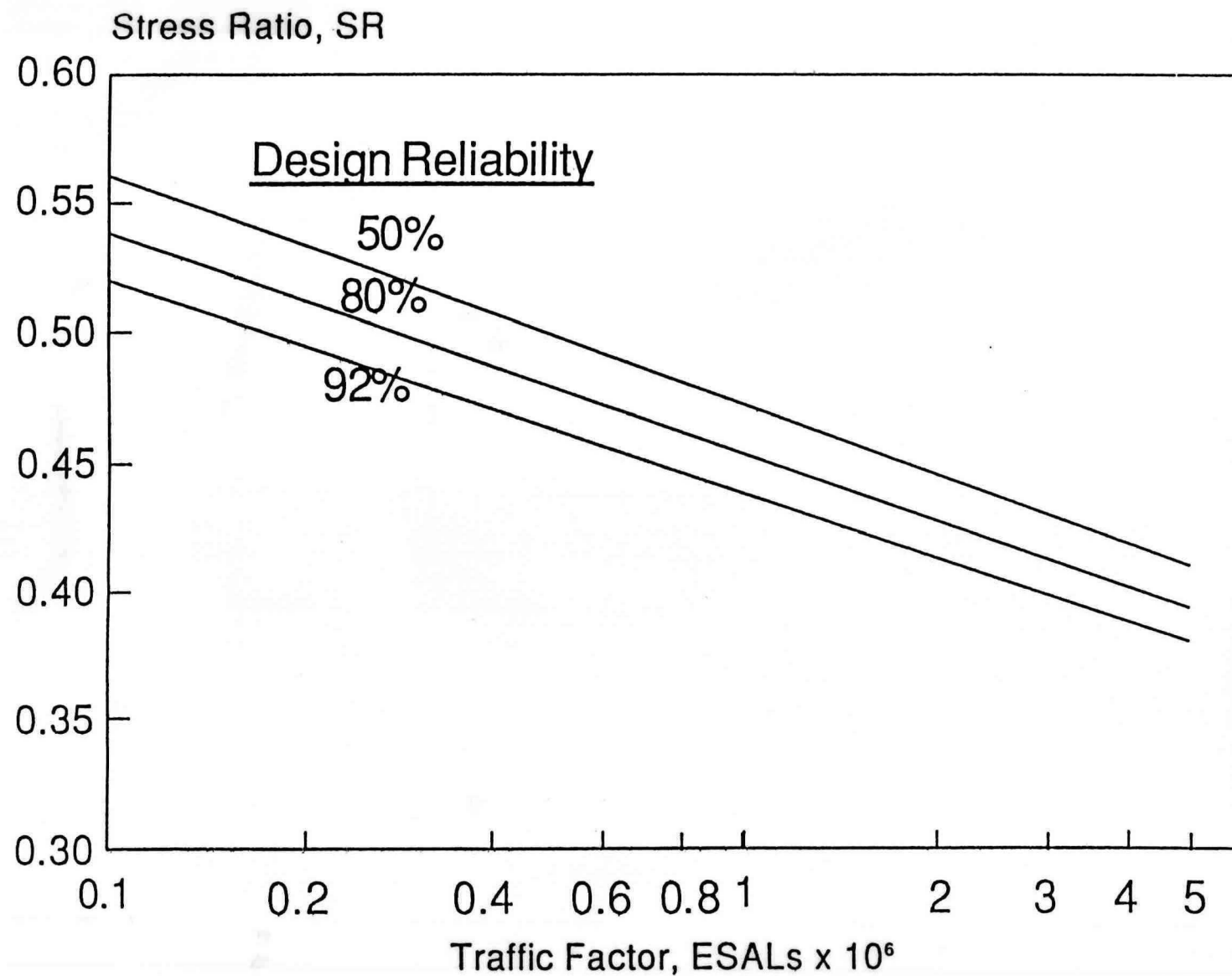


Figure A-49 Typical relationship of stress ratio to traffic conditions (Flexible Pavement Manual, 1991).

The flexural strength and elastic modulus of a PSM can be estimated from its unconfined compressive strength (Q_U in psi). The flexural strength is approximately 20% of Q_U . The elastic modulus is estimated as:

$$E_{PSM} \text{ (ksi)} = 500 + [Q_U \text{ (psi)}] \quad (A-68)$$

Figure A-50 is used to determine the required T_{EQ} for routine pavement design. The PSM base layer thickness is calculated as:

$$T_{PSM} = T_{EQ} - 0.5 T_{AC} \quad (A-69)$$

The recommended minimum PSM base layer thickness is 15 cm (6 in).

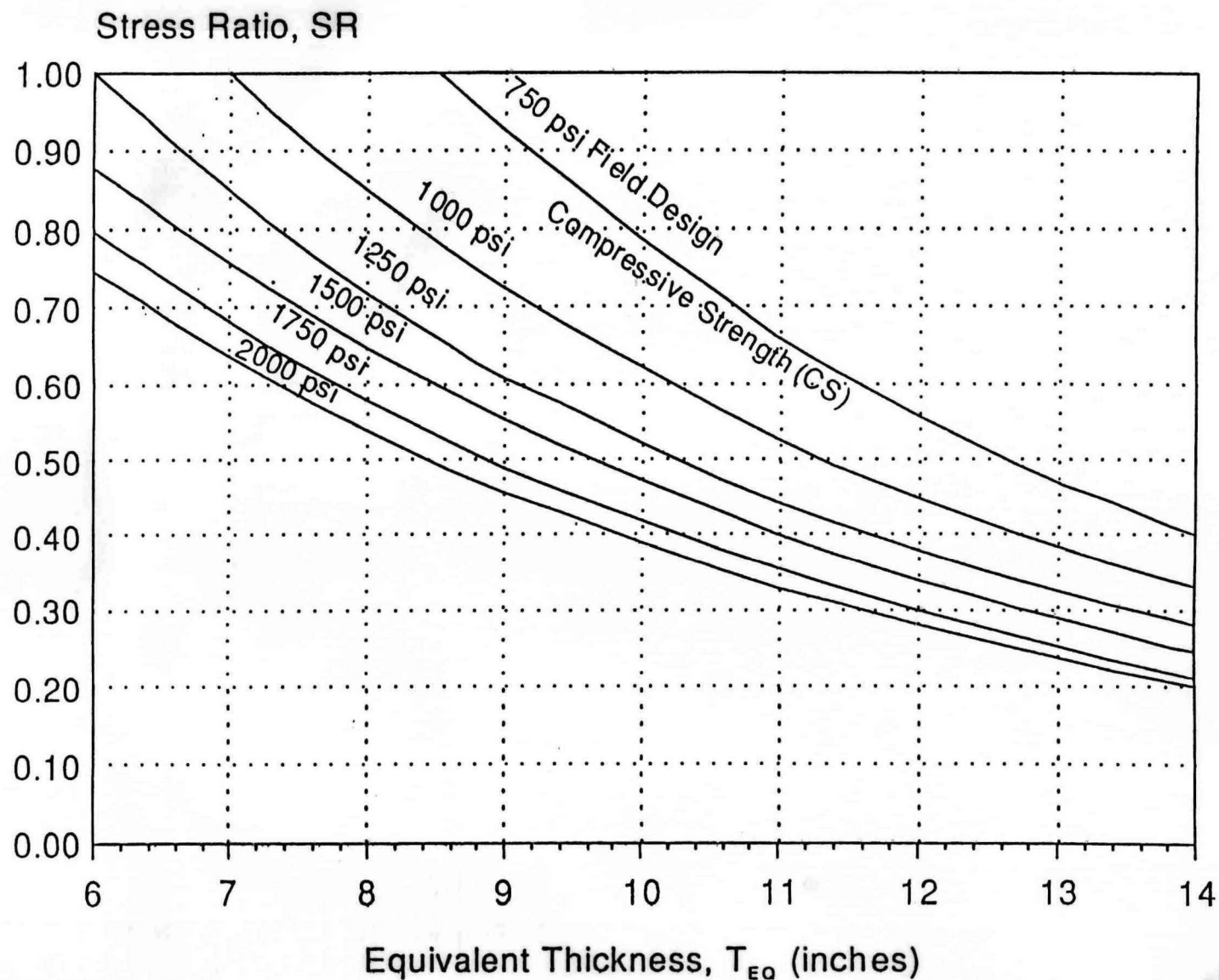


Figure A-50 Typical PSM thickness design chart (Flexible Pavement Manual, 1991).
1 in = 25.4 mm 1 psi = 6,894 Pa